BiochemiCa^{2+}l studies in Alzheimer's disease: the *APP*arent diagnostic and therapeutic role of antipsychotics on calcium homeostasis and amyloid-precursor-protein metabolism

ANDRÁS PALOTÁS, M.D.

Ph.D. THESIS

UNIVERSITY OF SZEGED
2004

INTRODUCTION

The amyloidogenic processing of the membrane-associated amyloid precursor protein (APP), regulated by calcium signaling pathways, results in the formation of the neurotoxic β-amyloid peptide (βAP), that is the major component of senile plaques in Alzheimer's disease (AD). βAP-induced cytotoxicity involves disruption of resting intracellular free calcium level ($[Ca^{2+}]_i$). Certain agents used in the treatment of co-morbid conditions in AD, such as haloperidol (HAL), have been shown to interact with calcium homeostasis and βAP formation. Toxic effects of βAP are ubiquitously present in the body, however its pathomechanism is difficult to be examined in the central nervous system. A substantial body of data exists indicating that biochemical changes of brain cells in various neurobiological diseases with systemic manifestation (*eg.* AD) are reflected in peripheral tissues, such as in fibroblasts and lymphocytes.

OBJECTIVES OF THE STUDY

In order to investigate calcium and other factors (*ie.* genes) involved in βAP toxicity and APP processing, the present study focuses on calcium homeostasis in the periphery, also on APP metabolism and gene expression profile in the brain. The effect of certain antipsychotics, including HAL and risperidone (RISP), is also evaluated for their effects on βAP-induced calcium-imbalance and their role on APP metabolism and gene expression.

EXPERIMENTAL PROCEDURES

Resting intracellular calcium levels were assessed by fluorescence ratio imaging of the calcium indicator dye Fura-2AM ($FL_{340/380}$) in human fibroblasts and lymphocytes. Rat cortical APP levels after acute and chronic intra-peritoneal treatment of rodents with HAL or RISP were determined using Western-immunoblot techniques. Cortical gene expression was analyzed by cDNA microarrays after the same treatment modalities. Results were confirmed by real-time quantitative reverse transcription polimerase chain-reaction (QRT-PCR).

RESULTS

1. **Calcium homeostasis.** $FL_{340/380}$ of control lymphocytes was 1.001±0.117, whereas Alzheimer lymphocytes exhibited a ratio of 1.131±0.100. In contrast, $FL_{340/380}$ of control fibroblastic cultures revealed 2.48±0.162, and Alzheimer fibroblasts exhibited 2.052±0.207 $FL_{340/380}$. Exposure of both control lymphocytes and fibroblasts to βAP for 2 and 16 hours, respectively, caused a rise in the free cell calcium ($FL_{340/380}$: 1.507±0.368 and 2.666±0.08, respectively). Alzheimer lymphocytes and fibroblasts showed a $FL_{340/380}$ of 1.130±0.075 and 2.055±0.125, respectively after βAP treatment. Chronically, $FL_{340/380}$ was initially elevated in fibroblastic cultures, but after 16-weeks $FL_{340/380}$ gradually fell below resting levels. Co-incubation of HAL or RISP with βAP resulted in no significant alteration in the resting calcium levels of fibroblasts.

$FL_{340/380}$ of lymphocytes

Comparative fluorimetric measurements on lymphocytes of human Alzheimer and control donors on $FL_{340/380}$ using Fura-2AM. Resting $[Ca^{2+}]_i$ appeared to be higher in AD cells when compared to that seen with control lymphocytes. After incubating cells in the presence of βAP, the $[Ca^{2+}]_i$ of the control cells elevated, while that of AD lymphocytes did not differ considerably. (*P<0.05)

Samples	$FL_{340/380}$ (mean±SD)	Number of cuvettes
Control	1.001±0.117	23
Alzheimer	1.131±0.100*	18
Control+βAP	1.507±0.368*	23
Alzheimer+βAP	1.130±0.075	18

$FL_{340/380}$ of fibroblasts: treatment with HAL and RISP

Comparative fluorimetric studies on human control and Alzheimer fibroblasts on $FL_{340/380}$ utilizing the Ca^{2+}-indicator dye Fura-2AM. Cells were cultured with or without βAP and/or HAL/RISP for 16 hours at 37°C. Elevation in $FL_{340/380}$ after βAP-treatment was attenuated by co-administration of HAL or RISP. (*P<0.05, when Alzheimer samples are compared to the controls, and **P<0.05, when samples are compared to their untreated counterparts only)

Cultures	$FL_{340/380}$ (mean±SD)	Number of coverslips
Control	2.48±0.162	16
Alzheimer	2.052±0.207*	42
Control+βAP	2.666±0.08**	16
Alzheimer+βAP	2.055±0.125*	42
Control+HAL	2.41±0.119	16
Alzheimer+HAL	2.049±0.202*	16
Control+βAP+HAL	2.46±0.123	16
Alzheimer+βAP+HAL	2.054±0.198*	16
Control+RISP	2.479±0.200	16
Alzheimer+RISP	2.054±0.172	16
Control+βAP+RISP	2.482±0.114	16
Alzheimer+βAP+RISP	2.053±0.099	16

Time-course of βAP on $[Ca^{2+}]_i$ of human fibroblasts

Short-term exposition of fibroblasts to βAP results in an increased $[Ca^{2+}]_i$. The rise in the calcium-level peaks after an approximately half-a-week treatment with the peptide. The flow-chart demonstrates that the reversible elevation of $[Ca^{2+}]_i$ turns into a fall at around the 16th week of exposition to βAP, and yields a sustained decrease in the $[Ca^{2+}]_i$. Calcium-level of control cultures with no βAP treatment appeared to be unchanged during the experiment.

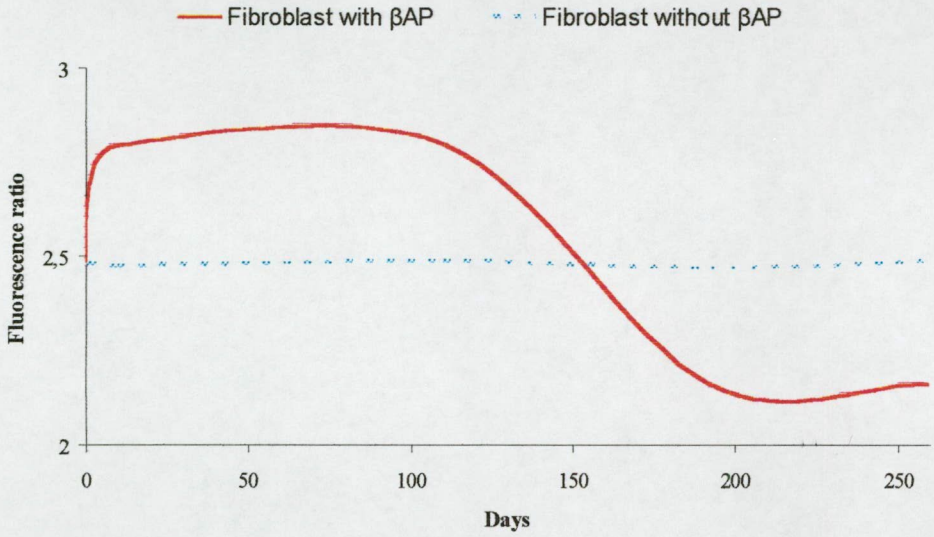

2. **APP-levels.** Significant rises in the relative values of rat cortical APP levels were between 2-6% when compared to that seen with control levels after 12-96 hours of treatment with HAL. Neither chronic HAL, nor acute or chronic RISP treatment has resulted in altered APP concentration.

Time-course of HAL on rat cortical APP concentrations
Intraperitoneal administration of HAL resulted in significant increase in rat cortical APP-level in therapeutic dose within 24 hours. This elevation was seen even in 12 hours in toxic dose of the drug. Both therapeutic and toxic HAL leaved APP concentrations unchanged on the long-run. (*P<0.05)

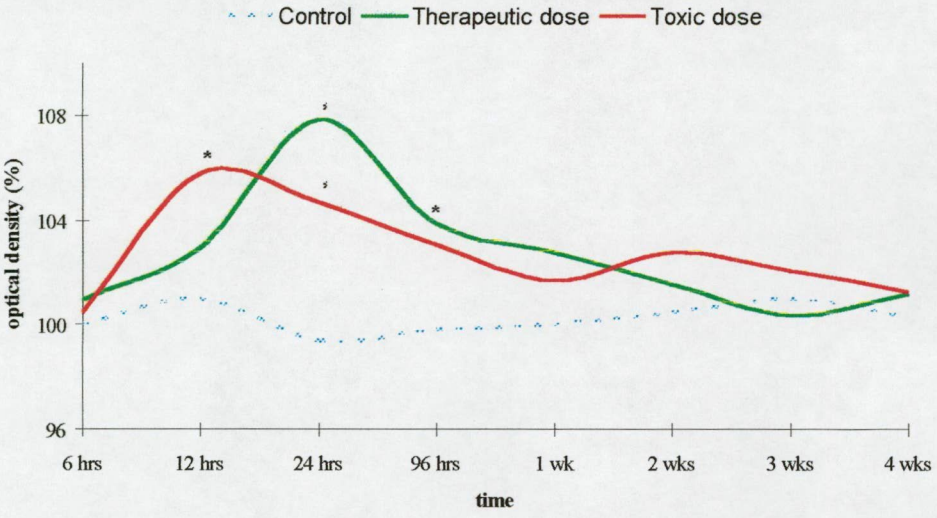

Time-course of RISP on rat cortical APP concentrations
The flow-chart delineates the effect of the typical antipsychotic drug on the APP metabolism in an acute or chronic time-frame. RISP did not significantly interfere with the APP-levels either in therapeutic or toxic doses.

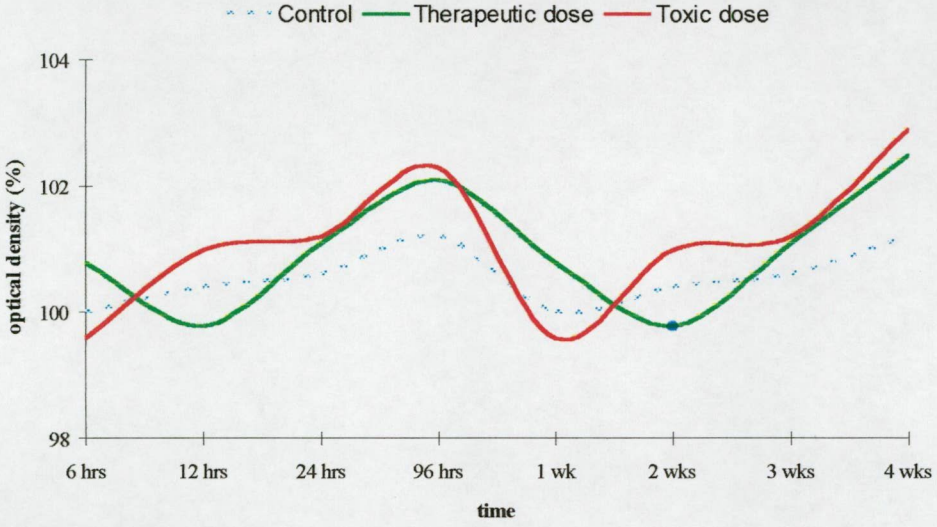

3. **Gene expression profile.** HAL significantly over-expressed 8 and repressed 6 genes, whereas RISP induced the expression of 7 and down-regulated 27 genes in a cDNA microarray system containing 8,000 clones. QRT-PCR results were in accordance with the expression of these genes, and therefore the semi-qualitative results of cDNA-micro-chips were validated.

Of the significantly altered transcripts, only genes involved in AD or directly linked to this thesis (*ie*. ionic homeostasis and protein metabolism), and those with a Δ *Fold* > 2.00 are listed in the following tables.

List of differentially expressed genes in rat fronto-temporo-parietal cortex after acute (96 hours) treatment with HAL. A: over-expressed, and B: repressed genes

A:

Clone name (mRNA)	Δ Fold (mean)	Accession number	Functional group
Rattus norvegicus cDNA clone, similar to Human B12 protein mRNA	1.96	AA900186	Ion transport
S100 calcium-binding protein A8 (calgranulin A) (S100A8)	1.41	NM_053822	Ion transport
Glutamate receptor subunit GluR2-flip mRNA, complete cds	1.22	AF164344	Ion transport
Calmodulin 2, mRNA, complete cds	1.13	BC058485	Ion transport
Rattus norvegicus APP770 mRNA, complete cds	1.76	AF513015	Other

B:

Clone name (mRNA)	Δ Fold (mean)	Accession number	Functional group
Serotonin N-acetyltransferase	-2.15	NM_012818	Circadian rhythm
Inwardly rectifying K^+-channel	-1.89	D61687	Ion transport
Voltage-dependent calcium channel γ-7 subunit (Cacng7) mRNA, complete cds	-1.21	AF361349	Ion transport
Tyrosine aminotransferase	-2.68	NM_012668	Metabolism
Disintegrin and metalloprotease domain 2	-2.15	NM_020077	Protein metabolism
Type I pro-α_2 collagen-like sequence	-3.25	AF050214	Other
TPCR09 protein	-2.07	X89698	Other

List of differentially expressed genes in rat fronto-temporo-parietal cortex after chronic (4 weeks) treatment with HAL

Clone name (mRNA)	Δ Fold (mean)	Accession number	Functional group
K^+-channel (erg2)	1.11	AF016192	Ion transport

List of significantly A: induced, and B: down-regulated genes in rat fronto-temporo-parietal cortex after acute (96 hours) treatment with RISP

A:

Clone name (mRNA)	Δ Fold (mean)	Accession number	Functional group
Plakoglobin	2.20	U58858	Cell adhesion
RING finger protein	2.07	AF036255	Development
Small inducible cytokine subfamily A20	2.31	NM_019233	Immune response
RAB15	2.24	M83679	Protein metabolism
ryk-tyrosine kinase-related protein	2.67	AB073721	Protein metabolism
CLN2 tripeptidyl peptidase I	2.35	AB043870	Protein metabolism
K^+-channel (erg2)	2.08	AF016192	Ion transport
Na^+-channel, voltage-gated, type 10a	1.01	NM_017247	Ion transport
Vacuolar adenosine triphosphatase-β	1.40	Y12635	Ion transport
ATPase, Na^+/K^+ transporting, α_1	2.00	NM_012504	Ion transport
Acyl-Coenzyme A dehydrogenase, C-4-12	2.13	NM_016986	Metabolism
Activating transcription factor 3	2.50	NM_012912	Transcription regulator
SH-PTP2 protein tyrosine phosphatase 11	2.74	NM_013088	Signal transduction
Interleukin 6 receptor	3.12	NM_017020	Signal transduction
Endothelin receptor	2.04	NM_017333	Signal transduction
Integrin-binding sialoprotein	2.14	NM_012587	Others
Neurexin IIIα (axon guidance)	2.84	L14851	Others

B:

Clone name (mRNA)	Δ Fold (mean)	Accession number	Functional group
CD5	-2.60	X78985	Cell adhesion
Activity regulated cytoskeletal-associated protein	-2.31	NM_019361	Development
Protein phosphatase 1, regulatory 14a	-2.61	NM_130403	Immune response
Disintegrin and metalloprotease domain 2	-2.15	NM_020077	Protein metabolism
Voltage-dependent calcium channel g8	-2.21	NM_080696	Ion transport
Plasma membrane CA^{2+}-ATPase 3	-1.47	M96626	Ion transport
Inwardly rectifying K^+-channel	-2.32	D61687	Ion transport
γ-glutamylcysteine synthetase	-2.12	NM_017305	Metabolism
Interleukin 10 receptor-α	-2.68	NM_057193	Signal transduction
Basignin (Ox47 antigen or CE-9)	-2.02	NM_012783	Signal transduction
Soluble adenylyl cyclase (SAC)	-2.37	AF081941	Transport
Type I pro-α_2 collagen-like sequence	-3.77	AF050214	Others
Putative zinc-finger protein	-3.40	AJ007467	Others
U2 RNA 3' end	-2.63	M10882	Others
Glucagon (Gcg)	-2.17	NM_012707	Others

List of significantly A: up-regulated, and B: repressed genes in rat fronto-temporo-parietal cortex after chronic (4 weeks) treatment with RISP

A:

Clone name (mRNA)	Δ Fold (mean)	Accession number	Functional group
Protein phosphatase 1, regulatory 14a	2.30	NM_130403	Immune response
Receptor activity modifying protein 2	3.35	AB042888	Signal transduction

B:

Clone name (mRNA)	Δ Fold (mean)	Accession number	Functional group
Inwardly rectifying K^+-channel	-1.65	D61687	Ion transport
Uncoupling protein 2, mitochondrial	-1.25	NM_019354	Ion transport

Other than the above transcripts, a number of genes involved in metabolism in general (*eg.* glutathione S-transferase), cell cycle (*eg.* growth accentuating protein 43), adhesion (*eg.* integrin β_1), immune response (*eg.* T-cell receptor α-chain), and others (*eg.* FSH-regulated protein) were also differentially expressed.

DISCUSSION

1. **Calcium homeostasis.** Alzheimer lymphocytes maintain increased, whereas Alzheimer fibroblasts show decreased resting intracellular calcium levels when compared to their respective control counterparts. Exposure to βAP results in elevated calcium concentration in control samples, however both Alzheimer lymphocytes and fibroblasts appeared to be refractive to βAP. On the long-run, βAP had a time-dependent biphasic-effect by initially increasing calcium-levels, but chronically antagonizing it in control fibroblastic cultures. This novel finding, and the fact that lymphocytic turnover is higher than that of fibroblasts, give an explanation between the differential resting calcium levels in the cell-types studied. Both HAL and RISP have proved to efficiently antagonize βAP-induced calcium imbalance in fibroblasts without directly interfering with calcium homeostasis.

2. **APP-levels.** The levels of APP have been significantly increased after acute HAL treatment only in both therapeutic and toxic doses. Chronic administration of HAL and treatment with RISP in general had no impact on APP metabolism. By being a calcium-antagonist, HAL may prevent APP-processing from shifting to the amyloidogenic pathway, therefore it prevents βAP formation and, in turn, precludes calcium imbalance in a process that might be referred to as "protective cycle."

3. **Gene expression profile.** The expression of several genes was interfered with in this study in a similar manner by HAL and RISP. Members of signal transduction, structural elements, factors related to protein metabolism in general, components involved in cell survival, determinants of membrane conductance and ion transport, and basics of nuclear functions, were some of the genes with altered expression.

CONCLUSIONS

1. *Fibroblasts and lymphocytes show biochemical differences in AD by exhibiting abnormal Ca^{2+} homeostasis.*
2. *Biphasic effect of βAP may shed new light on understanding cellular alterations in dementia and differences between tissue-specific pathologies in the same condition.*
3. *Biochemical alterations in the periphery may support the diagnosis of AD, may help monitoring the progression of the disease and responsiveness to treatments.*
4. *HAL and RISP are potent in antagonizing βAP-induced Ca^{2+}-imbalance.*
5. *These antipsychotics are safe with respect to APP metabolism, and acute HAL (ie. pulse-therapy) might be beneficial on APP processing in AD.*
6. *A "protective cycle" of antipsychotics is proposed in AD.*
7. *HAL and RISP are involved in interfering with the expression of a large array of genes involved in Ca^{2+}-signaling, survival and cellular plasticity.*
8. *Antipsychotics with different pharmacological characteristics share targets at the molecular level, including Ca^{2+}-homeostasis.*
9. *Ca^{2+} is central in the pathogenesis of AD, and agents targeting Ca^{2+} may slow or inhibit the progression of and might even reverse AD and its corollary symptoms.*
10. *Ca^{2+} might be a unifying molecule in most neurodegenerative disorders and also in metabolic diseases afflicting extraneuronal organs.*

BIBLIOGRAPHY

Cumulative impact factor:
64.573

Number of publications:
22

List of articles relevant to this thesis

Palotás A, Penke B, Palotás M, Kenderessy SzA, Kemény L, Kis E, Vincze G, Janka Z, Kálmán J. Haloperidol attenuates β-amyloid-induced calcium imbalance in human fibroblasts. Skin Pharmacol. Physiol. 2004; 17: 195-199.
Impact factor (2003): 1.529

Palotás A, Pákáski M, Palotás M, Hugyecz M, Molnár J, Penke B, Janka Z, Kálmán J. Effect of haloperidol and risperidone on amyloid precursor protein levels *in vivo*. Brain Res. Bull. 2003; 62: 93-99.
Impact factor: 2.609

Palotás A, Janka Z, Penke B, Kálmán J. Risperidone antagonizes β-amyloid peptide-induced intracellular calcium level changes in fibroblasts. Neuropsychopharm. Hung. 2003; V/3: 138-142.
Impact factor: 0

Palotás A, Kálmán J, Palotás M, Kemény L, Janka Z, Penke B. Long-term exposition of cells to β-amyloid results in decreased intracellular calcium concentration. Neurochem. Int. 2003; 42: 543-547.
Impact factor: 3.261

Palotás A, Kálmán J, Palotás M, Juhász A, Janka Z, Penke B. β-amyloid-induced increase in the resting intracellular calcium concentration gives support to tell Alzheimer lymphocytes from control ones. Brain Res. Bull. 2002; 58: 203-205.
Impact factor: 2.283

Palotás A, Kálmán J, Laskay G, Juhász A, Janka Z, Penke B. Comparative studies on $[Ca^{2+}]_i$-level of fibroblasts from Alzheimer patients and control individuals. Neurochem. Res. 2001; 26: 817-820.
Impact factor: 1.638

ACKNOWLEDGEMENTS

First of all, the active participation of the *volunteers* in the ongoing study is highly appreciated.

I thank *Dr. Gábor Laskay* for always giving me a helping hand in understanding the pickiest details of fluorimetric studies. He taught me everything I will ever know about spectrofluorimetry. Sharing his teaching and research experiences with me has been a springboard for my scientific career.

I am grateful to *Prof. Dr. Lajos Kemény, Dr. Anna Kenderessy-Szabó* and their colleagues at the Department of Dermatology, University of Szeged, Hungary, for providing me with the skin samples and fibroblast cultures.

I would also like to thank my colleagues at the Department of Experimental Surgery, University of Szeged, Hungary, in granting me unlimited access to the Hitachi F-2000 spectrofluorimeter.

I acknowledge the assistance of each and every co-workers at the Alzheimer's Disease Research Center, University of Szeged, including *Prof. Dr. Péter Kása, Dr. Magdolna Pákáski, Marietta Hugyecz* and colleagues. The assistance and friendship of *László Kálmán* of the same institute is highly valued.

I am indebted to *Dr. László G. Puskás* and his colleagues of the Laboratory of Functional Genomics, Biological Research Center of the Hungarian Academy of Sciences, for assisting in the cDNA-micro-chips.

I am gratified that my clinical directors, *Prof. Dr. György Lázár* of the Department of Surgery and *Dr. Gábor Bogáts* of the Division of Cardiac Surgery, University of Szeged, Hungary, permitted me to conduct this research parallel with my daily routine in cardiac surgical patient care.

I am obliged for the co-operation of the staff of the Department of Psychiatry, University of Szeged, Hungary. I also appreciate *Dr. Anna Juhász* for her assistance in taking care of the biological samples and cultures. Predominantly, I owe gratitude with deepest respect to *Prof. Dr. Zoltán Janka* and *Dr. János Kálmán* for their scientific partnership, helping hand, encouragement, incessantly magnificent aid, lift, moral support, and friendship.

Above all, words cannot convey how thankful I am to *Prof. Dr. Botond Penke* of the Department of Medical Chemistry, University of Szeged, Hungary, for his contribution to this work in endlessly giving perpetual advice, hand, comfort, care, encouragement, and for being the most sincere counterpart & friend of mine I have ever worked with.

My admiration to my family and loved ones for closing ranks behind me all my life, and to my brother, *Dr. Miklós Palotás*, of the Department of Anesthesiology and Intensive Therapy, University of Szeged, Hungary, for collaborating with me throughout this study is self-explanatory.

I would also like to express my gratefulness to my fellow scientific colleagues and friends, *Dr. Yoo-Hun Suh* of Seoul National University, South Korea, *Dr. Mark P. Mattson* at the National Institute on Aging, USA, *Dr. Jefferey L. Cummings* of UCLA School of Medicine, USA, and *Dr. Alexei Koudinov* of the Russian Academy of Sciences, Russia, for permitting me to reproduce some of their theoretical work in this thesis, and for giving me future directions.

Finally, I highly value the assistance of all of my work-mates whom are not listed here by name.

BiochemiCa^{2+}l studies in Alzheimer's disease: the *APP*arent diagnostic and therapeutic role of antipsychotics on calcium homeostasis and amyloid-precursor-protein metabolism

ANDRÁS PALOTÁS, M.D.

Ph.D. THESIS

UNIVERSITY OF SZEGED
2004

TABLE OF CONTENTS

INTRODUCTION

Clinical aspects of Alzheimer's disease

Each year millions of people go through a stage of mental deterioration in which their ability to remember gradually fades. At certain stages of the disease a simple task that is taken for granted, such as how to make a phone call, becomes insurmountable. Most of the people who are afflicted with this illness are elderly, but their symptoms are not caused by their aging. After three to ten years from the onset of the disease the patients become unable to recognize close relatives. Eventually fading remembrances slowly destroy their emotional balance, their sense of judgment, and their personal identity. Due to their inability to support themselves they gradually become bedridden. Complications arising from this vegetative state ultimately lead to death.

In the early 1900's the symptoms of this disorder were recognized by a German psychiatrist, Alois Alzheimer, for whom this disease is named[1]. Scientists have recently made major advances in understanding the mechanism which triggers the illness. The ultimate goal of Alzheimer research is to elucidate the pathway underlying the massive neuronal death seen in the brain with this syndrome leading to this specific kind of dementia – a condition denoting a progressive decline in mental function, in memory, and in acquired intellectual skills. About 70% of dementia cases are due to Alzheimer's disease (AD).

AD is a major public health problem secondary to the increased life expectancy of the general population and a better appreciation of the socio-economic consequences of the disease. AD is a disease with several million living victims worldwide[2]. With an annual incidence of about more than half a million cases, and given the aging of the population, improvements in life expectancy, and in treatment of AD, the prevalence of this condition will quadruple in the next 50 years[2].

A definitive diagnosis of this disorder requires pathological examination of the brain, but diagnosis on clinical grounds according to the *Diagnostic and Statistical Manual of Mental Disorders, 4th Edition (DSM-IV)* criteria[3] alone is correct in the majority of cases, especially if other causes have been ruled out. Neuropathological examination from autopsy studies suggests a 90% accuracy rate in the clinical detection of AD[4].

Computerized tomographic (CT) and magnetic resonance imaging (MRI) of the brain of Alzheimer patients show thin cortical gyri of the postero-temporal and postero-parietal lobes (*ie.* brain atrophy), enlarged (lateral) ventricles, and atrophy of the hippocampus. These findings are not specific, however, since other conditions may also produce atrophy of the brain. Furthermore, there is some degree of atrophy in normal aging[5,6].

Dementia in AD steadily worsens, with a loss of 3 to 4 points per year on a standard assessment instrument such as the Mini-Mental State Examination (MMSE)[7]. Various patterns of deficits are seen, with the most common being an insidious onset, with recent memory loss followed by the development of aphasia, apraxia, and agnosia after several years. Some patients present with irritability and personality changes in the early stages. Later during the course of the disease, patients usually develop gait and motor disturbances, eventually becoming mute and bedfast. On average, AD patients live for 8 to 10 years after they are diagnosed, although the disease can last for up to 20 years[8].

In addition to debilitating the patient, AD impacts on families. This impact is emotional, with caregivers experiencing depression, guilt, anger, and physical stress leading to caregiver frailty, as well as economic consequences, with costs of care in the tens of thousands of dollars per year[9,10].

Histopathological findings in AD

The formation of senile plaques in the brain is a main pathological feature of AD. These plaques contain deposits of a 38-43-amino-acid protein-residue, called the β-amyloid peptide (βAP)[11]. In the presence of senile plaques neurites (*ie.* neuronal processes: the dendrites and axons) degenerate; ultimately brain cells necrotize. The dystrophic neurites and cells surround the senile plaques and together they are referred to as the neuritic plaques[12]. This morphological characteristic has led to the speculation that the amyloid masses, particularly the presence of βAP in the extracellular space cause the death of adjacent neurons.

Apart from forming the senile plaques, β-amyloid fibrils are deposited along the walls of the cerebral and meningeal vascular system, too, causing vascular amyloid angiopathy[13].

Another microscopic hallmark of AD is the profound neurodegeneration in the frontal, temporal and parietal cortices. A variety of neurochemical deficits affect the serotonergic, noradrenergic, and cholinergic systems[14]. The cholinergic deficit of AD is well documented; there is a marked loss of neurons in the basal forebrain nuclei (particularly in the Meynert's nucleus) that usually exceeds 75% of the total neuronal population at the time of an autopsy[15].

Cytopathological manifestation of AD is the presence of paired helical filaments (PHF) within the brain cells[16]. These intraneuronal filaments aggregate and form neurofibrillary tangles (NFT)[17]. This amorphous material is assembled from an abnormally phosphorylated and transformed cytoskeletal protein called *tau* (τ)[18]. Normally, *tau* plays an important role in stabilizing microtubules and thus helps to maintain neural vesicular transport. The most conspicuous effect of the phosphorylation of *tau* is the decrease in its binding capacity to the microtubules. This causes a loss of axonal transport, since microtubules provide the tracks for vesicle traffic driven by motor proteins.

β-amyloid peptide

βAP is derived from the highly regulated and sequential cleavage of amyloid precursor protein (APP) as a normal physiological product[19,20]. It is a soluble component at nanomolar concentrations of the plasma and the human cerebrospinal fluid (CSF)[21] as a range of isoforms between 38 and 43 amino acids in length.

The presence of βAP under normal conditions suggests the possibility of a physiological role for βAP. βAP may serve an essential role in synapse and synaptic plasticity that underlie learning and memory[22,23]. A role for βAP in neural and synaptic structure-functional plasticity is additionally supported by an increase of synaptic APP with learning capacity[24], by neuronal activity dependent secretion of natural βAP[25], and up-regulating a synaptic vesicle protein transcript by $βAP_{1-42}$[26].

Because soluble βAP is apparently a physiological peptide, it was proposed that the key to the cellular toxicity of βAP appears to be proportional to its aggregation state[27]. The aggregation of soluble βAP peptide into fibrillar cross-β pleated-sheet conformation to form oligomers, polymers or protease-resistant fibrils over time is generally considered to be a critical event in the pathology of AD[28]. This is signified by the finding that the predominant carboxyl-terminal isoforms in CSF of healthy individuals are $βAP_{1-40}$ (90%) and the fibrillogenic $βAP_{1-42}$ (10%). In patients with AD, however, the relative proportions of 1-40 and 1-42 change to ~50% each[29]. Moreover, $βAP_{1-42}$ is the major component of amyloid deposits in brain with AD[30].

Interestingly, βAP deposition has been observed in various brain areas without accompanying neurodegeneration[31,32,33], whereas neurodegeneration can occur in areas with no βAP deposition[34]. Therefore, attention is turning away from the deposits of extracellular insoluble aggregated amyloid

in plaques and toward soluble, oligomeric and even intracellular βAP[35,36]. Accumulation of intracellular βAP ($βAP_i$) and preamyloid protrofibrils are being recognized as a contributing factor or initiating event towards neuronal death and synaptic loss in early AD pathogenesis[37].

The theory that βAP plays a key role in neurodegeneration in AD has been proven both *in vivo* and *in vitro*[38,39,40], leading to the "amyloid cascade" hypothesis[41,42]. The neurotoxicity exerted by aggregated βAP can be mediated by several mechanisms.

Several reports suggest that the neurotoxic effects of βAP are mediated by the disruption of calcium homeostasis, resulting in increased neuronal intracellular calcium levels ($[Ca^{2+}]_i$)[43,44]. βAP is a potent L-type voltage-gated calcium-channel activator[45], and causes reduction in the activity of Na^+/K^+-ATPase[46], Na^+/Ca^{2+} exchanger[47] and K^+-channel[48]. βAP is also proved to directly form non-selective calcium-channels[49]. Neurons exposed to βAP exhibit calcium responses sensitive to excitatory amino acids and membrane depolarization: enhancement of glutamate-mediated excitotoxicity[50] adds to the elevated calcium-levels.

When in an aggregating form, βAP induces membrane lipid peroxidation by generating reactive oxygen species[51,52,53]. The increased ROS and intracellular calcium levels induced by βAP impair mitochondrial function and can trigger a programmed cell death process called apoptosis[54,55,56].

Early association of activated microglial cells and reactive astrocytes in neuritic plaques and the appearance of inflammatory markers indicate a state of chronic inflammation in AD. Immune activation and/or inflammatory activity have been shown to be significantly elevated in the brains of AD patients[57]. Microglia and astrocytes would be activated, perceiving βAP oligomers and fibrils as a foreign material, because these kinds of βAP assemblies are apparently never observed during brain development and in the immature nervous system[58]. βAP also directly activates the complement system[59]. The importance of the inflammatory component to the disease mechanism is supported by the consistent finding that anti-inflammatory drugs have a beneficial effect on disease progression.

Extracellular interaction of β-amyloid aggregates with cell membranes could induce a wide variety of alterations through numerous potential target sites that are consistent with the pathological activation of signal transduction. These include the mitogen-activated protein kinase (MAPK), calpain, cyclin-dependent kinase-5 (cdk-5), glycogen synthase kinase-3β (GSK-3β), and tyrosin kinase Src pathways[60,61]; by progressive and sustained activation thereof, βAP induces tyrosine phosphorylation of numerous neuronal proteins, including *tau* and microtubule-associated protein-2c (MAP-2c)[62].

The calcium theory in AD

Calcium plays fundamental roles in the development, function, and plasticity of nerve cell circuits[63]. The regulation of Ca^{2+} dynamics in neurons is very complex, involving proteins localized in essentially all major subcellular structures including the plasma membrane, cytosol, mitochondria, and endoplasmic reticulum[64]. The concentration of Ca^{2+} outside the cell (1-2 mM) is 10,000-fold higher than in the cytosol (50-200 nM), and this concentration gradient is maintained largely by removal of Ca^{2+} from the cytoplasm by plasma membrane and endoplasmic reticulum (ER) Ca^{2+}-ATPases.

Pathophysiologically, interfering with the intracellular ionic homeostasis of neurons is thought to be one of the most conspicuous brain cell destroying activities of βAP[43]. Destabilization of Ca^{2+} homeostasis in neurons plays a central role in AD pathogenesis[44]. In the presence of the peptide, the intracellular calcium concentration of cells has been reported to increase through various, but not fully understood mechanisms, including the putative calcium channel activity of βAP[49], or its

interaction with membrane structures. Measurements of calcium concentrations in brain tissue from AD patients reveals evidence for increased overall levels (free and protein-bound) of calcium[65]. Levels of activated calcium-dependent enzymes and proteases are also increased[66].

Increase in the calcium concentration due to βAP is balanced by pumping out the excess. This feature expends a large amount of the cells' energy, preventing them from providing for their own physiological and biochemical pathways any longer. Concentration of ROS will then increase which may further damage cells. The effects disable cells to control their fluid and ion balance. Water and charged particles (especially even more Ca^{2+}) that are normally pumped out now stream in. Additionally, alterations in intracellular Ca^{2+}-levels are known to induce cell loss by apoptosis, a degenerative pathway typically associated with gene-directed cellular suicide termed programmed cell death. Neurons that are meant to last a lifetime can be transformed at an early stage to this form of death.

β-amyloid-precursor-protein

β-amyloid peptide derives from the proteolytic processing of its precursor, the β-amyloid-precursor-protein (APP)[67]. Full-length APPs are considered integral membrane glycoproteins containing a large extracytoplasmic domain, a transmembrane region, and a small cytoplasmic sequence[68]. The APP spans the cell membrane between amino acids 700-723. The β-amyloid site is represented by the amino acids 672-713; that is, the C-terminal of βAP takes part in forming the transmembrane region.

In mammals, the APP protein is expressed ubiquitously in all tissues examined including neurons, glias, and non-neuronal cells[69,70], including fibroblasts[71], but there are differences in the expression levels of the splicing variants. Alternative splicing of the APP gene gives rise to at least 10 protein isoforms. Three of them known to contain βAP are APP_{770} (full-length APP), APP_{751} (minus exon 8) and APP_{695} (minus exons 7 and 8). Exon 7 encodes the Kunitz protease inhibitor (KPI)[72]; KPI-containing APP isoforms are more amyloidogenic[73]. Neuronal cells predominantly express APP_{695}, whereas the $APP_{751/770}$ form is mainly expressed in non-neuronal tissues such as heart, lung, liver, kidney, muscle and spleen[74,75]. In the brain, APP is expressed with high levels in the hippocampal formation[76].

α-secretion

APP can undergo at least two post-translational processing pathways. In the non-amyloidogenic or normal pathway, constitutively secreted APP (referred to as sAPPα), lacking the transmembrane and cytoplasmic sequences, is produced after full-length molecules are cleaved by an enzyme called α-secretase between amino acids Lys_{16} and Leu_{17} of the β-amyloid sequence[77] (between the amino acid 687-688 of the full-length precursor protein). Because sAPPα is produced after full-length molecules are cleaved by the α-secretase within the β-amyloid sequence, this cleavage event is incompatible with the production of the neurotoxic β-amyloid (Figures 1, 2).

sAPPα has several neuroprotective properties. sAPPα protects neurons from ischemic injury[78,79], has effects on ion fluxes[80], stimulates neurite outgrowth[81], promotes proliferation[82], cell survival[83], and protects neurons from oxidative, excitotoxic[84] and metabolic, including βAP[85]-induced insults. Regarding signal transudation pathways, sAPPα is implicated to play a role in activation of neuroprotective NF-κB-dependent transcription[86], phospholipase C – protein kinase C (PKC) and inositol trisphosphate (IP_3)[87] pathways.

Figure 1: Amino acid sequence of APP in the βAP region

Sites of proteolytic cleavage by α-, β-, and γ-secretases are shown. Mutations in APP which cause familial forms of AD or a related amyloidosis are also presented. βAP region within the precursor protein is highlighted.

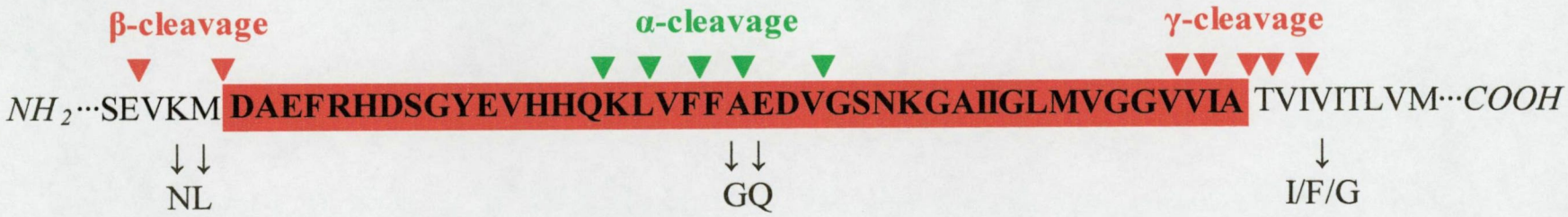

Figure 2: Schematic diagram of APP and its principle metabolic derivatives

The figure depicts the largest of the known APP alternate transcripts, comprising 770 amino acids. Regions of interest are indicated at their correct relative positions. A single membrane-spanning domain at amino acids 700-723 is indicated by the horizontal hatched bars. The βAP fragment (red box) includes 28 residues just outside the membrane plus the first 11-15 residues of the transmembrane domain. The left lower diagram indicates the site of the constitutive proteolytic cleavage that enables secretion of the soluble ectodomain of APP (sAPPα) and retention of the 83-residue C-terminal fragment (~10kDa) in the membrane (CTFα). This non-amyloidogenic processing of APP by α-secretase precludes βAP-formation. The right lower portion of the diagram depicts the alternative proteolytic cleavage by β-secretases that results in the formation of sAPPβ (an ectodomain similar to sAPPα), and a potentially neurotoxic ~12kDa C-terminal fragment (CTFβ), which serves as an intermediate in the generation of βAP. A subsequent γ-cleavage after the α- or β-secretion yields non-toxic p3 and neurotoxic βAP, respectively. As a by-product of the γ-activity, non-toxic CTFγ is formed, which is subject to ε-cleavage.

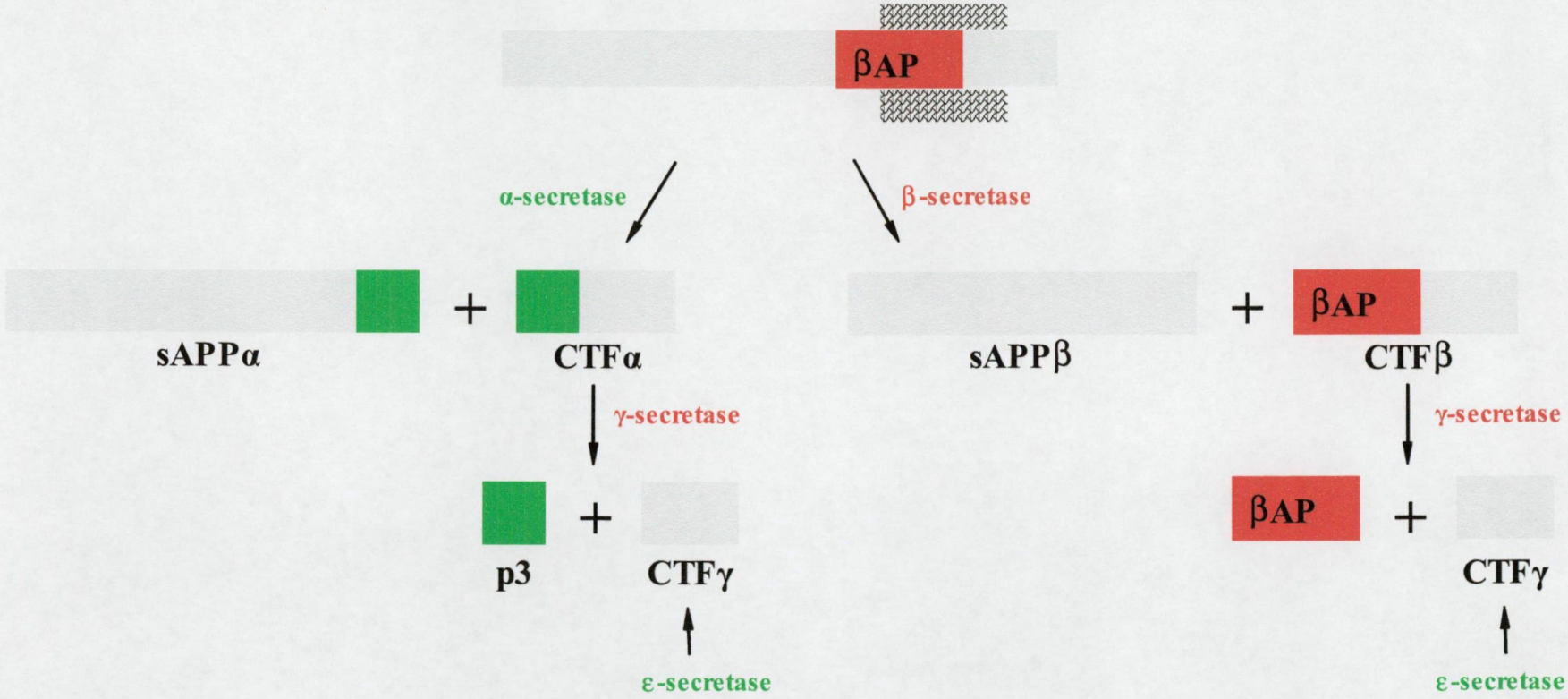

β-secretion
βAP is derived from the highly regulated and sequential cleavage of APP by proteases designated β-secretase and γ-secretase. This amyloidogenic β-secretion pathway is an alternative of normal APP processing, involving cleavage of APP by β-secretase adjacent to the N-terminal residues of the βAP sequence. β-secretase generates the N-terminus of βAP, cleaving APP to produce a soluble version of the precursor (sAPPβ) and a 99-amino-acid residue C-terminal fragment that remains membrane bound (CTF_{99}, or CTFβ).

γ-secretion
Cleavage after β-secretion by a subsequent γ-secretase at position 40, 42 or 43 of the βAP sequence within CTFβ results in the release of neurotoxic βAP, a 4kDa derivative from APP[88], and a remaining 57-59 residue C-terminal tail: CTFγ (Figure 2). In addition, cleavage of the by-product of α-secretion, CTF_{83} (CTFα) by γ-secretase yields non-pathogenic derivative referred to as *p3* and CTFγ. In contrast with α-secretion that almost exclusively occurs in the plasma membrane, APP may be internalized and processed in the endosomes (proteasomes/lysosomes) during sequential β/γ-secretion to produce βAP.

γ-activity is heterogeneous: most of the full-length βAP species produced is a 40-residue peptide ($βAP_{1-40}$), whereas a small proportion is 42-43-residue C-terminal variant ($βAP_{1-42/43}$). The longer and more hydrophobic $βAP_{1-42/43}$'s are much more prone to fibril formation than is $βAP_{1-40}$[89], and even though $βAP_{1-42}$ is a minor form of βAP, it is the major βAP species found in cerebral plaques[90]. Moreover, γ-secretase has remarkably loose sequence specificity for its substrate because many mutations in APP near the γ-secretase site still allow βAP production.

Identifying γ-activity revealed that γ-secretase is a multimeric entity: presenilins (PS), nicastrin, Aph1 and Pen2 generate an active γ-secretase complex.

Presenilins (PSs) may be the active center of γ-activity. γ-secretase has been demonstrated to have an acidic pH optimum, consistent with the notion that the presenilins are intramembranous aspartyl proteases[91]. Also, PSs are chaperoning molecules that may bring APP to the proximity of γ-secretase.

The missense mutations in the gene encoding APP, as well as those in the genes encoding PS1 and PS2, share the common feature that they alter the γ-secretase cleavage of APP to increase the production of the amyloidogenic $βAP_{1-42}$[92].

Behavioral and psychological symptoms of dementia (BPSD)
AD is characterized clinically by decline in memory and cognitive functions, however manifestations of BPSD, including psychosis, delusions, hallucinations, agitation, *etc.* during the course of the disease are significant events[4-7]. Their frequency ranges from 50 to 90% and they can occur at any point in the disease process, often being the presenting symptom. The number and severity of behavioral problems increase with worsening of cognitive impairment[93]. BPSD can be mainly grouped into behavioral and psychological symptoms of dementia disorders. The former are usually identified on the basis of patient observations, while the latter are mainly assessed on the basis of interviews with patients and relatives[94].

Interestingly, AD pathology is infrequent in patients with schizophrenia (SCH)[95,96]. It has been proposed that medications used to treat SCH, such as haloperidol (HAL), might have a protective effect against developing AD neuropathology, which would account for a low frequency of these changes in elderly SCH. The mechanism by which antipsychotic drugs might exert such an effect is not known.

A systemic approach to neurometabolic disorders

β-amyloid is reported to be ubiquitously present in the body[97], and has every now and then been demonstrated to form depositions in the skin of Alzheimer patients[98], presumably interfering with intracellular biochemical pathways of peripheral tissues. Indeed, several alterations in the blood of AD patients have been reported. In lymphocytes, changes in ionic and signal transduction pathways[99], elevated number of apoptotic peripheral mononuclear cells[100], increased vulnerability to programmed cell death[101] and raised levels of oxidative DNA damage[102] was reported. With respect to platelets, disrupted membrane fluidity[103,104], hypofunction of mitochondrial enzymes[105], and modified activation of cells[106] have been found. Dysfunctions of red blood cells including decreased erythrocyte AchE activity are also observed[107]. In case of fibroblasts, disturbances of Ca^{2+}-uptake[108], ionic homeostasis[109], glucose metabolism[110], proteolysis[111], signal transduction[112] and DNA repair[113] are some of the biochemical changes reported in AD.

Apart from brain-specific changes, abnormalities attributed to AD seen in many peripheral cell types such as erythrocytes, lymphocytes, platelets and fibroblasts have lead to the speculation that AD might be a systemic disorder, with the most prominent pathology in the cognitive functions of the CNS.

A substantial body of data exists indicating that biochemical changes of brain cells in various neurobiological diseases with systemic manifestation are reflected in peripheral tissues, such as fibroblasts and lymphocytes[114,115]. In the course of surveying a wide variety of these mirror changes, previous reports have proved that fibroblasts and lymphocytes can serve as models and diagnostic markers of several neurodegenerative disorders, including metachromatic leucodystrophy, Tangier's disease, and generalized glycogenosis[114,116].

Lymphocytes and cultured fibroblasts offer many advantages for the study of various pathobiochemical alterations in AD. These pathways are more robust in these living cells than in postmortem material, such as brain, and the results are not complicated by agonal or postmortem events[117].

OBJECTIVES OF THE STUDY

1. **Involvement of the periphery in AD**
   The identification of the mirror shifts in AD described in the *introduction* has been of my interest. The aim was to study whether readily available tissues such as fibroblasts and lymphocytes may serve as simple supportive systems to monitoring intracellular ionic imbalance, particularly that of the basal intracellular free calcium levels ($[Ca^{2+}]_i$) in AD. Broadly in line with this hypothesis, the present communication summarizes techniques which have been used to study the biochemistry and physiology of skin fibroblasts and lymphocytes isolated from patients with certain neurometabolic disorders including AD. Consistent with this, alterations in calcium homeostasis of fibroblasts and lymphocytes associated with AD are discussed in the present thesis.

2. **Pharmacological studies**
   Several investigators have found a low frequency of AD in patients with SCH, and it has been proposed that antipsychotic medications may be responsible[95,96].

   The prototype classical antipsychotic HAL is dopamine-2 (D_2) and sigma-1 (σ_1) receptor antagonist with apoptotic activity[118,119,120]. HAL is involved in neurotoxicity, causing clinically troublesome adverse events such as extrapyramidal and cardiac side-effects[121]. The "gold-standard" neuroleptic HAL has been reported to be a calcium and calmodulin antagonist[122], and was also demonstrated to efficiently inhibit βAP-formation from APP[123]. The mechanism by which it might exert such an effect is not known. However, HAL and other traditional antipsychotics have several adverse effects. Therefore, the use of atypical antipsychotics is taking over medical indications of conventional neuroleptics with very much success without notable side effects[124,125]. The widely used high-potential atypical antipsychotic risperidone (RISP) is a potent D_2-, $5HT_2$- and NA-antagonist with less adverse effects. RISP has no known effect on AD pathology, including APP metabolism.

   In light of evidence that HAL, one of the most frequently prescribed antipsychotic medications used in the treatment of SCH[126], interferes with Ca^{2+}-homeostasis[122] and APP processing[123], we evaluated it for its effects on βAP-induced Ca^{2+}-imbalance *in vitro* and its role on APP metabolism. To gain more insight on its cellular effects at the molecular level, we have also studied its role on gene expression *in vivo*. In the course of surveying a wide variety of agents directed against βAP-toxicity, we also examined RISP with respect to $[Ca^{2+}]_i$, APP and gene expression profile.

EXPERIMENTAL PROCEDURES

Participants

- *Demographics*

Primary cultures of human fibroblasts and suspension of lymphocytes were obtained and prepared from forearm skin-biopsies and blood samples after informed consent from participants. Sporadic AD patients of late-onset and age-matched controls volunteered as donors (Table I).

Table I: Demographic data of participants

Sporadic late-onset AD patients and age-matched controls volunteered as donors. Selection of individuals was made after their informed consent. Fibroblasts were harvested from forearm excisional biopsies; lymphocytes were separated from venous blood samples drawn in the usual fashion.

	Studies on fibroblasts		Studies on lymphocytes	
	Age of donors (mean±SD)	*Number of volunteers*	*Age of donors (mean±SD)*	*Number of volunteers*
Control	71±8.8	8	66.8±10.2	12
AD	73±10.11	8	71±8.5	10

At the time of obtaining samples, every single individual was outpatient. The diagnosis of AD was made according to DSM-IV criteria[3]. All AD donors met the DSM-IV definition of dementia of the Alzheimer's type, which requires evidence of cognitive deficits (criterion A) and a process of decline from previous levels (criterion C); none of them had history of familial AD. Control individuals were tested negative for any forms of dementia.

- *Medications*

None of the participants in our study received any medication known to interfere with calcium metabolism, such as antihypertensive drugs, calcium-antagonists, or antidepressants. None of the patients was on AchEIs before and during the measurements.

Culture methods

- *Fibroblast culturing*

For outgrowth of fibroblasts, small pieces of skin material were placed in cell culture flasks ($25cm^2$) and grown for 3-5 weeks in Dulbecco's modified Eagle's medium (DMEM) containing 5% of heat inactivated fetal calf serum (FCS) as well as penicillin (100 U/mL), streptomycin (100 µg/mL) and 2mM glutamate in a humidified atmosphere of 95% air and 5% of CO_2. Cells were detached for serial passaging using 0.01% of trypsin and 0.02% of EDTA. Stocks of each cell line (passage number: 5) were frozen to -80°C and stored at -130°C until use. After thawing and/or trypsinization, cells were used to seed on glass coverslips, 10mms in diameter, pretreated with collagene, in a 24-multiwell plate in the DMEM medium containing 5% of FCS. Cultures maintained in this way were generally confluent by day 7 and were used directly for measurements of $[Ca^{2+}]_i$.

To monitor the long-term effect of βAP, a single sample was used for chronic culturing. Here, the seeding-and-passaging cycle was repeated as needed. In short, after 7 days *in vitro*, cells developed a monolayer, and subcultures were provided by trypsinization.

All fibroblasts had a characteristic spindle-shaped appearance and were attached firmly to the coverslips.

- *Separation of lymphocytes*
Blood samples were gently layered on Ficoll solution, and were centrifuged at 1800 rpm for 20 mins. Lymphocyte-containing bands were rinsed with phosphate-buffered saline (PBS) three times. Cell concentration was estimated using Bürker's chamber. Lymphocytes in PBS were used for measurements of $[Ca^{2+}]_i$.

- *Viability*
Viability of cells was estimated by the method of intravital staining with Trypan Blue after exposition of cells to the preparation (0.2% Trypan Blue in Hank's balanced saline solution, HBSS). After 5 minutes of incubation in the solution, less than 2-3% of fibroblasts and lymphocytes absorbed the dye. In line with this finding we concluded that more than 97-98% of cells present in the cuvettes were viable.

- *Treatment*
Cells were cultured in the presence of 10^{-7}M, 10ng/mL [127,128] and/or 50μg/L [129,130] final concentrations of βAP, HAL and RISP, respectively. HAL and RISP – designated for intravenous use – were purchased commercially (Haloperidol®; *Gedeon Richter Ltd* and Risperdal®; *Ris-Int-63, Ref.No.: 336341; Janssen-Cilag, division of Johnson&Johnson Ltd., Hungary*, respectively) and were used directly on the cells without further purification or sterilisation. Final concentrations of these antipsychotics were calculated in accordance with their therapeutic blood levels.

Fibroblasts and lymphocytes used for control study were free of any treatment.

Measurements of $[Ca^{2+}]_i$

- *Fluorescence imaging*
$[Ca^{2+}]_i$'s were quantified by fluorescence ratio imaging of the calcium indicator dye Fura-2AM. Cells were incubated for 20-30mins at 37°C in the presence of 1μM of the acetoxy-methylester form of Fura-2AM. Cultures loaded with the dye were then washed twice with PBS solution and were transferred to cuvettes containing PBS at 25°C for measurements. Fluorescence imaging in standard 1×1cm cross section quartz cuvettes were performed with Hitachi F-2000 spectrofluorimeter. The ratio of the fluorescence emission of the cultures using two different excitation wavelengths of 340nm and 380nm, at emission wavelength of 495nm was applied to determine $[Ca^{2+}]_i$. Values of the 340/380 fluorescence excitation ratio at 495nm emission wavelength ($FL_{340/380}$), which represents the $[Ca^{2+}]_i$, were computed after each fluorescence measurement. In line with several papers examining calcium levels[43,114,131], the authors found the rate of the fluorescence ratios to be more informative of the change of the calcium-level than the absolute values of $[Ca^{2+}]_i$.

- *Validity of Fura-2AM labeling*
To check that loading of the cells with the dye and intracellular cleavage of the ester occurred, we sampled the fluorescence excitation ratios before and after loading the cultures with the dye. In case of fibroblasts, ratios of unloaded cells observed at 495nm were 10.67±3.26, around 3-times lower when compared to the ratio of 35.43±8.03 after incubation with the dye. As for lymphocytes, sampling of the fluorescence excitation ratios after incubation with the dye revealed 79.89±10.11, which represents a roughly 10-fold increase from the unlabeled ratio of 7.68±2.2. This is characteristic of Fura-2AM fluorescence.

No significant alteration was detectable among labeled cultures in Fura-2AM fluorescence using the calcium-insensitive excitation wavelength of 367nm, indicating that the observed response reflects a real change in the calcium-level of the cells.

- *Protein content of cultures*

Because gross alterations in the cell number/cell mass actually present in the cuvettes may interfere with the fluorescence intensities, the total protein content of the samples was determined according to Lowry et al[132]. Coverslips with control fibroblasts were found to contain 146.9±8.4μg protein/coverslip, whereas Alzheimer cells contained 139.1±5.1μg protein/coverslip. Protein content of control lymphocytes revealed 252.1±11.6μg protein/cuvette, and cultures of AD leucocytes contained 239.9±14.0μg protein/cuvette. This difference is not significant in statistical terms, suggesting that the total protein content of Alzheimer and control cells did not differ considerably.

- *Rationale of the effect of βAP, HAL and RISP*

During the experiments, the treated and control cell populations were cultured in media of identical composition except for the presence or absence of βAP, HAL and/or RISP. Therefore, it is reasonable to conclude that the observed difference in the 340/380 fluorescence excitation ratio of Fura-2AM-loaded cells is only associated with the presence or absence of the agents used, and hence can be regarded as an effect induced by βAP, HAL and/or RISP itself.

Synthesis and purification of βAP

- *Amino acids*

All amino acid derivatives, solvents, chemicals and the resins were obtained commercially and were used without further purification. Protected amino acids used in the syntheses were of the L-configuration. The α-amino function group was protected with tert-butoxy-carbonyl (Boc) group, and the reactive side chain functional groups were protected as follows: para-toluene-sulfonyl for Arg, cyclohexyl for Asp and Glu, benzyl-oxy-carbonyl for His, 2-chlorobenzyl-oxycarbonyl for Lys, benzyl for Ser, and 2-bromobenzyl-oxycarbonyl for Tyr. The side chains of Asn and Gln were unprotected.

- *Solid phase peptide synthesis*

βAP was prepared by solid phase methodology [133] using ABI-430A automated peptide synthesizer. For peptides with an amidated carboxy-terminus, para-methyl-benzhydryl-amine (MBHA) resin (0.57mmole/g) and for peptides with free carboxy-terminus Merrified resin (1mmole/g) was used. The coupling reactions were achieved with 3-fold excess of Boc-amino acids using DCC or DCC/HOBt as activating agent in dichloro-methane, dimethyl-formamide or a combination of thereof. Boc-Asn and Boc-Gln were coupled with preformed 1-hydroxy-benzotriazole ester to avoid side reactions. After a coupling time of 2 hours, the completeness of acylation was monitored at each stage by the standard ninhydrin test[134]. In cases where incomplete coupling was found, the coupling procedure was repeated, or the acetylation was carried out before the removal of the N-α-amino protecting group prior to the coupling of the next amino acid. Acetylation was performed with 30% of acetic anhydride in dichloro-methane for 10 and 20 minutes. Intermediate deblocking was achieved with 50% of trifluoro-acetic acid in dichloro-methane containing 0.5% of dithio-threitol followed by neutralization with 10% of triethyl-amine in dichloro-methane. Final deprotection as well as the cleavage of the peptides from the resin were performed with anhydrous hydrogen fluoride in the presence of 8% of anisol, 2% of dimethyl-sulfide, 2% of p-cresol, and 2% of thio-cresol at 0°C for 60 mins. After the removal of the hydrogen fluoride under a steam of nitrogen and *in vacuo*, the free peptides were precipitated with diethyl ether, filtered, washed with diethyl ether and extracted with 95% of TFA, diluted with water, and lyophilized.

- *Purification*

Crude peptides were purified by using a Shimadzu LC-8A preparative HPLC system equipped with Backbond WP-C4 column (300×47 mm, 300Å pore size, 15-20 μm particle size). The column was eluted with a solvent system consisting of (1) 0.1% of aqueous trifluoro-acetic acid and (2) 0.1% of trifluoro-acetic acid in 80% of aqueous aceto-nitrile in a linear gradient mode for 30 minutes at 80mL/min flow. The eluent was monitored at 220nm. The fractions were checked by analytical HPLC, and those with purity higher than 95% were pooled and lyophilized. The HPLC analyses of the peptides were carried out with a Hewlett-Packard Model 1050 liquid chromatograph using a Nucleasil 300 C4 (280×4 mm) reversed-phase column and a gradient elution with two solvent systems described above at a flow rate of 1mL/min. The peaks were monitored at 220nm. Amino acid analyses of the purified peptides were carried out on a Hewlett-Packard Amino-Quant amino acid analyzer after hydrolysis of the samples in 6 M of hydrochloric acid at 110°C for 48hrs in tubes sealed under vacuum. Amino acid analysis of the hydrolysates of peptides showed the expected amino acid composition (data not shown). Data of electrospray mass spectrometry (ES-MS, FinniganMat TSQ 7000 mass spectrometer) were in accordance with the calculated average molecular masses.

- *"Aging" of the peptides*

Freshly prepared aqueous βAP solutions were "aged" for 1 hour before use.

Treatment of animals

Male, Sprague-Dawley rats weighing 200-250g were maintained in plastic cages (three per cage) containing wood shavings and were given rodent chow and filter-purified tap water *ad libitum*. Murines were housed in rooms of our animal facility maintaining temperature of 25±2°C and a 12-h light/dark cycle.

All rodents were in good condition, and showed no signs of stress. Each was allowed to acclimate to the housing conditions for 1 week prior to beginning the experiment. With respect to the traditional antipsychotic haloperidol (Haloperidol®; *Gedeon Richter Ltd, Hungary*), groups of six rats were injected intra-peritoneally (i.p.) on a daily basis with therapeutic (0.05mg/kg) or toxic (0.5 mg/kg) doses dissolved in saline[135,136]. In case of the atypical drug risperidone (Risperdal®; *Ris-Int-63, Ref.No.: 336341; Janssen-Cilag, division of Johnson&Johnson Ltd., Hungary*), therapeutic (0.1mg/kg) or toxic (1.0 mg/kg) doses, dissolved in water, were administered[137,138]. Control rats received the vehicle alone. No other animals were housed in the room or allowed contact with the study animals.

Experiments were performed in accordance with a protocol approved by the university ethics committee on laboratory animals.

Preparation of rat cortical samples

After acute (6, 12, 24 and 96 hours) and chronic (1, 2, 3 and 4 weeks) administration of the antipsychotics in both therapeutic and toxic doses, rats were decapitated under ether anesthesia. The cerebellum was removed and the fronto-temporo-parietal cortices were dissected. In order to eliminate post-mortem decay, preparation was performed on dry ice. The samples were homogenized in 50mM of Tris buffer (pH 7.5) containing 0.15M NaCl, 2mM phenyl-methyl-sulfonyl-fluoride, 2mM EDTA, 2 μg/mL leupeptin, 1 μg/mL pepstatin, 1% Nonidet–P-40 and 0,1% sodium deoxycholate by using a glass-teflon potter (1500 rpm, 1 min). The homogenates were centrifuged at 10,000 × *g* for 30mins at 4°C. The supernatants were used for the detection of total APP. Protein concentrations of samples were determined by the method of Folin as modified by Hess et al.[139]

Western immunoblot

Proteins (30μg/lane) were separated on a 9% of sodium-dodecyl-sulfate (SDS)-polyacrylamide gel and electroblotted onto nitrocellulose membranes by using the BioRad Mini-Protean II system. After protein quenching with 5% non-fat dry milk in 50mM of Tris-buffered saline (TBS, pH 7.5) containing 0.2% of Tween-20, the blotted samples were incubated overnight at room temperature in monoclonal 22C11 antibody (5 μg/mL, against residues 68-81 of APP). After being washed (5×), the membranes were incubated with horse-radish-peroxidase (HRP)-conjugated anti-mouse-IgG (1:500, Sigma-Aldrich, USA). For the detection of blots, the Renaissance Western Blot Chemiluminescence Reagent (Pierce, USA) was employed, followed by exposure to an autoradiographic film. Optical densities of immunoreactive bands were detected and quantified by means of the NIH-Image Analyser Program (NIH, USA). The levels of APPs in the control group were taken as 100%, and changes were calculated with respect to this value (data are given in relative units).

Microarray Protocols

- *Samples and RNA preparation*

  Total RNAs were extracted and purified from rat fronto-temporo-parietal cortices (40mg/animal) using NucleoSpin RNA purification kit (Macherey-Nagel, Dürren, Germany) according to the manufacturer's instructions. The quantity and the quality of all RNA preparations were assessed by gel electrophoresis and spectrophotometry (optical density: OD_{260}/OD_{280} ratios) (NanoDrop, Rockland, DE, USA). RNA samples were aliquoted and stored at -80°C. Total RNA was used for microarray analysis as well as for Real-time quantitative reverse transcription-PCR (QRT-PCR).

- *Construction of microarrays*

  8,000 cDNA inserts (amino-modified oligo-nucleotides) from rat mixed-tissue cDNA libraries (peripherial ganglion, brain, heart, *etc.*), containing named genes, expressed sequence tags (ESTs), housekeeping genes and genomic control spots (Sigma-Operon) were resuspended in 50% dimethyl-sulfoxide/water at a final concentration of 300fmol/μL. Oligonucleotides were arrayed from 384-well plates onto PXM oligo-nucleotide slides (Full Moon Biosystems, Sunnyvale, CA, USA) by using a MicroGrid Total Array System (BioRobotics, Cambridge, UK) spotter with 16 pins in a 4×4 format. DNA elements were deposited in duplicate in distinct area of the array. The diameter of each spot was approximately 200 μm. After printing, slides were incubated in a humid chamber for 14h at 42°C. Prior to hybridization, the slides were processed as described previously[140,141].

- *Microarray probe preparation and hybridization*

  For probe preparation, 2μg of total RNA was reverse transcribed using poly-dT primed Genisphere Expression Array 900 Detection system (Genisphere, Hatfield, PA, USA) in 20μL total volume using 20 units of RNAsin (Fermentas, Vilnius, Lithuania), 1× first strand buffer and 200 units of RNAse H(-) point mutant murine myeloid leukemia virus (M-MLV) reverse transcriptase (Fermentas, Vilnius, Lithuania). All other probe preparation steps were done according the manufacturer's instructions (Genisphere, Hatfield, PA, USA). Both the first step cDNA hybridization and the second step capture reagent hybridization were carried out in a Ventana hybridization station (Ventana Discovery, Tucson, AZ, USA) by using the "antibody" protocol. First hybridization was performed at 40°C for 6h in "FGL2" hybridization buffer (10× Denhart solution, 0.25M sodium phosphate buffer pH: 7.0, 1mM EDTA, 1× SSC, 0.5% SDS), then 2.5μL of each Cy5 and Cy3 capture reagents were added to the slides in 200μL "Chiphyb" hybridization buffer (Ventana Discovery, Tucson, AZ, USA) and incubated at 42°C for 2h. After hybridization, the slides were washed in 0.2×SSC twice at RT for 10min, then dried and scanned.

- *Scanning*

Each array was scanned under a green laser (543nm for Cy3 labeling) or a red laser (633nm for Cy5 labeling) using a ScanArray Lite (GSI Lumonics, Billerica, MA) scanning confocal fluorescent scanner with 10μm resolution (Laser power: 85% for Cy5 and 90% for Cy3, Gain: 80% for Cy5 and 75% for Cy3)[142]. Scanned output files were analyzed using GenePix Pro5.0 software (Axon Instruments Inc., Foster City, CA, USA). Each spot was defined by automatic positioning of a grid of circles over the image. For each channel the median values of feature and local background pixel intensities were determined[142, 143]. The background-corrected expression data were filtered for flagged spots and weak signal. Technical replicates on the same array were averaged. Data were excluded in cases where technical replicates were significantly different. Normalization was performed using the print-tip Lowess method[144,145], followed by Student's *t*-test in order to determine the genes to be regarded as regulated in response treatment. Logarithm was taken from each expression ratio to fulfill the *t*-test's requirement for a normal distribution. Genes for which the mean of log-ratios across the biological replicates was equal to zero at a significance level α=0.05 are considered to have an unchanged expression. On the other hand, genes having a *P* value smaller than α and the average-fold change (increase or decrease) of the four data points were at least 2.0-fold were considered as regulated genes.

- *Expression profile verification*

QRT-PCR was performed on a RotorGene 2000 instrument (Corbett Research, Sydney, Australia) with gene-specific primers and SybrGreen protocol to confirm the gene expression changes observed by microarrays. 2μg of total RNA from each sample was reverse transcribed in the presence of poly(dT) sequences in a total volume of 20μL. After dilution with20 μL of water, 1μL of the diluted reaction mix was used as template in QRT-PCR. The 20μL reaction volume contained 0.2mM of dNTP, 1× PCR reaction buffer (ABGene, Epsom, UK), 6mM of each primer, 4mM of $MgCl_2$, 1× SYBR Green I (Molecular Probes, Eugene, Oregon, USA) at final concentration, and 0.5 units of thermostart *Taq* DNA polymerase (ABGene, Epsom, UK). The amplification was carried out with the following cycling parameters: 600 sec heat start at 95°C, 45 cycles of denaturation at 95°C for 25sec, annealing at 60°C for 25sec and fluorescence detection at 72°C for 15sec. Relative expression ratios were normalized to β-actin. Non-template control sample was used for each PCR run to check the genomic DNA contaminations of cDNA template. Analysis of results was performed by Pfaffl method[146]. Using this calculation method differences between the amplification efficiencies of reactions could be corrected.

Data analysis

Results presented are "arithmetic means ± standard deviation" of experiments performed in triplicate. Data were analyzed using Excel 98 (Microsoft, Redmond, WA) utilizing Student's *t*-test to determine the significance of observed changes. All differences stated in the text are statistically significant ($P<0.05$).

RESULTS AND DISCUSSION

1. Involvement of the periphery in AD

1.a. $[Ca^{2+}]_i$ of lymphocytes

Lymphocytes were successfully harvested and purified on Ficoll gradient from both Alzheimer and control donors. Cells were 97-98% viable as confirmed by intravital staining with Trypan Blue, and were competent to be labeled with Fura-2AM at 37°C by passive diffusion during the experiments. The ratio of fluorescence at 340 and 380nm ($FL_{340/380}$) representing $[Ca^{2+}]_i$ of control cells was 1.001±0.117, whereas Alzheimer lymphocytes exhibited a ratio of 1.131±0.100 (Table II). These findings indicate that AD cells demonstrate increases in free cell calcium when compared to leukocytes of age-matched controls.

Table II: $FL_{340/380}$ of lymphocytes

Comparative fluorimetric measurements on lymphocytes of human Alzheimer and control donors on $FL_{340/380}$ using Fura-2AM. Resting $[Ca^{2+}]_i$ appeared to be higher in AD cells when compared to that seen with control lymphocytes. After incubating cells in the presence of βAP, the $[Ca^{2+}]_i$ of the control cells elevated, while that of AD lymphocytes did not differ considerably. (*$P<0.05$)

Samples	$FL_{340/380}$ (mean±SD)	Number of cuvettes
Control	1.001±0.117	23
Alzheimer	1.131±0.100*	18
Control+βAP	1.507±0.368*	23
Alzheimer+βAP	1.130±0.075	18

Lymphocytes of our sporadic AD patients were distinguished from normal ones in our experiments, which clearly shows that detectable biochemical alterations are present in Alzheimer lymphocytes. Considering βAP central to AD pathomechanism, elevated $[Ca^{2+}]_i$ of AD cells is broadly in line with the notion that βAP has the potential to increase Ca^{2+}-levels[43,44,49,65,66]. However, serum βAP-level in AD patients does not significantly differ from that seen in healthy individuals to convincingly explain the findings. Moreover, βAP is considered a physiological peptide[19-21]; it exerts pathologic effects either in its aggregated form[27], or its cytotoxicity has been attributed to attending intracellularily[35-37]. Nevertheless, even though blood concentrations of βAP is not significantly higher, its level might be slightly elevated enough to disrupt Ca^{2+}-homeostasis in lymphocytes, and AD-specific changes in βAP aggregation or distribution inside the cells might be present to further the calcium-imbalance.

To justify the Ca^{2+}-rising effect of βAP, measurements of $[Ca^{2+}]_i$ with the calcium indicator dye Fura-2AM in control lymphocytes maintained in the presence of 10^{-7}M βAP for 2 hours revealed an increase in the 340/380 fluorescence excitation ratio (FL_{LYMPH}: 1.507±0.368), the mark of an increase in free calcium level during the 2-hour exposure period. By directly monitoring $[Ca^{2+}]_i$, we found that Alzheimer cells, maintained in the same conditions, showed no significant change in the free cell calcium (FL_{LYMPH}: 1.130±0.075). AD lymphocytes appeared to be resistant to βAP.

These findings might be explained by our hypothesis which assumes that slightly, but chronically elevated serum βAP levels disrupt Ca^{2+} in a tonic manner, causing continuous Ca^{2+}-overload into the neurons. This may indirectly confirm why resting $[Ca^{2+}]_i$ of

untreated AD lymphocytes is higher than that of control ones. The incessant amyloid-stimulus will ultimately make lymphocytes resistant to βAP. Furthermore, βAP can cause sustained alterations in cell membrane fluidity[163]. Aggregated and intracellular βAPs interact with membrane structures (both protein-peptide and lipid-peptide interactions), which can cause permanent change in the structure of the cell membrane and in $[Ca^{2+}]_i$. These alterations might promote the resistance of lymphocytes to βAP with respect to $[Ca^{2+}]_i$.

Because Ca^{2+} is a central secondary messenger, tonic elevation of its concentration has various effects. In blood, Ca^{2+} plays role in activation of lymphocytes.

Elevation of intracellular free Ca^{2+} is one of the key triggering signals for T-cell activation by antigen. βAP is known to interfere with various (including Ca^{2+}- and K^+-) channels, and is able to form non-selective cation pores in the cell surface, both known to yield elevated intracellular free Ca^{2+}-levels. Tonic βAP-trigger may lead to incessant antigen-independent activation and clonal expansion of lymphocytes, which is required to generate an efficient generalized immune response to a specific antigen (*eg.* βAP). However, the immune system is complex enough that activation of CD_4^+ T-cells can lead to several different functional outcomes: activation and cytokine secretion, death, or functional non-responsiveness (anergy).

Activation of lymphocytes in AD by Ca^{2+} might be of critical importance. When Alzheimer first described the clinical and pathologic features of the dementing disorder in early 1900s, he noticed signs of an inflammatory reaction; however, only in the last decade has the notion that the brain is "immunologically privileged" begun to be dismissed as an oversimplification, supported by mounting evidence that senile plaques and NFTs in brains of patients with AD are associated with a unique endogenous inflammatory reaction that is orchestrated by microglial cells. Activated microglia, the residing macrophage of the brain, in conjunction with astrocytes, which sustain the functional integrity of neurons, contribute extracellular matrix proteins, and can be considered to be cells of the innate immune system, are central to the inflammatory hypotheses for the neurodegenerative processes that are associated with AD. Microglial activation may be induced by soluble βAP fragments through causing Ca^{2+}-imbalance, plaque deposition, degenerating neurons, or all three. Activated microglia may release neurotoxins, toxic inflammatory mediators, and free radicals, but may also be involved in scavenging βAP. Inflammatory stress may increase generation of βAP through upregulation of APP. Apart from directly activating microglia by increasing $[Ca^{2+}]_i$, βAP might also circuitously stimulate microglia. This activatory scenario might not uniquely happen in the CNS.

It is well established that cross-talk takes place between the brain and the peripheral immune system. CD_4^+ helper cells are triggered by peptide antigens bound to class II MHC molecules. A class II allele that can bind to a given self-antigen (*eg.* amyloid-aggregate) may facilitate an autoimmune response. T-cell antigen receptor (TCR) is comprised of a ligand-binding subunit, the α and β chains, and a signaling subunit, namely the CD_3 units. The physiologic ligand for the TCR is foreign peptide bound to the MHC expressed on APCs, including dendritic cells, macrophages, and B cells. βAP may bind to either units, and therefore fibrillar βAP deposits and βAP fibrils may serve as activator of the immune system both in and outside of the CNS. Activation of autoreactive (amyloid-reactive) T-cells in periphery leads to release of cytokines/adhesion molecules and passage of cells through altered blood-brain-barrier into CNS.

Activated lymphocytes do penetrate into the normal brain in small numbers[147] and, during CNS inflammatory reactions, such as in AD, their migration is dramatically upregulated[148]. Leptomeningeal infiltrates primarily around amyloid-laden blood vessels with T-lymphocytes (mostly CD_4^+ type) suggests that lymphocytes freely enter the brain in AD[149]. In order for leukocytes to perform their immune function in tissue surveillance they must be capable of leaving the vasculature and entering tissues. The way in which specific leukocyte subsets may achieve this in different vascular beds is in many cases unresolved. In the CNS, extravasating leukocytes must penetrate the highly impermeable tight junctions, which link the vascular endothelial cells, or use an alternative unresolved parajunctional mechanism. However it is apparent that whichever mechanism is used for leukocyte diapedesis, the cells of the blood-brain barrier are not passive in this respect and are actively involved in facilitating lymphocyte migration into the CNS. Ca^{2+}-mediated intracellular events are essential for lymphocyte migration through the blood-brain barrier[150], as triggered by βAP.

T-cells cross the intact blood-brain-barrier, home to neuritic plaques, and cause local inflammation either directly, or by activating microglia. However, relatively few T- and B-lymphocytes are detected in the vicinity of plaques. Nonetheless, an increase in the levels of IFNγ, the principal T_{H1} cytokine, is correlated with the severity of AD [151] by synergistically enhancing the βAP-dependent microglial activation, resulting in neuronal cell injury[152]. This hypothesis is confirmed by the finding that the activity of certain T_{H2} cytokines, such as IL-10, which seem to be potent in reducing the activity and neurotoxicity of microglia, is reduced in patients with AD, and a decrease in the numbers and activity of suppressor T-cells has been reported[151]. Therefore, local inflammatory up-regulation seen in the brains of patients with AD may arise from an inadequately regulated systemic immune response[153], presumably triggered by βAP.

A complete understanding of these signaling mechanisms may lead to the identification of target pathways for the therapeutic treatment of brain inflammatory disorders, including AD. In addition, by understanding the mechanisms responsible for triggering lymphocyte migration it may be possible to manipulate peripheral blood lymphocytes to deliver therapeutic agents, that are normally excluded by the blood-brain barrier, to the CNS particularly in inflammatory diseases where these cells would be self targeting. During an influx of leukocytes, the initial interaction of the infiltrating cells is with the endothelial lining of the vessels. After migration through the endothelium, however, the principal interaction of leukocytes is with fibroblasts. This interaction is mediated through the increased expression of intercellular adhesion molecule-1 (ICAM-1). An immediate response to the cross-linking of ICAM-1 on fibroblasts or endothelial cells is the triggering of a rise in $[Ca^{2+}]_i$[154], and activation of NF-κB, which is a transcription factor ubiquitously associated with the induction of a range of pro-inflammatory cytokines and adhesion molecules[155]. Therefore, the Ca^{2+} homeostasis of Alzheimer fibroblasts has also been examined in this study.

1.b. $[Ca^{2+}]_i$ of fibroblasts

Seven days after seeding, cultured fibroblasts from both Alzheimer and control donors were 80% confluent. More than 97-98% of cells on coverslips were viable as confirmed by intravital staining using Trypan Blue. Cells were competent to be labeled with Fura-2AM at 37°C by passive diffusion during the study. With respect to control cultures, $FL_{340/380}$ revealed 2.48±0.162, whereas Alzheimer fibroblasts exhibited a ratio of 2.052±0.207 (Table III). Just as with lymphocytes, fibroblasts of our sporadic AD patients were also distinguished from normal ones in our experiments, demonstrating detectable biochemical alterations in Alzheimer fibroblasts.

Table III: $FL_{340/380}$ of fibroblasts – short-term study

Comparative fluorimetric studies on human control and Alzheimer fibroblasts on $FL_{340/380}$ using the Ca^{2+}-indicator dye Fura-2AM. Cells were maintained with or without βAP for 16 hours at 37°C. The fluorescence excitation ratios were calculated from fluorescence intensities observed at 495nm using dual wavelength spectrofluorimetry (excitation wavelengths: 340 and 380nms). Alzheimer cells exhibited lower $[Ca^{2+}]_i$ when compared to the control cultures. Exposure of fibroblasts to βAP resulted in increased $[Ca^{2+}]_i$ of the control cells, but not of AD cultures. (*P<0.05)

Cultures	$FL_{340/380}$ (mean±SD)	Number of coverslips
Control	2.48±0.162	16
Alzheimer	2.052±0.207*	42
Control+βAP	2.666±0.08*	16
Alzheimer+βAP	2.055±0.125	42

These findings indicate that cultured cells from donors of AD demonstrate significant decreases in resting free cell calcium when compared to that of age-matched controls. However, when taken together with leukocytes, the resting free calcium of AD lymphocytes is apparently opposing that of AD fibroblasts, in that basal $[Ca^{2+}]_i$ of fibroblasts from AD patients is significantly lower, whereas $[Ca^{2+}]_i$ of lymphocytes is higher than that of the matched controls. To reconcile these opposite changes in AD cells, βAP-induced biochemical alterations were also studied in fibroblasts.

Exposure of cells to βAP for 16 hours caused a rise in free cell calcium only in control cultures ($FL_{340/380}$: 2.666±0.08). βAP apparently disrupts calcium-regulating processes in control cells resulting in elevations of free cell calcium. This finding is in line with previous reports[43,109,114,131], demonstrating elevated calcium level as an underlying pathomechanism of βAP-induced cellular degeneration. However, AD cells do not show this response. Alzheimer cultures maintained in the same conditions showed little or no change in $[Ca^{2+}]_i$, with the fluorescence ratio being 2.055±0.125 (Table III). Alzheimer fibroblasts, like lymphocytes, are therefore refractive to βAP. These results are in line with findings demonstrating a decreased βAP-sensitivity in Alzheimer cells[156,157].

Rise in $[Ca^{2+}]_i$ results in triggering of various pathways of a particular cell. As discussed with the immune system, B-cell receptor (BCR)- and TCR-signaling is initiated through the actions of non-receptor tyrosine kinases in conjunction with B- and T-cell-specific adaptor proteins, transduce signals required for the activation of the downstream signaling pathways, including Ca^{2+}[158]. Just as with lymphocytes, fibroblasts are also activated by Ca^{2+}-signals. In this scenario, fibroblasts undergo activation and secrete cytokines. Upregulation of mRNA encoding for the inflammatory cytokines IL-1β and IL-6 as well as for chemokines IL-8 and MCP-1 might therefore represent potent activators of local inflammatory cytokine and chemokine production[159] to activate lymphocytes. Signaling through ICAM-1 provides a co-stimulatory signal with that of CD_3 leading to T-cell proliferation, migration, and the induction of cytokines [160]. Migration is primarily dependent on the stage and mode of lymphocyte activation, and activated T-cells, irrespective of their antigen specificity, are able to penetrate the blood-brain barrier[161]. ICAM-1, overexpressed by activated fibroblasts and lymphocytes, is central to the migration of T-cells into the CNS[162]. Production of cytokines, moreover, may indirectly lead to microglial activation in the brain.

The most parsimonious explanation for the role of fibroblasts in AD is, therefore, activating members of the immune system, including T-cells and microglia. Both processes may be initiated by βAP. In order to suppress the βAP-induced activation of both fibroblasts and lymphocytes in AD, several pharmacological interventions should be considered. The use of Ca^{2+} channel blockers (L-type calcium blockers, such as verapamil, diltiazem and nifedipine; non-selective calcium blocker amlodipine, *etc.*), activating plasma membrane Ca^{2+}-ATPase, overexpression of SR/ER Ca^{2+}-ATPase, mitochondrial targeting, and NF-AT signaling pathway targeting may be promising.

βAP-induced rise in the $[Ca^{2+}]_i$ leads to activation of fibroblasts and therefore participates in lymphocyte migration. Interestingly, however, AD fibroblasts demonstrate decreases in the resting free Ca^{2+} when compared to control cells.

1.c. Long-term effect of β-amyloid

Short-term (8-16 hours') exposure of cultures to βAP resulted in elevation of the fluorescence ratio (FL: 2.691±0.121), which is an indicative of the increase in the $[Ca^{2+}]_i$ (Table IV). This finding is in line with previous reports, demonstrating that a sustained rise in the basal calcium level is one of the underlying pathomechanisms of neural degeneration. The βAP-induced increase in the $[Ca^{2+}]_i$ peaked in fibroblasts on the 4th day of exposure to the peptide (FL: 2.798±0.101), and turned into a plateau for around 16 weeks (Figure 3). After the approximately 4 months' time the calcium-level of fibroblasts gradually started to decrease. Within 11 weeks, the $[Ca^{2+}]_i$ became significantly lower in the cells (FL: 2.164±0.199) when compared to that of the resting levels seen with cultures before exposure to βAP (FL: 2.479±0.221). The decreased calcium-level appeared to be constant for 10 weeks. In contrast with fibroblasts exposed chronically to βAP, $[Ca^{2+}]_i$ of control cultures did not change significantly over time (Table IV, Figure 3).

Table IV: $FL_{340/380}$ of fibroblasts – long-term study

Comparative fluorimetric studies on human fibroblasts on $FL_{340/380}$ utilizing the Ca^{2+}-indicator dye Fura-2AM. The cells were cultured with βAP for 37 weeks at 37°C. The table marks a rapid increase in the $FL_{340/380}$, representing elevation in $[Ca^{2+}]_i$. This elevation continues to be significant for 16 weeks, after which a decline in the calcium-level develops. The decrease in the fluorescence-ratio appears to be permanent. $[Ca^{2+}]_i$ of untreated cultures did not change significantly during 37 weeks. (*P<0.05)

Duration of treatment	βAP	Control
resting level	2.479±0.221	2.479±0.221
8 hrs	2.691±0.121*	2.483±0.107
16 hrs	2.666±0.080*	2.480±0.162
~half-week	2.798±0.101*	2.475±0.200
~16 weeks	2.802±0.157*	2.489±0.113
~27 weeks	2.164±0.199*	2.469±0.132
~37 weeks	2.165±0.176*	2.489±0.206

Figure 3: Time-course of βAP on $[Ca^{2+}]_i$ of human fibroblasts

Short-term exposition of fibroblasts to βAP results in an increased $[Ca^{2+}]_i$. The rise in the calcium-level peaks after an approximately half-a-week treatment with the peptide. The flow-chart demonstrates that the reversible elevation of $[Ca^{2+}]_i$ turns into a fall at around the 16th week of exposition to βAP, and yields a sustained decrease in the $[Ca^{2+}]_i$. Calcium-level of control cultures with no βAP treatment appeared to be unchanged during the experiment.

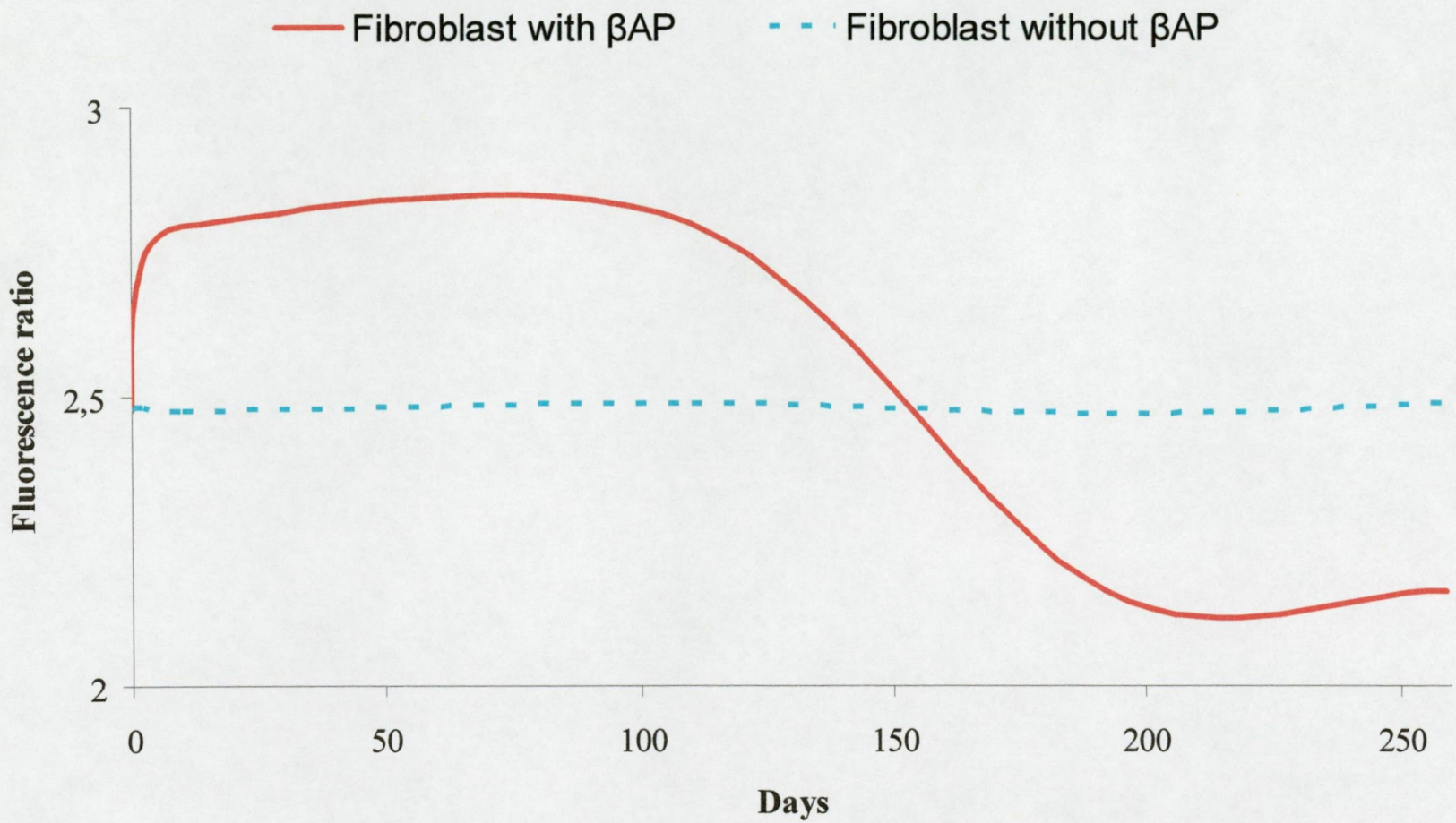

Treatment of control fibroblasts with βAP has resulted in a transient rise in the calcium-concentration. Elevation in the $[Ca^{2+}]_i$ appeared to be constant for 16 weeks, after which period the calcium level of cells gradually started to fall. Chronic exposition of fibroblast cultures to βAP, therefore, causes a decline in the calcium-level. This decrease was apparently sustained in our experiments. Thus, cells in our study have responded to βAP treatment in a time-dependent manner. Consistent with previous findings[43,109,114,131], $[Ca^{2+}]_i$ is increased as a result of βAP; this, however, seems to be only a short-term effect of the peptide. Piling evidence suggests that βAP interacts with cell membrane structures and also causes changes in membrane fluidity[163]. Exposure to βAP elicits sustained activation of Ca^{2+}-permeable receptor channels, which results in a pathological enhancement of inward Ca^{2+}-currents and a subsequent increase in the $[Ca^{2+}]_i$[50,131,164]. Elevation of $[Ca^{2+}]_i$ may further progress through the activation of second messengers (*eg.* IP_3) that mobilize intracellular calcium ions resulting in Ca^{2+}-release from its intracellular stores[165,166]. We hypothesize that the acute rise in $[Ca^{2+}]_i$ is attributable to these interactions of βAP.

Chronic exposition of cells to βAP apparently decreases $[Ca^{2+}]_i$. This observation is a real *novum*, and the exact pathomechanism behind this finding is yet unknown. Falling of the calcium-level may indicate that βAP causes a total ionic imbalance. Initially, βAP peptides can increase calcium influx through voltage-gated calcium channels (N- and L-type channels); form a cation-selective ion channel after βAP incorporation into the cellular membrane; reduce magnesium blockade of NMDA receptors to allow increased Ca^{2+} influx; and inhibit K^+ channel and Na^+/Ca^{2+} exchanger. Opening elevation of $[Ca^{2+}]_i$ triggers Ca^{2+}-mediated Ca^{2+}-release from intracellular stores[167]. Also, based on the channel hypothesis[49], βAP may further the calcium imbalance by directly forming Ca^{2+}-channels. As a result, $[Ca^{2+}]_i$ may reach pathological levels which exhausts the buffering capacity of intracellular Ca^{2+}-pools, particularly that of the mitochondria and endoplasmic reticulum. Due to the altered concentration gradient, Ca^{2+} is expelled from the cell through outward channels to compensate the Ca^{2+}-overload. As a result of their pathological interaction with βAP, the function of Ca^{2+}-exchangers and pumps that translocate Ca^{2+} to the interstitium may become hyperactive and uncontrolled. These pumps transport Ca^{2+} from the cytoplasm to the extracellular fluid against large electrochemical potential gradients using energy from ATP, which causes an incessant outward calcium flow leading to a Ca^{2+} loss inside of the cell. This can not be balanced by the cells' internal buffer systems on the long term, yielding a sustained decrease in the $[Ca^{2+}]_i$[168] and loss of energy. At later stages, damage to the mitochondria results in the enhanced production of free radicals, and activation of factors involved in apoptotic cell death. Accordingly, chronic fall in Ca^{2+} predisposes cells to self-degeneration[169]. As a result, derange of the intracellular calcium homeostasis ensues, and cells ultimately succumb to the chronic ionic imbalance.

The biphasic Ca^{2+}-response to βAP may play an important role in the pathomechanism of AD. Initially fibroblasts, activated by Ca^{2+}, assist lymphocytic migration. A decreased calcium-level on the long-run, however, might deactivate fibroblasts. Dormant fibrocytes with no cytokine and ICAM-1 expression chronically arrest lymphocytic activation and migration to the brain through blood-brain-barrier. This may explain why relatively few T- and B-lymphocytes are detected in the vicinity of neuritic plaques.

Despite the major pathological findings in the central nervous system of Alzheimer patients, the present thesis, as well as previous studies, indicate that metabolic deficits occur in non-neuronal tissues, including fibroblasts and lymphocytes[97-109]. Interestingly, however, basal $[Ca^{2+}]_i$ of fibroblasts is opposing that of lymphocytes. The difference between an increased $[Ca^{2+}]_i$ in lymphocytes and decreased $[Ca^{2+}]_i$ in fibroblasts may be

attributable to the specific ion-regulation of the respective cell-type, or to an altered affinity of βAP to different cells of peripheral tissues. To reconcile these opposite changes in AD cells, the fact that the turnover rate of cells in the blood is way higher than that of the fibroblasts may give a more convincing explanation. βAP initially increases the $[Ca^{2+}]_i$ of cells, which has been demonstrated herewith and earlier[43,109,114,131]; this correlates with an increase in the $FL_{340/380}$ of the lymphocytes in this study. βAP, however, completely disrupts calcium homeostasis on the long run, resulting in a decreased resting calcium level, as seen with fibroblasts. On theoretical grounds as explained above, the $[Ca^{2+}]_i$ would also be decreased in white blood cells, had they lived longer (*ie.* had their turnover rate been slower), like fibroblasts.

Importantly, both AD fibroblasts and lymphocytes are resistant to βAP. Alzheimer cells – in contrast to control ones – could be rendered resistant to βAP because of the chronic, long-term expositions, lasting several weeks (with respect to lymphocytes) or years (in case of fibroblasts), of cells to the peptide[98]. A tonic βAP-load seen in AD ultimately decreases $[Ca^{2+}]_i$ and makes cells insensitive to β-amyloid on the long run.

βAP apparently has a time-dependent biphasic effect: acutely, it increases the calcium-concentration of cells; in contrast, on the long-run, βAP acts as a calcium-antagonist. Therefore, the idea that βAP leads to neural degeneration solely by increasing cells' calcium concentration must be replaced with a more complex view of its dual function in intracellular ionic homeostasis. The neurotoxicity of βAP is therefore due to its dual effect, but mainly to its long-term calcium-antagonistic activity. The observed changes can be considered as long-term cell physiological action and can be used as a sensitive marker for testing for the long-term activities of βAP.

These data signify that Alzheimer-specific biochemical alterations are present in the peripheral tissues. It is yet unknown whether these changes reflect the very dysfunctions in the brain, or these changes are specifically present only in the cell-types studied. Because fibroblasts express metabolic alterations that reflect dysfunction in other organs, such as the brain, it is reasonable to suggest that these changes might also be present in the CNS.

These findings therefore may shed new light on understanding the pathomechanism of AD. This new observation on Ca^{2+} homeostasis might be used as a springboard for studying AD pathology, and for developing novel treatment options in AD. Moreover, fluorimetric differences in AD fibroblasts and lymphocytes might serve as useful models for establishing diagnostic tools in Alzheimer dementia, monitoring progression of the disease and responsiveness to treatments by screening biochemical alterations in the periphery.

2. Role of antipsychotics in the periphery

2.a. *Effect of haloperidol on $[Ca^{2+}]_i$ of fibroblasts*

$[Ca^{2+}]_i$ of neither control, nor AD fibroblasts have changed significantly as a result of HAL treatment ($FL_{340/380}$: 2.41±0.119, and 2.049±0.202, respectively). Preincubation of cultures with HAL together with βAP has also resulted in no elevation in $[Ca^{2+}]_i$ (Table V).

In the brain, HAL has been previously reported to interfere with calcium metabolism through various mechanisms, including interaction with D_2 and σ_1-receptors[122,170,171]. Moreover, HAL has been shown to induce apoptosis of brain cells, which involves activation of σ-receptors, and also translocation of calcium into the cytoplasm[171,172,173]. Because differences certain to be encountered with respect to tissue-specific macromolecules, lack of various neuronal receptors on fibroblasts may give an explanation. Since fibroblasts do not express D_2 and σ_1-receptors, HAL is not potent in

interfering with Ca^{2+}-homeostasis in cutaneous cells. However, other than receptor-mediated pathways may also lead to HAL-induced changes in Ca^{2+}-levels. Therefore, evaluating HAL for its effects on βAP-induced Ca^{2+}-imbalance on fibroblasts in this study was inevitable.

Table V: $FL_{340/380}$ of fibroblasts: treatment with haloperidol

Comparative fluorimetric studies on human control and Alzheimer fibroblasts on $FL_{340/380}$ utilizing the Ca^{2+}-indicator dye Fura-2AM. Cells were cultured with or without βAP and/or HAL for 16 hours at 37°C. Elevation in $FL_{340/380}$ after βAP-treatment was attenuated by co-administration of HAL. (*P<0.05, when samples compared to their untreated counterparts only)

Cultures	$FL_{340/380}$ (mean±SD)	Number of coverslips
Control	2.48±0.162	16
Alzheimer	2.052±0.207	42
Control+βAP	2.666±0.08*	16
Alzheimer+βAP	2.055±0.125	42
Control+HAL	2.41±0.119	16
Alzheimer+HAL	2.049±0.202	16
Control+βAP+HAL	2.46±0.123	16
Alzheimer+βAP+HAL	2.054±0.198	16

Co-administration of both βAP and HAL yielded unchanged Ca^{2+}-levels of the cultures (Table V). This finding is important in light that βAP has proved to change $[Ca^{2+}]_i$, and might be explained on the basis that HAL has been shown to block Ca^{2+}-channels[170,174]. Evidence from a number of studies has demonstrated that βAP can form ion channels in lipid bilayers, liposomes, neurons and other cells[49,175]. βAP-channels are heterogeneous in size, selectivity, blockade, and gating. They exhibit multiple cation selectivity, admitting Ca^{2+}, Na^{+}, K^{+}, Li^{+}, *etc.*, leading to unregulated Ca^{2+}-influx via βAP-channels. Based on the Ca^{2+}-channel hypothesis of βAP, HAL may efficiently block the channel activity of βAP.

Also, because HAL was demonstrated to efficiently inhibit βAP-formation[123], the protective effect of HAL might be achieved through two connected mechanisms. HAL decreases the concentration of βAP; accordingly, less Ca^{2+}-channels, formed of βAP, will be present. However, even these few channels are blocked by HAL. Moreover, HAL may act as a β-sheet breaker. This hypothesis strongly supports the theory that both regulating βAP production and blocking βAP-channels/βAP aggregation may underlie the molecular mechanism of HAL (neuro)protection. Therefore, HAL is a multimodal antagonist of βAP.

Chronic treatment with HAL may result in decreased βAP-induced neurotoxicity in the brain over time through various, but not fully understood mechanisms as discussed above. This may explain why several investigators have found a low frequency of AD neuropathology in SCH, as many patients with SCH are likely to have been chronically treated with HAL, a commonly prescribed drug for this disorder.

Because AD is frequently associated with BPSD, which is treated with antipsychotic medications such as haloperidol[176,177], future randomized controlled studies should target AD patients with BPSD with a history of chronic HAL treatment for neuropathologic examination. The prediction is that these patients should show a lower progression rate than untreated subjects or subjects treated with structurally divergent antipsychotic drugs.

2.b. Effect of risperidone on $[Ca^{2+}]_i$ of fibroblasts

Exposure to the atypical antipsychotic RISP alone did not significantly alter the $[Ca^{2+}]_i$ of both control and AD fibroblasts, leaving the $FL_{340/380}$ technically unchanged. This suggests that RISP itself does not interfere with Ca^{2+}-homeostasis of these cutaneous cells. No significant alteration was observed when cells were co-treated with RISP and βAP (Table VI).

Table VI: FL340/380 of fibroblasts: treatment with risperidone

Comparative fluorimetric measurements on fibroblasts of Alzheimer and control donors on $FL_{340/380}$ using Fura-2AM. Cells were maintained with or without βAP and/or RISP for 16 hours at 37°C. βAP-induced increase in $FL_{340/380}$, representing a rise in $[Ca^{2+}]_i$, was efficiently antagonized by RISP. (*$P<0.05$, when samples compared to their untreated counterparts only)

Cultures	$FL_{340/380}$ (mean±SD)	Number of coverslips
Control	2.48±0.162	16
Alzheimer	2.052±0.207	42
Control+βAP	2.666±0.08	16
Alzheimer+βAP	2.055±0.125	42
Control+RISP	2.479±0.200	16
Alzheimer+RISP	2.054±0.172	16
Control+βAP+RISP	2.482±0.114	16
Alzheimer+βAP+RISP	2.053±0.099	16

Contrary to HAL, there is no information on the effect of RISP on Ca^{2+}-homeostasis, nor on its ability to interfere with βAP production. However, activation of dopamine-receptors leads to transient increase in $[Ca^{2+}]_i$. Atypical antipsychotics, such as RISP, have been shown to stabilize $[Ca^{2+}]_i$ through antagonizing dopamine-receptors. Furthermore, atypical but not classical neuroleptic drugs reduce astroglial dopamine-sensitivity[178]. Moreover, dopamine-receptor antagonists such as RISP, just as antioxidants, have been shown to protect neurons against the damaging effects of βAP and catecholamines[179].

RISP did not change $[Ca^{2+}]_i$, and alleviated βAP-induced Ca^{2+}-imbalance. These very same phenomena were found in this study with respect to typical antipsychotic HAL, and therefore they may share common targets. When taken together with the hypothesis that fibroblasts may serve as models of several neurometabolic disorders including AD[114-116], administration of RISP and HAL in the treatment of BPSD appears to be safe with respect to $[Ca^{2+}]_i$. Moreover, both RISP and HAL have proved to efficiently antagonize Ca^{2+}-disrupting cytotoxic effects of βAP. In spite of their inability to directly interfere with Ca^{2+} in the periphery, the observation that RISP and HAL efficiently attenuate βAP-induced Ca^{2+}-imbalance further confirms the possibility that RISP and HAL directly interact with βAP. However, further studies are needed to evaluate the putative neuroprotective effect of both agents. These might include selective pre- and postincubation of cultures with RISP or HAL and βAP; comparing the findings on fibroblasts with results on cultures from central nervous system that do (*eg.* neurons) and those do not (*eg.* glias) express dopamine and sigma receptors; and biophysical studies on the direct interaction between these antipsychotics and βAP. In light of these evidences, RISP and HAL may be useful leads in the development of effective AD therapeutic agents.

Apart from directly modulating calcium levels and blocking Ca^{2+}-channels, RISP and HAL may also alter the metabolism of APP and expression of genes involved in Ca^{2+}-regulation.

3. Antipsychotics in the brain – the Alzheimer approach

3.a. *Effect of haloperidol and risperidone on APP metabolism*

Using monoclonal 22C11 antibodies against residues 68-81 of APP, we were able to detect wide, APP containing bands at 110-120 kDa (Figures 4, 5). Traditional antipsychotic HAL efficiently elevated cortical APP-levels in a concentration-dependent manner (Table VII, Figures 4, 6). Significant rise in APP was evident as a result of acute administration of HAL in therapeutic and toxic doses within 24 and 12 hours, respectively. Significant changes in APP concentrations were between 2-6% when compared to that seen with control levels. On the other hand, chronic HAL treatment slightly increased APP concentrations, however, did not change APP levels considerably.

Table VII: Semi-quantitative evaluation of rat cortical APP-Western-blot after or without acute and chronic intra-peritoneal HAL administration

Rat cortical APP-levels were approximated utilizing Western-immuno-blotting, and chemi-luminescent visualization of bands were quantified by densitometry. Acute HAL-treatment revealed significant increase both in therapeutic and toxic doses within 24 and 12 hours, respectively, with regards to APP when compared to that seen with control animals. Chronic (1-4-week) administration of HAL resulted in incessant APP-levels in SPRD rat cortices *in vivo*, as detected by chemiluminescent Western-blot techniques. Optical densities are depicted in relative units, with the controls taken as 100%. (*$P<0.05$)

Duration of treatment	Control	Therapeutic dose	Toxic dose
6 hrs	100	101	100.5
12 hrs	101	103	105.8*
24 hrs	99.4	107.9*	104.7*
96 hrs	99.8	103.9*	103.1
1 week	100	102.8	101.7
2 weeks	100.5	101.6	102.8
3 weeks	101	100.4	102.1
4 weeks	100.3	101.2	101.3

The atypical antipsychotic risperidone slightly, but not significantly increased cortical APP levels in both therapeutic and toxic doses during all treatment periods (Table VIII, Figures 5, 7). In case of this atypical antipsychotic drug there was neither time-, nor concentration-dependence with respect to APP levels.

Table VIII: Time-course of acute and chronic RISP treatment on rat cortical APP concentrations

Semi-quantitative evaluation of cortical APP-Western-blot after or without acute (6, 12, 24, and 96-hour) and chronic (1-4-week) RISP treatment, administered through the intra-peritoneal route, delineates no significant changes both in therapeutic and toxic doses with respect to APP when compared to that seen with untreated SPRD rats. APP-containing bands were assessed by chemiluminescent Western-immunoblot techniques, and optical densities are displayed in relative units (controls being 100%).

Duration of treatment	Control	Therapeutic dose	Toxic dose
6 hrs	100	100.8	99.6
12 hrs	100.4	99.8	101
24 hrs	100.6	101.1	101.2
96 hrs	101.2	102.1	102.3
1 week	100	100.8	99.6
2 weeks	100.4	99.8	101
3 weeks	100.6	101.1	101.2
4 weeks	101.2	102.5	102.9

Figure 4: APP immunoblots after haloperidol administration *in vivo*

Quantification of immunoblot analysis by densitometry delineates **A:** a marked increase after acute haloperidol treatment. **B:** Chronic haloperidol reveals no significant changes either in therapeutic (Th) or toxic (Tx) doses when compared to that seen with controls (C).

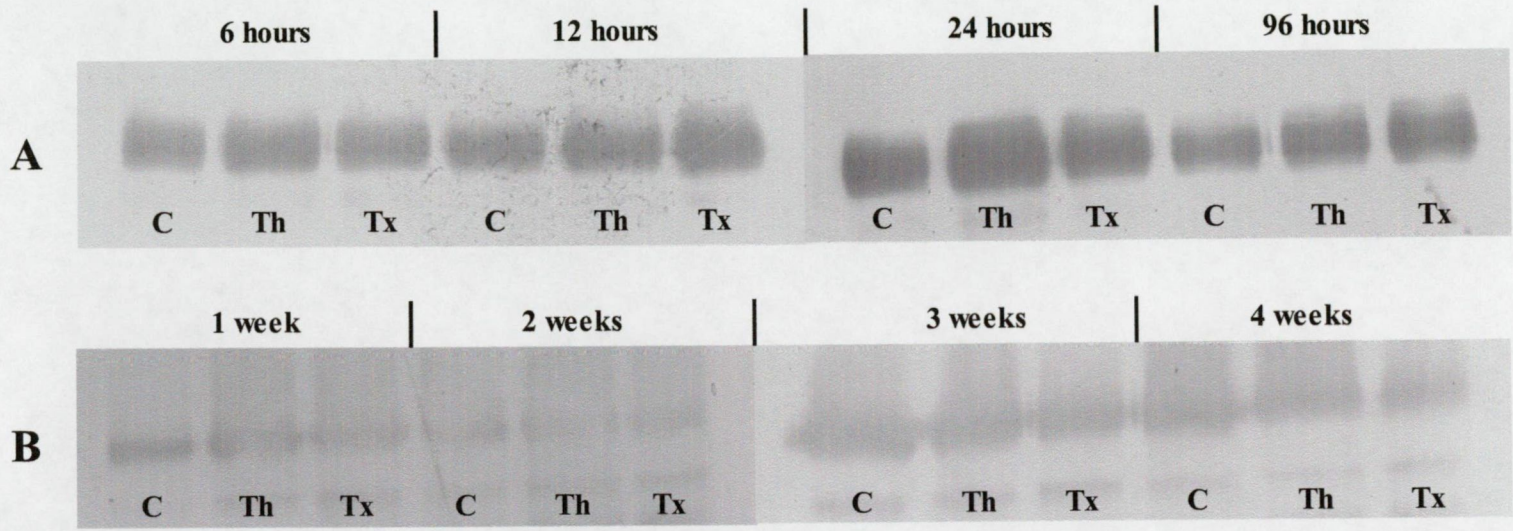

Figure 5: APP immunoblots following risperidone administration *in vivo*

Rat cortical APP immunoblots show technically unchanged densities after acute (A) or chronic (B) risperidone treatments, respectively.

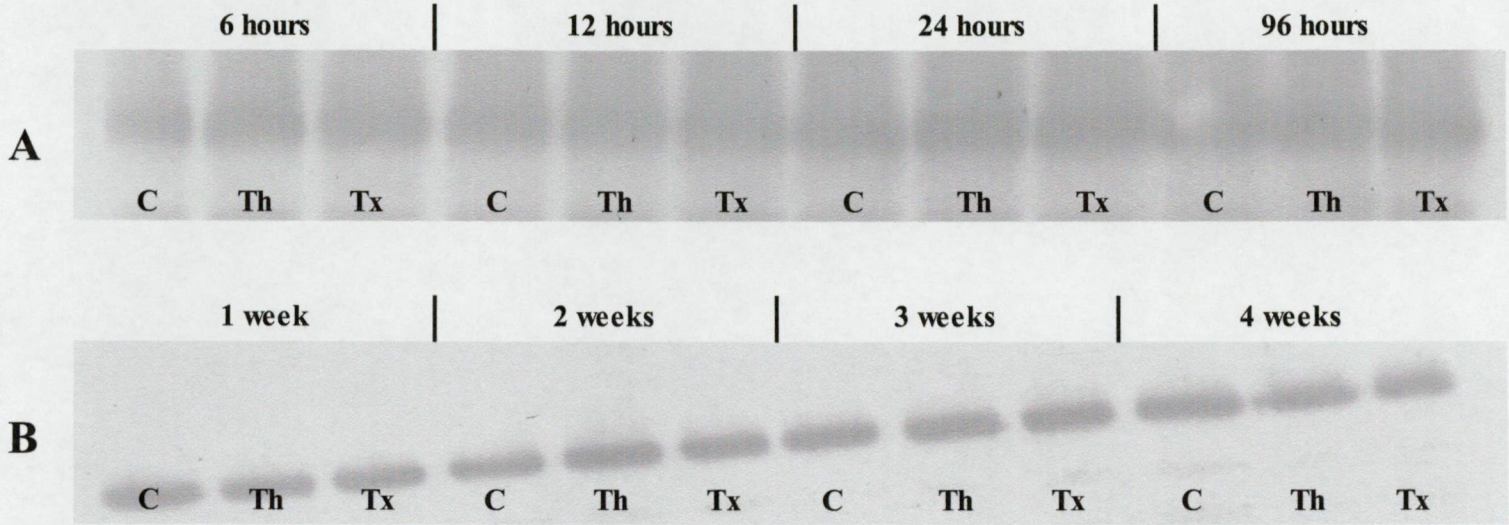

Figure 6: Time-course of HAL on rat cortical APP concentrations

Intra-peritoneal administration of HAL resulted in significant increase in rat cortical APP-level in therapeutic dose within 24 hours. This elevation was seen even in 12 hours in toxic dose of the drug. Both therapeutic and toxic HAL leaved APP concentrations unchanged on the long-run. ($P<0.05$)

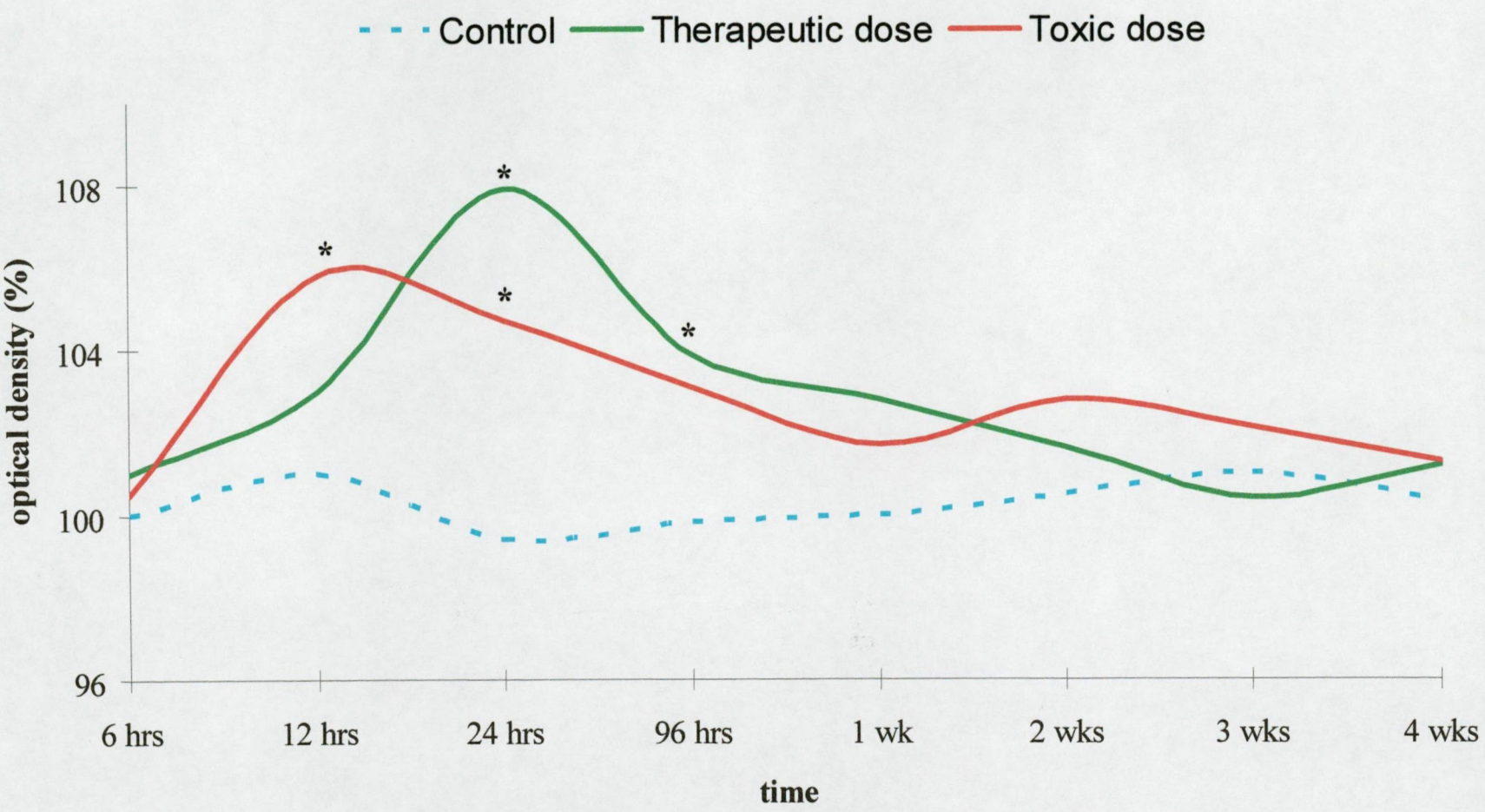

Figure 7: Time-course of RISP on rat cortical APP concentrations

The flow-chart delineates the effect of the typical antipsychotic drug on the APP metabolism in an acute or chronic time-frame. RISP did not significantly interfere with the APP-levels either in therapeutic or toxic doses.

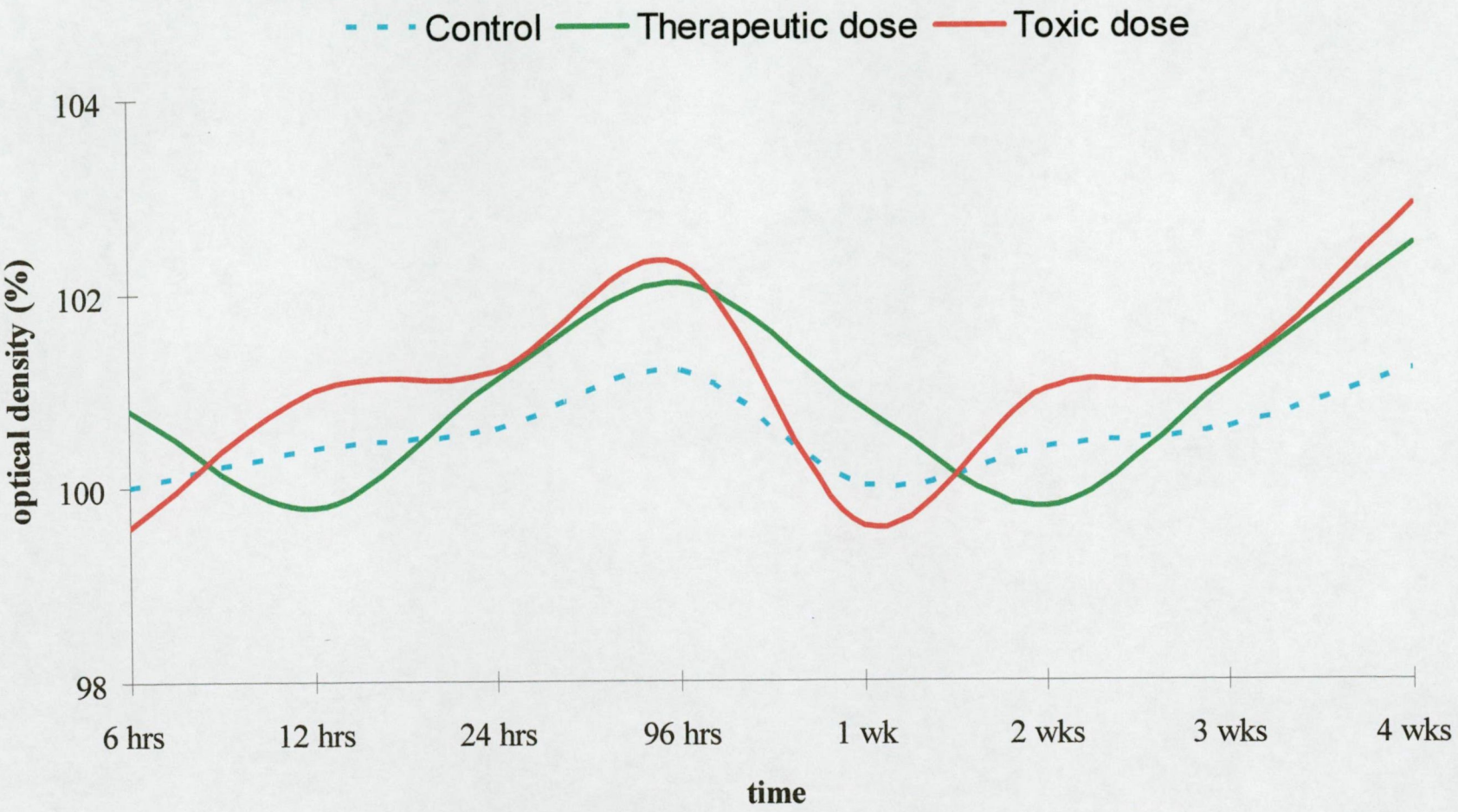

3.a.i. Effect of HAL on APP levels

Acute administration of HAL apparently yields APP elevation in both therapeutic and toxic doses. Because HAL acts as an inhibitor of select proteinases[180], including secretases that cleave APP[123], acute HAL leads to increase in the non-metabolized form of APP. This is supported by the finding that APP metabolism is increased by environmental effects that activate Ca^{2+}-signaling pathways[44]; by being a calcium antagonist[122], HAL efficiently inhibits APP processing, leading to elevated full-length APP levels.

- *Neurotoxicity and neuroprotection*

HAL has been proved to be neurotoxic, and the involvement of oxidative free radicals and apoptotic factors is strongly implicated[120,121].

σ_1-ligands, such as neurosteroids, play a role in neuroprotection[181,182]. σ_1-agonists modulate ionotropic, metabotropic and voltage-gated Ca^{2+}-signals, and enhance intracellular Ca^{2+}-mobilization[183]. Ca^{2+} increases APP metabolism in general[44], and also stimulates sAPPα secretion[184]. sAPPα can reduce neuronal cytosolic Ca^{2+}-levels and have demonstrated neuroprotective efficacy against a variety of insults[84]. Moreover, σ_1-receptor agonists play an important role in learning and memory. They have been demonstrated to possess neuromodulatory effects; they potentiate cholinergic neurotransmission and the glutamatergic system[185,186]. Also, neuroprotection against βAP-induced neurotoxicty was reported[187]. Because the traditional neuroleptic HAL acts as sigma σ_1-antagonist[119], it inhibits this complex neuroprotective pathway to yield sAPPα, and therefore increases full-length APP levels.

By being a D_2-receptor antagonist[118], HAL decreases PKC activity and level[188]. Activating PKC would lead to secretion of neuroprotective sAPPα[189,190], and to modulation of Ca^{2+}-currents by regulating Ca^{2+}-channels through second messengers[191,192]. Ca^{2+}, one of the most important second messengers in the brain, decreases APP mRNA levels[193]. Taken together, decreased PKC by HAL increases APP mRNA.

Even though increased APP level is a precondition to excessive neurotoxic βAP formation, one of the inducible neuroactive (trophic) factors at site of neural injury is the APP that may participate in cell-to-cell recognition, re-establishment of synaptic contacts, alleviation of glutamate-induced membrane depolarization and over-excitation, and stabilization of the intracellular Ca^{2+} homeostasis[164,181,194,195]. Therefore, it is assumed that APP is an important protein for tissue repair and that its expression is upregulated following nerve damage[196], as might be expected to occur following amyloid fibril formation or administration of toxic agents, such as HAL. In addition, persistent induction of APP expression without subsequent accumulation of βAP in response to acute brain injury substantiates the neuroprotective potential of APP[194,197]. This may account for the elevated APP level seen in these experiments after HAL treatment. Because HAL is neurotoxic, acute increase in APP after HAL-treatment might be considered as such a compensatory mechanism. This is supported by the observation that the presumably non-toxic RISP does not exert such effects. Further hypothesizing the advantageous roles of HAL, elevated APP levels might be a preconditioning effect of HAL to other nocuous agents, such as βAP.

Moreover, HAL is known to increase the activity of NF-κB[198]. Activation of NF-κB by either sAPPα[199] or HAL stabilizes cellular Ca^{2+} homeostasis by modulating the expression of genes that encode Ca^{2+}-binding proteins, ionotropic glutamate receptor subunits, and anti-apoptotic *bcl-2* family members[200]. This is in line with HAL-induced cellular protection with respect to neurotoxic APP metabolites, *ie.* βAP, in peripheral tissues (Table V).

- *HAL and Ca^{2+} in AD*

Abnormal signal transduction systems have been implicated in the pathophysiology of AD and in APP metabolism, but their precise role has been difficult to establish. It is therefore reasonable to hypothesize that the action of HAL on APP processing is a fine-tuning mechanism involving various second messengers, such as Ca^{2+}.

Calcium, as discussed above, plays central role in HAL-induced neurotoxicity and neuroprotection both in general and in AD. However, HAL modulates extracellular Ca^{2+}-influx and intracellular Ca^{2+}-mobilization through σ_1-receptors, therefore stabilizes Ca^{2+}. This fine-tuning mechanism leads to constitutive sAPPα secretion, which precludes βAP formation. This is in line with the finding on peripheral cells that HAL attenuates βAP-induced Ca^{2+}-imbalance and stabilizes $[Ca^{2+}]_i$ (Table V). Moreover, because it has been shown to non-selectively block Ca^{2+}-channels[122], HAL may also directly protect in AD against pores formed in the membrane by βAP that act as cation (*eg.* Ca^{2+}) channels[49].

Yielding an elevated APP concentration in the aforementioned Ca^{2+}-dependent manner by HAL is two-fold: suppressing its cleavage or elevating $mRNA_{APP}$-level. HAL has been reported to block the amyloidogenic processing of APP, which, in turn, precludes βAP production[123], and therefore may stimulate neuroprotective sAPPα secretion which may attenuate both self-induced (*ie.* direct toxicity of HAL) and βAP-derived neurotoxicity.

Nevertheless, chronic treatment with HAL results in stable APP levels, which leads to decreased deposition of βAP in the brain over time by inhibiting βAP formation[123] and alleviating βAP-induced toxicity as presented above. When previous reports are taken together with our findings, the impact of HAL in AD is 3-fold: it stabilizes Ca^{2+}, stimulates sAPPα secretion and inhibits βAP formation; these effects are inter-connected. This may further confirm why a low frequency of AD is present in SCH patients, as many of them are likely to have been treated chronically with antipsychotics, including HAL.

- *APP-receptor*

Various ligand-operated ion channels that control intracellular Ca^{2+}-levels may also regulate APP processing[44]. Both sAPPα and βAP have been demonstrated to modulate cytoplasmic Ca^{2+} concentration[43,84], raising the possibility that these compounds may regulate their own formation. This fine-tuning mechanism may be characteristic of AD because of the involvement of various APP-related substances. However, by being a putative cell-surface receptor, APP itself might also be directly involved in this scenario[68]. APP might be a single metabotropic receptor coupled to GTP-binding proteins[201201], or it may be a part of a larger receptor complex potentiating D_2- and/or σ_1-receptors. Elevated APP levels after acute HAL treatment argue for this hypothesis, in that inhibitory ligands (*eg.*

HAL) result in compensatory up-regulation of their receptors (*eg.* APP itself). Therefore, HAL-APP receptor-kinetics should be investigated in the future.

3.a.ii. Effect of RISP on APP levels

Atypical RISP has common action with HAL on D_2-receptors. However, it also acts as serotonergic-antagonist, of which 5-HT_2 and 5HT_4-receptors have been shown to stimulate sAPPα secretion[202]. Moreover, lesions of cholinergic, serotonergic, and adrenergic neurotransmitter systems all result in the induction of APP levels[203]. By antagonizing both 5-HT and NA (*ie.* adrenergic) receptors, slight elevation in APP concentration elicited by RISP treatment is apparently evident. This suggests that RISP may induce neuroprotection against various internal or external nocuous stimuli by slightly stimulating APP expression[164,194,197]. Furthermore, considering that increase in APP level is seen after exposition to potentially toxic agents (*eg.* HAL), marked elevation in APP concentration is not present after treatment with the presumably non-toxic RISP.

In contrast with HAL, high potential atypical antipsychotic RISP did not have a significant effect on APP, nor does the literature have any information on its importance at any level in AD, be it clinical or molecular. The observed changes elicited by HAL are therefore better explained. Even though both drugs act as D_2-antagonists, involvement of σ_1-receptors, altered affinity to APP, direct cytotoxicity, or other unknown mechanisms may account for the differing impact of HAL from RISP on APP metabolism. However, the slight increase in APP levels as a result of RISP treatment (Figure 7) might also be regulated by gordian mechanisms; apart from D_2-receptors, the involvement of numerous factors beyond the first messenger level along with 5-HT_2 and NA-receptors, and above all Ca^{2+}, might be implicated.

3.a.iii. Implication in AD

The pharmacological actions of HAL and RISP are important in the course of dementia. Antipsychotics did not affect intracellular Ca^{2+} levels in AD fibroblasts in the presence or absence of βAP treatment. In case of APP, however, their molecular impact is crucial in AD.

The major route of APP processing is via α-secretion, in which APP is cleaved by α-secretase at or adjacent to Lys_{16} in the βAP sequence[77] (Figures 1, 2). This route of processing has two important consequences. On one hand, C-terminally truncated form of APP (*ie.* sAPPα) is released from the membrane and can be subsequently secreted from the cell. Also, this pathway destroys the complete βAP sequence and therefore may mitigate amyloid formation. The amyloidogenic APP metabolic route produces βAP via the activation of β- and γ-secretases.

Intact cellular homeostasis, including relatively stable Ca^{2+}-level, leads to constitutive sAPPα-secretion. Because sAPPα is known to stabilize cytosolic Ca^{2+}-dynamics, normal processing of APP stimulates sAPPα production. Because HAL and also probably RISP stabilize Ca^{2+}, a protective circle is proposed in this thesis. By producing relatively constant Ca^{2+} concentrations, HAL and RISP stimulate sAPPα formation, which in turn stabilizes Ca^{2+} levels. Apart from constitutively secreted sAPPα, receptor-activated sAPPα release mediated by protein kinases – such as PKC – is a crucial pathway in APP metabolism[204,205]. As discussed above, activated PLC affects APP processing by either of two pathways, one involving an increase in PKC (PLC-DAG-PKC cascade) and the other an elevation in

cytoplasmic Ca^{2+}-levels (PLC-IP_3-Ca^{2+} limb of the pathway). Both pathways, probably also activated by HAL and RISP, are known to stimulate sAPPα production and inhibit βAP formation[204].

Unlike usual conditions, however, cells in AD are exposed to neurotoxic βAP. The βAP-limb of the APP pathway has been shown to induce significantly altered Ca^{2+} levels both in this thesis and elsewhere. Increased or decreased levels of cytoplasmic Ca^{2+} plays a role in the abnormal proteolytic processing of APP resulting in increased βAP formation[206,207]. This feed-forward neurodegenerative pathway leads to cell death by sustained Ca^{2+}-levels and inhibited sAPPα secretion. By antagonizing βAP-induced Ca^{2+}-imbalance, stabilizing Ca^{2+}-levels, and inhibiting βAP formation, the protective circles of HAL and RISP are important events in slowing the progression of AD.

Protein kinases, such as PKC, are involved in receptor-mediated sAPPα production. These protein kinases can be activated by second messengers, such as Ca^{2+}, or in turn, these kinases may activate second messengers, including Ca^{2+}. Even though Ca^{2+}-cascade can regulate APP metabolism in a PKC-independent fashion, hyperactivation of kinases by incessant Ca^{2+}-imbalance can activate PKC-reliant amyloidogenic APP processing.

Because propeptides of β- and γ-secretases undergo phosphorylation in order to yield active proteases[208], PKC-mediated phosphorylation plays a critical role in the regulation of sAPPα and βAP secretion, and PKC-mediated pathways may help control amyloid formation. However, PKC appears to mediate APP secretory processing not directly but via additional intracellular messengers. Apart from Ca^{2+}, one reasonable candidate for the phosphoacceptor is the APP secretase itself. In the course of the disease, "mal-activation" of kinases leads to hyper-phosphorylation, which may stimulate not only amyloidogenic APP processing, but also hyper-phosphorylation of the axonal transport-associated protein *tau*, which ultimately yields PHF. By acting on Ca^{2+}, both HAL and RISP are proposed to alleviate these effects seen in AD.

Taken together, βAP-Ca^{2+} feed-forward (Figure 8) and sAPPα-Ca^{2+} feed-back, *ie.* "protective circle" of HAL (Figure 9) is proposed in AD.

Figure 8: Proposed βAP-Ca^{2+} feed-forward

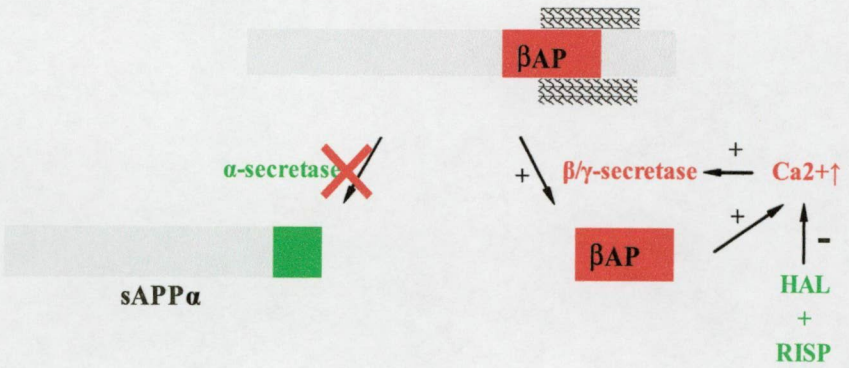

Figure 9: Proposed sAPPα-Ca^{2+} feed-back – "protective circle" of HAL

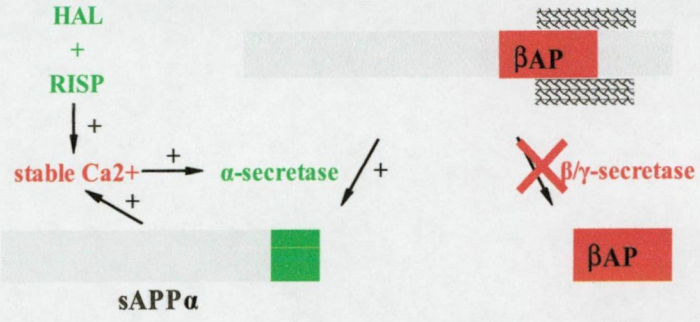

3.b. Gene expression profile of antipsychotics in the brain

It has been shown in this study that HAL and RISP interfere with Ca^{2+} and APP metabolism in AD. It is not yet fully understood whether this is a direct interaction taking place at the proteomic level, or their exact mode of action is interfering with genes and their expression – or perhaps both.

Recent advances in high-density cDNA microarray technique allow the possibility to analyze thousands of genes simultaneously for their differential gene expression patterns in various biologic processes, and determining mechanisms of drug action. The aim of this series of experiments was to gain experience in antipsychotic gene-expression profiling and characterize (in the parlance of genomics) the "antipsychotic transcriptome."

An important step to understanding the role of genes in the mechanism of drug action is to define gene expression profiles after drug manipulation. DNA expression array technology can monitor the expression of thousands of genes simultaneously and provide a format for identifying genes[209]. DNA microarrays allow genome-wide assessment of changes in relative messenger RNA abundance and thus can be used to monitor changes in gene expression as a result of various medications. Using this novel method we determined the effect of acute and chronic effect of HAL and RISP on the expression of approximately 8,000 gene targets in rat prefrontal/fronto-parieto-temporal cortex (Figure 10). This region of brain was chosen because this is an area in which abnormalities have been reported in SCH patients, where dopaminergic neurons largely project, and where antipsychotics have been shown to have numerous effects. Moreover, this is the area where AD-specific changes occur, and where HAL and RISP were shown in this study to have beneficial effects in dementia.

This study is very important, since the pharmacotherapy of psychiatric drugs continues to be based on trial and error, with psychiatric diagnosis serving as the principle guide for drug choice. Often drug selection within a therapeutic category (*eg.* antipsychotic) is based on side-effect profile (*eg.* sedation) to match a clinical need. Therapeutic response, even among diagnostically homogenous patient groups, is highly variable within classes of psychiatric drugs. Until now, little information is available on the molecular effect of antipsychotics.

Figure 10: cDNA microarrays

Gene-chips hybridized with Cy5 labeled cDNA probe (obtained from untreated rat cortical total RNA) and Cy3 labeled cDNA probe (obtained from antipsychotic-treated cortical total RNA)

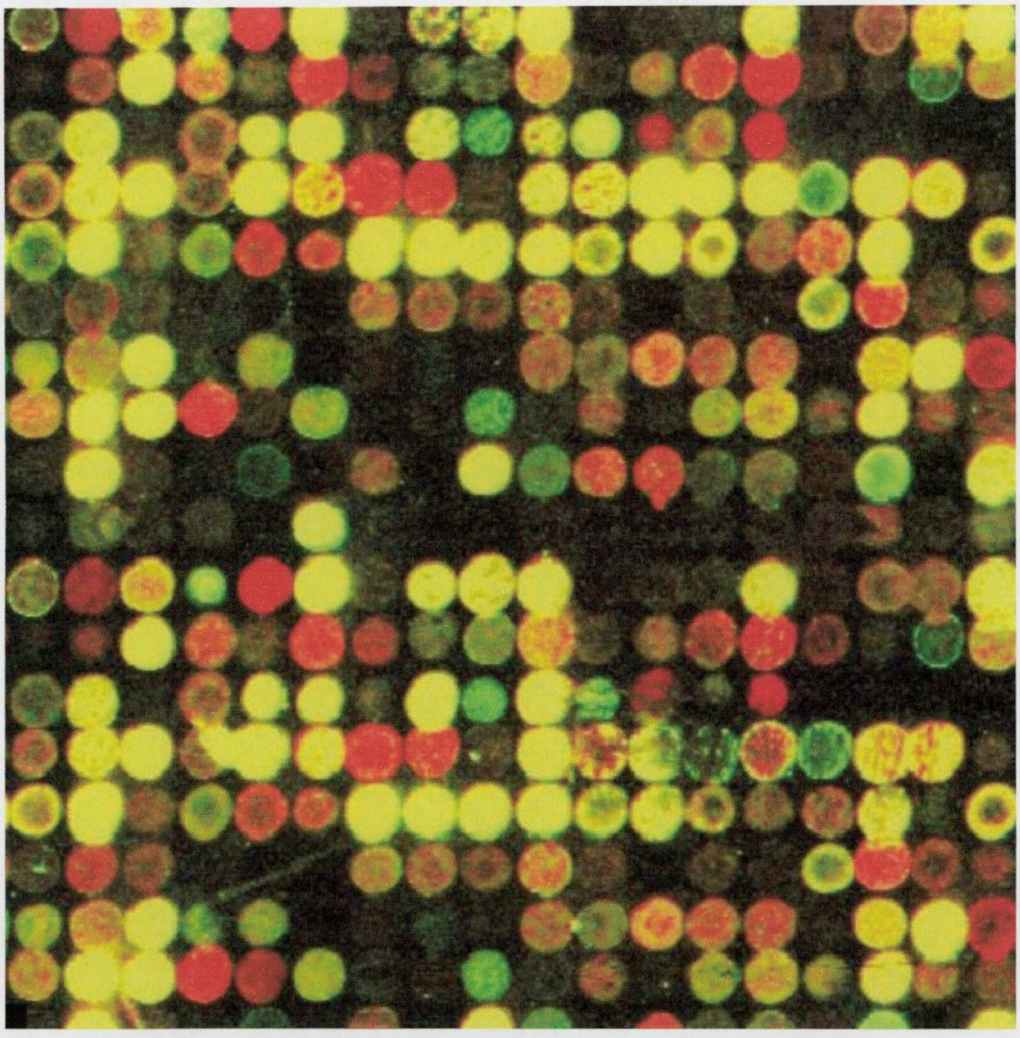

3.b.i. Analysis of DNA-chips

A number of transcripts were differentially expressed between control and treated samples. However, among the 8,000 genes examined in the present study the expression of only 36 genes (0.45%) was found to be significantly altered after treatment with HAL. In case of acute administration of HAL, 13 genes were more highly expressed and 15 transcripts were found to be significantly less abundant. After chronic HAL treatment, however, 9 transcripts were induced and none of them was considerably repressed.

The list of genes with significantly altered expression ($P<0.05$) is delineated in Tables IX-X. Values are presented as the expression ratio of treated / untreated cases for a certain gene. Apart from these known transcripts, a number of expressed sequence tags (ESTs) with unknown function were also differentially expressed in the antipsychotic-treated cortices; these are not listed.

Table IX: List of differentially expressed genes in rat fronto-temporo-parietal cortex after acute (96 hours) treatment with HAL. *A*: over-expressed, and *B*: repressed genes

A:

Clone name (mRNA)	Δ Fold (mean)	Accession number	Functional group
Follistatin-like protein	1.09	AA818445	Cell cycle and growth
Rat basic fibroblast growth factor (FGF) mRNA, complete cds	1.19	M22427	Cell cycle and growth
Protein O-mannosyltransferase 1	1.15	NM_053406	Development
Rattus norvegicus cDNA clone, similar to Human B12 protein mRNA	1.96	AA900186	Ion transport
S100 calcium-binding protein A8 (calgranulin A) (S100A8)	1.41	NM_053822	Ion transport
Glutamate receptor subunit GluR2-flip mRNA, complete cds	1.22	AF164344	Ion transport
Calmodulin 2, mRNA, complete cds	1.13	BC058485	Ion transport
Glutathione S-transferase A5 (Gsta5), mRNA	1.19	NM_031509	Metabolism
Rattus norvegicus similar to eosinophil peroxidase (LOC303414), mRNA	1.21	XM_220834	Metabolism
Adrenal mitochondrial protease	1.97	NM_153311	Protein metabolism
G protein-binding protein CRFG	1.06	NM_053689	Signal transduction
Ly-49 stimulatory receptor 3	1.20	NM_153726	Signal transduction
Rattus norvegicus APP770 mRNA, complete cds	1.76	AF513015	Other

B:

Clone name (mRNA)	Δ Fold (mean)	Accession number	Functional group
Pleiotrophin (heparine binding factor)	-1.11	NM_017066	Cell cycle and growth
Serotonin N-acetyltransferase	-2.15	NM_012818	Circadian rhythm
Activity regulated cytoskeletal-associated protein	-1.99	NM_019361	Development
α-prothymosin	-1.48	M86564	Immune response
Inwardly rectifying K^+-channel	-1.89	D61687	Ion transport
Voltage-dependent calcium channel γ-7 subunit (Cacng7) mRNA, complete cds	-1.21	AF361349	Ion transport
Tyrosine aminotransferase	-2.68	NM_012668	Metabolism
Rattus norvegicus mRNA for endothelial nitric oxide synthase, 3' region, partial	-1.57	AJ011116	Metabolism
Clathrin assembly protein long form	-1.04	AF041374	Protein metabolism
SH3 domain binding protein (CR16)	-1.82	U25281	Protein metabolism
Disintegrin and metalloprotease domain 2	-2.15	NM_020077	Protein metabolism
MIBP1 (c-myc intron-binding protein 1)	-0.99	D37951	Transcription regulator
Gap junction membrane channel β5	-1.24	NM_019241	Cell-cell interaction
Type I pro-α_2 collagen-like sequence	-3.25	AF050214	Other
TPCR09 protein	-2.07	X89698	Other

Table X: List of differentially expressed genes in rat fronto-temporo-parietal cortex after chronic (4 weeks) treatment with HAL

Clone name (mRNA)	Δ Fold (mean)	Accession number	Functional group
Follistatin-like protein	1.58	AA818445	Cell cycle and growth
Transducin-like enhancer of split 4	1.51	NM_019141	Development
K^+-channel (erg2)	1.11	AF016192	Ion transport
Acyl-Coenzyme A dehydrogenase, C-4-12	0.97	NM_016986	Metabolism
Extracellular signal-related kinase (ERK2)	1.02	M64300	Signal transduction
G protein-binding protein CRFG	1.31	NM_053689	Signal transduction
Relaxin-like factor	1.37	AF139918	Signal transduction
Endothelin receptor	1.69	NM_017333	Signal transduction
U2 RNA 3' end	1.59	M10882	Others

In case of RISP, 89 genes (1.11%) were found to significantly differ in expression. Acutely, 43 genes were induced and 46 were down-regulated (Table XI). Chronically, however, this number has decreased to 6 and 11, respectively (Table XII).

3.b.ii. Verification by QRT-PCR

To validate these semi-quantitative results, the expression of randomly selected 7 genes was analyzed by real-time quantitative PCR (QRT-PCR). The PCR primers used in this study are listed in Table XIII. The results for each sample were normalized to β-actin expression, then subjected to *t*-test analysis. All 7 transcripts were still identified as significantly more or less abundant, or unchanged, respectively (Figure 11). Comparison of the results derived from microarraying and the more accurate real-time PCR showed a qualitative agreement in that the differentially expressed genes in HAL or RISP-treated cortices were correctly assigned as up- or down-regulated, or significantly unchanged.

3.b.iii. Significance of genes with altered expression

In this study, we utilized the high-throughput gene chip, which contains 8,000 known genes and ESTs, to determine the alteration of gene expression profiles of rat cortex exposed to antipsychotics. Our results from microarray provided a genome-wide analysis of the cellular response to HAL and RISP treatment:

- *Neural plasticity*

Cellular and molecular responses of neurons to antipsychotic treatment are complex and are likely to be mediated by a variety of regulatory pathways. We found that the molecular response to these drugs in rat cortex involved inhibition or induction of genes, which have specific functions in signal transduction, transcriptional and translational regulation, protein turnover, and cellular metabolism (Tables IX-XII). All of these pathways are inevitable factors of neuronal plasticity. One of the central elements of this process is the activation of glutamatergic transmission.

Table XI: List of significantly A: induced, and B: down-regulated genes in rat fronto-temporo-parietal cortex after acute (96 hours) treatment with RISP

A:

Clone name (mRNA)	Δ Fold (mean)	Accession number	Functional group
Integrin α-subunit	1.13	S58528	Cell adhesion
Integrin β_1	1.70	NM_017022	Cell adhesion
Plakoglobin	2.20	U58858	Cell adhesion
Pleiotrophin (heparine binding factor)	1.11	NM_017066	Cell cycle and growth
KIAA1536 protein	1.28	NM_139190	Cell cycle and growth
Follistatin-like protein	1.96	AA818445	Cell cycle and growth
Protein O-mannosyltransferase 1	1.57	NM_053406	Development
HES-related repressor protein 1 (HERP1)	1.00	AY059382	Development
RING finger protein	2.07	AF036255	Development
Transducin-like enhancer of split 4	1.52	NM_019141	Development
Transmembrane receptor Robo1	1.71	AF041082	Development
T-cell receptor α-chain RT1L haplotype	1.57	L11027	Immune response
Small inducible cytokine subfamily A20	2.31	NM_019233	Immune response
Synaptotagmin VII	1.62	U20106	Protein metabolism
RAB15	2.24	M83679	Protein metabolism
ryk-tyrosine kinase-related protein	2.67	AB073721	Protein metabolism
Janus protein tyrosine kinase 1, JAK1	1.48	AJ000556	Protein metabolism
YME1 (*S. cerevisiae*)-like 1	1.14	NM_053682	Protein metabolism
Aminopeptidase PILS	1.15	AF148324	Protein metabolism
Adrenal mitochondrial protease	1.47	NM_153311	Protein metabolism
Cathepsin K	1.89	AF010306	Protein metabolism
CLN2 tripeptidyl peptidase I	2.35	AB043870	Protein metabolism
Similar to Human B12 protein	1.77	AA900186	Ion transport
K^+-channel (erg2)	2.08	AF016192	Ion transport
Na^+-channel, voltage-gated, type 10a	1.01	NM_017247	Ion transport
Vacuolar adenosine triphosphatase-β	1.40	Y12635	Ion transport
ATPase, Na^+/K^+ transporting, α_1	2.00	NM_012504	Ion transport
Acyl-Coenzyme A dehydrogenase, C-4-12	2.13	NM_016986	Metabolism
Kruppel-like factor LKLF	1.92	AA925780	Transcription regulator
Prophet of Pit1, paired-like homeodomain	1.96	NM_153627	Transcription regulator
Activating transcription factor 3	2.50	NM_012912	Transcription regulator
Splicing factor 1 homolog	1.75	AF079873	Signal transduction
SH-PTP2 protein tyrosine phosphatase 11	2.74	NM_013088	Signal transduction
Receptor activity modifying protein 2	1.00	AB042888	Signal transduction
Interleukin 6 receptor	3.12	NM_017020	Signal transduction
G protein-binding protein CRFG	1.89	NM_053689	Signal transduction
Endothelin receptor	2.04	NM_017333	Signal transduction
P-glycoprotein-like ATP cassette transporter	1.02	AF106563	Transport
Mg1	1.48	AY035343	Others
FSH-regulated protein	1.71	L26292	Others
Integrin-binding sialoprotein	2.14	NM_012587	Others
Ly-49 stimulatory receptor 3	1.84	NM_153726	Others
Neurexin IIIα (axon guidance)	2.84	L14851	Others

B:

Clone name (mRNA)	Δ Fold (mean)	Accession number	Functional group
Neural adhesion molecule F3	-1.37	D38492	Cell adhesion
BIT	-1.12	D38468	Cell adhesion
CD5	-2.60	X78985	Cell adhesion
Growth accentuating protein 43	-1.01	NM_017195	Cell cycle and growth
Serotonin N-acetyltransferase	-1.31	NM_012818	Circadian rhythm
Activity regulated cytoskeletal-associated protein	-2.31	NM_019361	Development
α-actinin 4	-1.19	AF190909	Development
Protein phosphatase 1, regulatory 14a	-2.61	NM_130403	Immune response
α-prothymosin	-1.62	M86564	Immune response
EFA6 exchange factor for ARF6	-1.40	AB040468	Protein metabolism
ARL5 ARF-like protein 5	-1.31	X78604	Protein metabolism
Ubiquitin C (Ubc)	-1.54	NM_017314	Protein metabolism
Clathrin assembly protein long form	-1.61	AF041374	Protein metabolism
SH3 domain binding protein (CR16)	-1.59	U25281	Protein metabolism
Hippocalcin (Hpca)	-1.63	NM_017122	Protein metabolism
Disintegrin and metalloprotease domain 2	-2.15	NM_020077	Protein metabolism
Disintegrin and metalloproteinase domain 1	-1.09	NM_020078	Protein metabolism
Voltage-dependent calcium channel g8	-2.21	NM_080696	Ion transport
Plasma membrane CA^{2+}-ATPase 3	-1.47	M96626	Ion transport
Inwardly rectifying K^{+}-channel	-2.32	D61687	Ion transport
Mitochondrial H^{+}-ATP synthase-α	-1.16	J05266	Ion transport
Uncoupling protein 2, mitochondrial	-1.53	NM_019354	Ion transport
Alkaline phosphatase, tissue-nonspecific	-1.17	NM_013059	Metabolism
Tyrosine aminotransferase	-1.52	NM_012668	Metabolism
γ-glutamylcysteine synthetase	-2.12	NM_017305	Metabolism
MIBP1 (*c-myc* intron binding protein 1)	-1.13	D37951	Transcription regulator
Extracellular signal-related kinase (ERK2)	-1.95	M64300	Signal transduction
Interleukin 10 receptor-α	-2.68	NM_057193	Signal transduction
Basignin (Ox47 antigen or CE-9)	-2.02	NM_012783	Signal transduction
Relaxin-like factor	-1.95	AF139918	Signal transduction
Soluble adenylyl cyclase (SAC)	-2.37	AF081941	Transport
Messenger RNA for preproalbumin	-1.17	V01222	Transport
Vesicular GABA transporter	-1.41	AF030253	Transport
gcd-10S	-1.17	AB046592	Transport
Gap junction membrane channel β5	-1.11	NM_019241	Cell-cell interaction
Type I pro-α_2 collagen-like sequence	-3.77	AF050214	Others
Putative zinc-finger protein	-3.40	AJ007467	Others
U2 RNA 3' end	-2.63	M10882	Others
Glucagon (Gcg)	-2.17	NM_012707	Others
LIM homeodomain protein 3β	-1.61	AF370447	Others
Limkain β1 (Lkap)	-1.38	NM_133421	Others
mud-2	-1.28	U70266	Others
Zinc finger protein 2 (DZF2)	-1.11	U78130	Others
Axomer-8, transported in axons	-1.00	AB097858	Others
DnaJ-like protein (heat shock response)	-1.15	U53922	Others
TPCR09 protein	-1.21	X89698	Others

Table XII: List of significantly A: up-regulated, and B: repressed genes in rat fronto-temporo-parietal cortex after chronic (4 weeks) treatment with RISP

A:

Clone name (mRNA)	Δ Fold (mean)	Accession number	Functional group
Follistatin-like protein	1.09	AA818445	Cell cycle and growth
Protein phosphatase 1, regulatory 14a	2.30	NM_130403	Immune response
Acyl-Coenzyme A dehydrogenase, C-4-12	1.24	NM_016986	Metabolism
Prophet of Pit1, paired-like homeodomain	1.69	NM_153627	Transcription regulator
Extracellular signal-related kinase (ERK2)	1.35	M64300	Signal transduction
Receptor activity modifying protein 2	3.35	AB042888	Signal transduction

B:

Clone name (mRNA)	Δ Fold (mean)	Accession number	Functional group
EFA6 exchange factor for ARF6	-1.04	AB040468	Protein metabolism
Clathrin assembly protein long form	-1.49	AF041374	Protein metabolism
Janus protein tyrosine kinase 1, JAK1	-1.37	AJ000556	Protein metabolism
Inwardly rectifying K^+-channel	-1.65	D61687	Ion transport
Uncoupling protein 2, mitochondrial	-1.25	NM_019354	Ion transport
Alkaline phosphatase, tissue-nonspecific	-1.67	NM_013059	Metabolism
Endothelin receptor	-1.03	NM_017333	Signal transduction
P-glycoprotein-like ATP cassette transporter	-1.13	AF106563	Transport
U2 RNA 3' end	-1.56	M10882	Others
Limkain β1 (Lkap)	-1.16	NM_133421	Others
TPCR09 protein	-0.91	X89698	Others

HAL has been proved to mediate glutamate transmission by interfering with the expression of NMDA-receptor subunits [210] and glutamate transporters [211]. Glutamatergic transmission at either the N-methyl-D-aspartate (NMDA) or α-amino-3-hydroxy-5-methyl-4-isoxazole-propionic acid (AMPA) receptors is one mechanism for an increase in synaptic strength and the induction of central sensitization [212]. Activation of these ionotropic receptors causes a sustained elevation in postsynaptic Ca^{2+} that induces a cascade of persistent intracellular events contributing to synaptic plasticity[212, 213]. Therefore, by acting on the glutamatergic system (*eg.* glutamate receptor subunit GluR2-flip), both HAL and RISP mediate Ca^{2+}-permeability of cells, and therefore mediates synaptic plasticity.

From the gene expression profiles of rat cortices exposed to HAL and RISP, it was also found that many genes are related to cell cycle control. Moreover, we also observed altered expression of genes encoding kinases including extracellular signal-related kinase (ERK2), *ryk*-tyrosine kinase-related protein, Janus protein tyrosine kinase 1, growth factors (*eg.* follistatin-like protein, basic fibroblast growth factor, pleiotrophin), and transcription factors, suggesting that HAL and RISP may also influence cell growth via mediation of multiple cell signal transduction pathways. These results confirm and provide mechanistic information about HAL- and RISP-induced neuro-plasticity.

Table XIII: Primers used in QRT-PCR analysis

Gene product	Forward primer	Reverse primer
Serotonin N-acetyltransferase	ACCGCTTGCCTTCTGAACA	CCCGCTGCTCCCGTTT
Follistatin-like protein	TTTCGTGTATGGCATCAACCA	GCGTCCAATTCCCAAGGA
Inwardly rectifying K^+-channel	AGTGTGGCTGTGGCAAAGG	CCGCAACTCAGGACAAGGA
Guanine nucleotide regulatory protein	CCAGCCTGGCTCCTCAGA	TGTTGCAGTCTCGAATTAGCTTCT
Endothelial nitric oxide synthase	AATAAATTCCCCTTCACGACCTT	CCTGCGGCTGCATCAATAT
Clathrin assembly protein long form	GATTCTGGTGGTGGACTTCTCAA	GGCGGAAGTTTGGCAACA
Rattus norvegicus cDNA clone	GGCCCAGAATGATGAGCAA	TGATTGGCGGCGTCGTA

Figure 11: Quantitative determination of transcript levels by real time PCR

Changes in transcript levels in rat fronto-temporo-parietal cortex after acute or chronic intraperitoneal treatment with HAL (light and dark green box, respectively) or RISP (light and dark blue box, respectively) were confirmed by real time PCR (dashed light and dark green box for HAL, respectively; and dashed light and dark blue box for RISP, respectively). The expression of serotonin-N-acetyltransferase, follistatin-like protein, inwardly rectifying K^+-channel, guanine nucleotide regulatory protein, endothelial nitric oxide synthase, clathrin assembly protein, and a *Rattus norvegicus* cDNA clone was determined. Dashed lines indicate the interval -1.8 to 1.8-fold regulation (corresponding to $\log_2 = 0.85$) in which changes in expression were considered not significant.

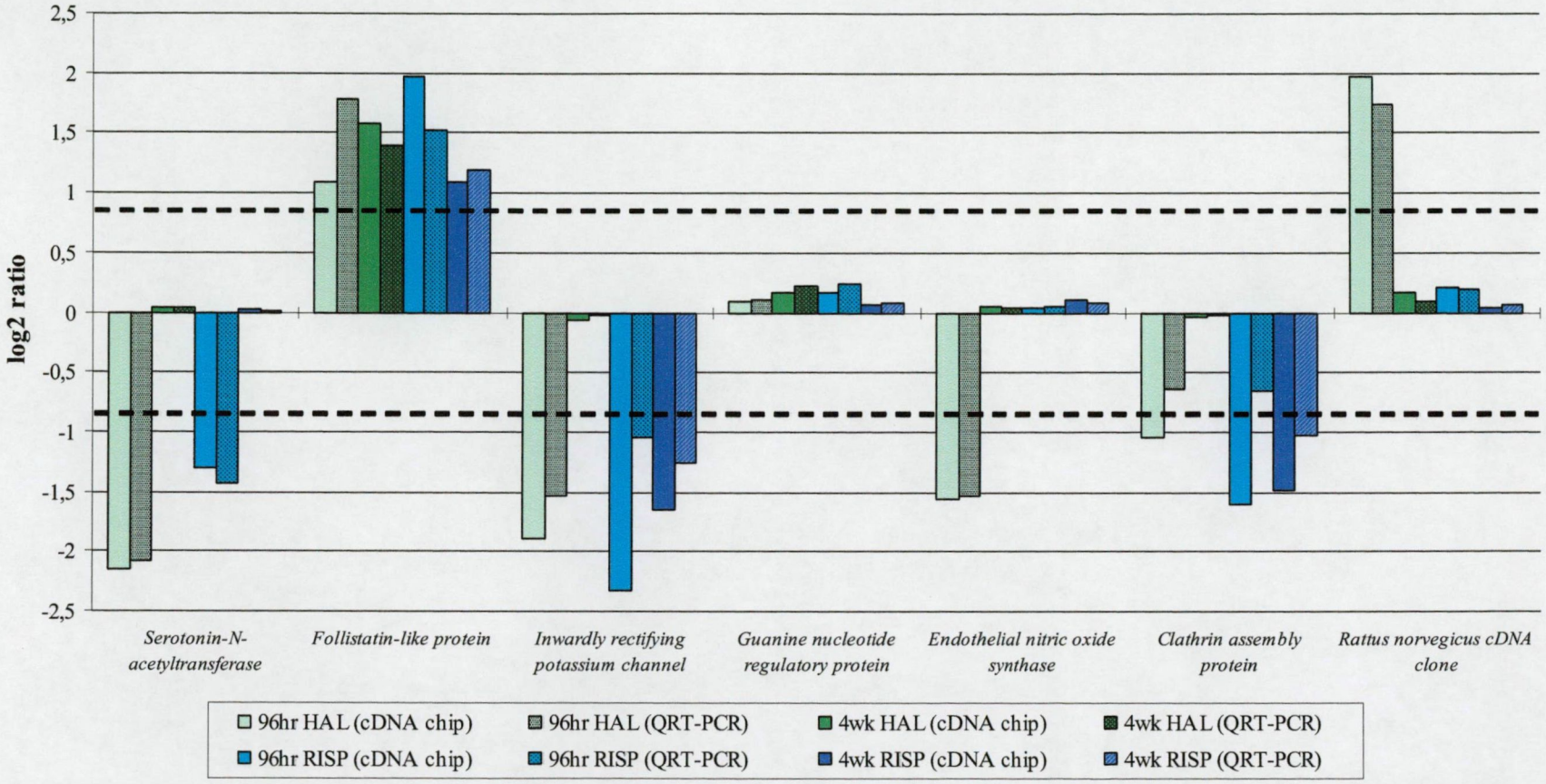

- *Role in neurometabolic disorders*

The results of our analysis implicate on the order of hundreds of genes as being involved in neurodegenerative diseases.

Several genes directly related to Ca^{2+} homeostasis were found to be differentially regulated by HAL and RISP, *eg.* S100 calcium-binding protein A8, calmodulin 2, voltage-dependent calcium channel γ-7 subunit, plasma membrane CA^{2+}-ATPase 3, *etc.* (Tables IX-XII). We have reported alterations of calcium homeostasis in neurometabolic conditions and other medical disorders in the present study. We have also shown that HAL and RISP are efficient in stabilizing $[Ca^{2+}]_i$, and therefore have a protective role in AD and various neuropsychiatric disorders. However, their mechanisms of action remained unknown. Broadly in line with the present findings on gene expression, the Ca^{2+}-stabilizing beneficial effects of these antipsychotics are based on the genomic level by interfering with Ca^{2+}-transporters, Ca^{2+}-channels, glutamatergic transmission, *etc.* (Tables IX-XII).

We have also reported above that HAL up-regulates the level of APP, a key precursor molecule in AD that yields neurotoxic βAP. Interestingly however, as aforementioned, APP might play a crucial role in neuroprotection by participating in cell-to-cell recognition, re-establishment of synaptic contacts, alleviation of glutamate-induced membrane depolarization and over-excitation, and stabilization of the intracellular Ca^{2+} homeostasis[164,194]. HAL therefore may stimulate cytoprotective pathways by inducing APP gene expression, as presented here and above. However, the direct neurotoxic effect of HAL[118-121] may also account for the elevated APP level as a defensive response seen in our experiments after HAL treatment.

The finding that HAL increases APP protein level, as discussed above, is now better explained, in that it is demonstrated here for the first time that HAL up-regulates APP mRNA. Ca^{2+} has been proposed to modify the production and processing of APP[44]. By acting on Ca^{2+}-homeostasis, as we have presented above and herewith, HAL may also indirectly interfere with APP both at the genetic and at the proteome level.

Because of its fundamental roles in regulating synaptic transmission, plasticity, and cell survival, Ca^{2+} homeostasis is undoubtedly altered, at some point in the pathogenesis of AD. The research described here suggests that altered Ca^{2+}-regulation contributes greatly to the pathogenic effects seen in neuropsychiatric conditions. Therefore, targeting Ca^{2+} for potential therapies is therefore worth consideration.

It is proposed in this study that relatively stable levels (*ie.* slight oscillations) of Ca^{2+} leads to normal or non-amyloidogenic APP processing (sAPPα-Ca^{2+} feed back, Figure 9), whereas pathological increase or decrease in Ca^{2+} triggers amyloidogenic APP metabolism (βAP-Ca^{2+} feed forward cascade, Figure 8), as discussed in this study. This provides a fine tuning mechanism in APP regulation. Both sAPPα and βAP have been demonstrated to modulate cytoplasmic Ca^{2+} concentration[43,84], raising the possibility that these compounds may regulate their own formation. Also, the biphasic regulation in AD fibroblasts presented in this thesis is well established. βAP results in aberrant regulation of $[Ca^{2+}]_i$ such that there is an enhancement of acute activation (*ie.* elevated levels), followed by a sustained depression of Ca^{2+}-concentration and signaling, when cells are exposed

to βAP and other insults[214]. Subtle alterations in this metabolic balance over a long period of time are likely to influence cellular homeostasis, be it proteomic, ionic, genetic, or other. Therefore, Ca^{2+}-stabilizing interventions should be considered the foundation of treating dementing neurodegenerative conditions.

Because abnormalities in Ca^{2+} homeostasis are also present in psychosis[215,216,217] and depression[218,219], both associated with AD, this study points out that these psychiatric disturbances manifest in dementia because of the Ca^{2+}-imbalance present in the primary disease. It is not difficult to see how disruption of a single interaction (*ie.* Ca^{2+} dysregulation) can have multiple flow-on effects to other cellular processes. Based on the protective role of antipsychotics regarding Ca^{2+}-imbalance, antipsychotics may constitute future treatment strategies aimed at alleviating BPSD and the cognitive symptomatology of AD. The use of antipsychotic drugs to treat dementia and co-morbidities associated with AD is apparently justified at the molecular level with respect to Ca^{2+}.

The involvement of Ca^{2+} has been implicated in neurometabolic disorders other than AD and its corollary symptoms, such as in Parkinson's[220], Huntington's[221], amyotropic lateral sclerosis[222], SCH[215-217], muscular dystrophy[223], *etc.*, suggesting a broad-spectral role of Ca^{2+} in neuropsychiatric disorders. A great number of articles were devoted to Ca^{2+} in brain physiology and pathology, but literally no paper has ever studied the role for Ca^{2+} at the holistic level. Broadly in line with the above findings, this study proposes that disturbing the central secondary messenger, Ca^{2+}, plays pivotal roles in various, if not all neurometabolic disorders. Impaired Ca^{2+} homeostasis has different functional consequences that mainly involve mechanisms to compensate Ca^{2+} imbalance. Environmental and genetic factors may determine that these functional compensatory mechanisms involve which of the many tertiary and quaternary messenger systems, yielding differing brain pathology, *ie.* altered Ca^{2+} leads to β-amyloid deposition in Alzheimer's, α-synucleinopathy in Parkinson's, accumulation of Lewy bodies, *etc.* This is supported by the existence of overlapping disorders (*eg.* AD with Lewy-bodies) and frequent co-morbid conditions (*eg.* depression in most neuropsychiatric maladies), as described earlier.

The central role of Ca^{2+} in various diseases of the man is signified not only in neuropsychiatric disorders, but also in many medical conditions. Ca^{2+}-channel blockers, for example, in arrhythmias, cardiac failure and hypertension, have proved to efficiently restore Ca^{2+} homeostasis. Moreover, Ca^{2+}-channel blockers were reported to limit cellular degeneration[224]. This thesis, therefore, proposes a new approach to Ca^{2+} imbalance at the holistic level (Figure 12).

Therefore, stabilizing calcium levels with Ca^{2+}-channel blockers, calmodulin antagonists, *etc.* may slow or inhibit the progression of and may reverse several neurometabolic disorders, and conditions afflicting other organs, too.

Figure 12: Proposed central role of Ca^{2+} in (neurometabolic) diseases

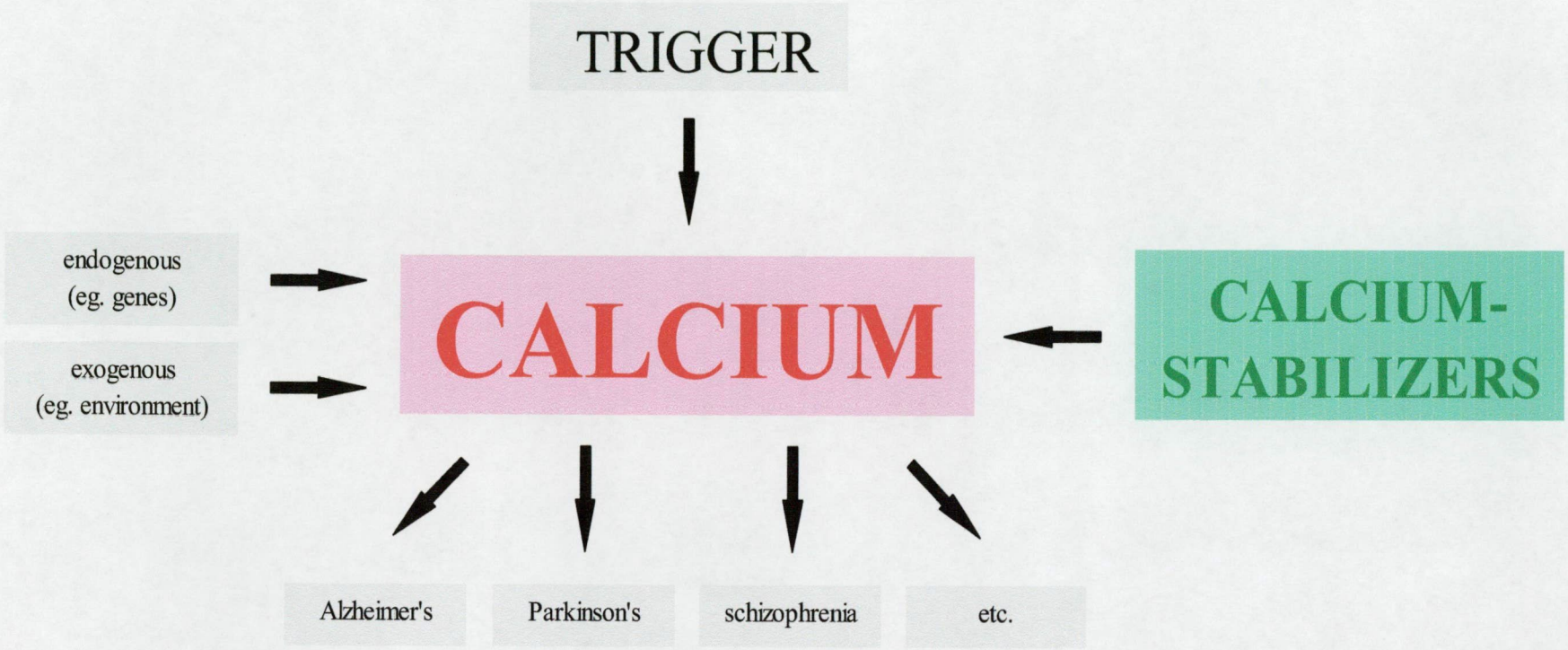

- *Stress and neurotoxicity*

Documented consequences of HAL treatment are neurotoxicity and apoptosis[118-121], which apparently may be attributable to its impact on the central secondary messenger, Ca^{2+}. Despite its molecular and clinical adverse effects, HAL is widely used in the treatment of psychiatric symptoms associated with various medical conditions where the involvement of Ca^{2+} is implicated, such as in AD. Interestingly, we have demonstrated above that HAL efficiently attenuates βAP-induced Ca^{2+}-imbalance in AD, which is in controversy with the present findings regarding Ca^{2+}. Most, if not all, genes in mammalian cells are regulated by multiple mechanisms acting in concert to regulate their expression. As gene products change in response to cellular needs, it is likely that the repertoire of regulatory mechanisms influencing the expression of these genes also changes. It is likely, therefore, that HAL disrupts Ca^{2+}-levels to cause apoptosis, however in an already disturbed setting, *eg.* in AD, it acts as a cytoprotective agent by inflaming defensive mechanisms such as inducing APP expression and level.

Another major category of differentially regulated genes encode for cell defense proteins, which include anti-oxidative stress proteins and heat shock proteins. The majority of these transcripts were differentially expressed in HAL and RISP-treated animals.

Oxidative stress can occur as a result of a number of stimuli. During aerobic metabolism under stress, reactive oxygen species (ROS) are produced as a result of partial reduction of oxygen. ROS were originally considered to be detrimental to cells, but recently it has been shown that it is involved in redox regulation by adjusting cellular activities[225]. These ROS induce the expression of defense-related genes such as those encoding glutathione-S-transferase (GST). In this study, the GST- and peroxidase enzyme-encoding genes were both up-regulated after treatment with HAL (Table IX/A). Glutathione acts as a redox-sensor and is involved in the multiple regulatory systems coordinating the expression of defense genes[226], therefore the increasing glutathione biosynthetic capacity could enhance resistance to oxidative stress. Because HAL is known to be toxic to cells, up-regulation of defense genes might be a compensatory mechanism, just as discussed with the induction of APP.

- *Effect on the dopaminergic system*

Antipsychotics had been assumed to suppress DA-mediated neurotransmission either by decreasing brain DA-levels (*eg.* reserpine) or by antagonizing D_2-receptors. Contrary to the hyper-dopaminergic hypothesis, some previous data indicate a reduced central DA output associated with SCH, a phenomenon that was found to correlate with negative symptoms, such as anergia, emotional blunting, lack of drive, *etc*[227]. Consequently, both hypo- and hyperfunctioning of brain DA-systems in SCH have been proposed and, tentatively, both types of dysfunction might even occur simultaneously, albeit in different brain regions. Responsiveness of both negative and positive symptoms of SCH to antipsychotics has been documented in clinical settings. Importantly, however, no effect on DA metabolism and transmission were significantly altered by HAL or RISP in our experiments at the genetic level. Their antipsychotic effect therefore is not by modifying DA turnover and bioavailability or modifying genes encoding for D_2-receptors, but by fine-tuning signal transduction pathways. By acting on intracellular signaling, HAL and RISP are potent inductors of neuronal plasticity.

As such, they are hypothesized to have an impact on remodeling pathological dopaminergic and glutamatergic neuronal circuits seen in SCH and other neuropsychiatric conditions as part of their modes of action.

Interestingly, however, both HAL and RISP significantly altered the expression of endothelin. There is increasing evidence that endothelins and endothelin receptors play a role in brain mechanisms associated with behavior and neuroendocrine regulation, as well as cardiovascular control. A growing mass of data suggests that they may be acting as true neurotransmitters or neuromodulators. They are known to stimulate DA-release in the CNS[228]. The effects of endothelin in the brain could be a continuum from physiologically relevant neuromodulatory effects at low concentrations, through reversible hypermetabolism at higher doses, to permanent neurotoxic neuronal damage at very high concentrations.

Altered expression of the endothelin-system as a result of administration of either of the two antipsychotics underlying these neurochemical effects do not necessarily have to be different. While it is clear that physiological activation of endothelin receptors induces a rise in intracellular Ca^{2+} levels [229], supra-physiological levels of Ca^{2+}-influx have been associated with neurotoxic events[230]. This may add to the well-known toxic effect of HAL. Alternatively, it is possible that the low-dose, physiological action of endothelin is mediated by a direct effect on dopaminergic terminals, whereas the high-dose effect also involves other mechanisms, such as glutamate and NO release[231]. It is well-known that the high levels of glutamate may induce neurotoxic effects in the brain, further explaining the neurotoxic effect of HAL.

Taken together, the impact of HAL and RISP on the dopaminergic system might be accomplished not directly, as suggested above, but via the novel neuro-transmitter/modulator endothelin system.

- *Commonalities*

The focus of this study was the identification of genes after treatment of rats with HAL and RISP. Even though there was an overlap of only a few genes at exposure to HAL and RISP, both drugs have interfered with the same cellular functions. RISP acutely had an impact on more genes than HAL. This might be attributable to the fact that the mode of action of RISP is more diverse: it is a high potential D_2-, $5HT_2$- and NA-antagonist, whereas HAL is a D_2-antagonist with some σ_1-activity. Taken together, this observation suggests that antipsychotics with different pharacological characteristics share targets at the molecular level.

Interestingly, some significantly enriched pathways differ after treatment with both drugs over time. Transcripts implicated in neuronal plasticity, survival, oxidative changes and metabolism in general are widely interfered with by HAL and RISP in our acute experiments, but these antipsychotic drugs had less diverse impact on these genes, or did not change chronically their expression profile (Tables IX-XII). This finding is well established, since high potential agents like HAL and RISP are thought to have more profound impact on initiating therapy. Chronically, however, drastic changes subside.

Whereas conventional neurological assessment utilizes behavioral, functional, and/or morphological techniques to estimate overt effect of drugs, new methods are being developed that identify molecular changes on the gene expression level that are associated

with medical treatment. Based on our findings, gene expression profiling is an invaluable method for delineating the neuro-psycho-pharmacological actions of antipsychotics by simultaneuously identifying thousands of genes modulated in response to drug exposure, and it allows the determination of genes responsible for treatment failure or development of drug resistance.

Additionally, cDNA arrays permit the measurement of early gene expression events in cells rather than cumulative systemic effects and, thus, may provide a means of early detection of therapeutic effects. Microarrays have considerable potential to define in molecular terms the progression of a disease and identify biochemical pathways that can be used as targets for future therapeutic intervention. The identification of unique gene expression patterns associated with cellular responses to a particular chemical or class of chemicals can be used in conjunction with a variety of pharmacological assessment platforms to identify the presence of both physiologically and medically useful substances. The feasibility of using DNA arrays for this assessment depends on the ability of this technology to identify reproducible gene expression signatures from relatively small quantities of RNA.

The use of QRT-PCR in combination with the microarray work ruled out the dissociation of protein translation from gene transcription. Therefore, gene expression profiling can be a powerful tool with which to compare the mechanisms of action of different agents, which elicit similar biological responses. As such, our study would serve as a platform for all further investigation of the molecular effects of HAL and RISP in rats and humans. Elucidation of the metabolic and signal transduction pathways and gene transcription factors that underlie the pathophysiology of neuropsychiatric disorders and the actions of various medications could also reveal targets for the development of novel therapeutic agents. The continued application of major advances in molecular and cellular neurobiology to psychiatric problems over the coming years holds a bright future for the treatment, and possibly prevention, of AD and other neurometabolic disorders.

SUMMARY

1. *Fibroblasts and lymphocytes show biochemical differences in AD by exhibiting abnormal Ca^{2+} homeostasis.*
2. *Biphasic effect of βAP may shed new light on understanding cellular alterations in dementia and differences between tissue-specific pathologies in the same condition.*
3. *Biochemical alterations in the periphery may support the diagnosis of AD, may help monitoring the progression of the disease and responsiveness to treatments.*
4. *HAL and RISP are potent in antagonizing βAP-induced Ca^{2+}-imbalance.*
5. *These antipsychotics are safe with respect to APP metabolism, and acute HAL (ie. pulse-therapy) might be beneficial on APP processing in AD.*
6. *A "protective cycle" of antipsychotics is proposed in AD.*
7. *HAL and RISP are involved in interfering with the expression of a large array of genes involved in Ca^{2+}-signaling, survival and cellular plasticity.*
8. *Antipsychotics with different pharmacological characteristics share targets at the molecular level, including Ca^{2+}-homeostasis.*
9. *Ca^{2+} is central in the pathogenesis of AD, and agents targeting Ca^{2+} may slow or inhibit the progression of and might even reverse AD and its corollary symptoms.*
10. *Ca^{2+} might be a unifying molecule in most neurodegenerative disorders and also in metabolic diseases afflicting extraneuronal organs.*

ACKNOWLEDGEMENTS

First of all, the active participation of the *volunteers* in the ongoing study is highly appreciated.

I thank *Dr. Gábor Laskay* for always giving me a helping hand in understanding the pickiest details of fluorimetric studies. He taught me everything I will ever know about spectrofluorimetry. Sharing his teaching and research experiences with me has been a springboard for my scientific career.

I am grateful to *Prof. Dr. Lajos Kemény, Dr. Anna Kenderessy-Szabó* and their colleagues at the Department of Dermatology, University of Szeged, Hungary, for providing me with the skin samples and fibroblast cultures.

I would also like to thank my colleagues at the Department of Experimental Surgery, University of Szeged, Hungary, in granting me unlimited access to the Hitachi F-2000 spectrofluorimeter.

I acknowledge the assistance of each and every co-workers at the Alzheimer's Disease Research Center, University of Szeged, including *Prof. Dr. Péter Kása, Dr. Magdolna Pákáski, Marietta Hugyecz* and colleagues. The assistance and friendship of *László Kálmán* of the same institute is highly valued.

I am indebted to *Dr. László G. Puskás* and his colleagues of the Laboratory of Functional Genomics, Biological Research Center of the Hungarian Academy of Sciences, for assisting in the cDNA-micro-chips.

I am gratified that my clinical directors, *Prof. Dr. György Lázár* of the Department of Surgery and *Dr. Gábor Bogáts* of the Division of Cardiac Surgery, University of Szeged, Hungary, permitted me to conduct this research parallel with my daily routine in cardiac surgical patient care.

I am obliged for the co-operation of the staff of the Department of Psychiatry, University of Szeged, Hungary. I also appreciate *Dr. Anna Juhász* for her assistance in taking care of the biological samples and cultures. Predominantly, I owe gratitude with deepest respect to *Prof. Dr. Zoltán Janka* and *Dr. János Kálmán* for their scientific partnership, helping hand, encouragement, incessantly magnificent aid, lift, moral support, and friendship.

Above all, words cannot convey how thankful I am to *Prof. Dr. Botond Penke* of the Department of Medical Chemistry, University of Szeged, Hungary, for his contribution to this work in endlessly giving perpetual advice, hand, comfort, care, encouragement, and for being the most sincere counterpart & friend of mine I have ever worked with.

My admiration to my family and loved ones for closing ranks behind me all my life, and to my brother, *Dr. Miklós Palotás*, of the Department of Anesthesiology and Intensive Therapy, University of Szeged, Hungary, for collaborating with me throughout this study is self-explanatory.

I would also like to express my gratefulness to my fellow scientific colleagues and friends, *Dr. Yoo-Hun Suh* of Seoul National University, South Korea, *Dr. Mark P. Mattson* at the National Institute on Aging, USA, *Dr. Jefferey L. Cummings* of UCLA School of Medicine, USA, and *Dr. Alexei Koudinov* of the Russian Academy of Sciences, Russia, for permitting me to reproduce some of their theoretical work in this thesis, and for giving me future directions.

Finally, I highly value the assistance of all of my work-mates whom are not listed here by name.

LIST OF PUBLICATIONS

1. **Cumulative impact factor:**
   64.573

2. **Number of publications:**
   22

3. **List of articles relevant to this thesis**

Palotás A, Penke B, Palotás M, Kenderessy SzA, Kemény L, Kis E, Vincze G, Janka Z, Kálmán J. Haloperidol attenuates β -amyloid-induced calcium imbalance in human fibroblasts. Skin Pharmacol. Physiol. 2004; 17: 195-199.
Impact factor (2003): 1.529

Palotás A, Pákáski M, Palotás M, Hugyecz M, Molnár J, Penke B, Janka Z, Kálmán J. Effect of haloperidol and risperidone on amyloid precursor protein levels *in vivo*. Brain Res. Bull. 2003; 62: 93-99.
Impact factor: 2.609

Palotás A, Janka Z, Penke B, Kálmán J. Risperidone antagonizes β-amyloid peptide-induced intracellular calcium level changes in fibroblasts. Neuropsychopharm. Hung. 2003; V/3: 138-142.
Impact factor: 0

Palotás A, Kálmán J, Palotás M, Kemény L, Janka Z, Penke B. Long-term exposition of cells to β-amyloid results in decreased intracellular calcium concentration. Neurochem. Int. 2003; 42: 543-547.
Impact factor: 3.261

Palotás A, Kálmán J, Palotás M, Juhász A, Janka Z, Penke B. β-amyloid-induced increase in the resting intracellular calcium concentration gives support to tell Alzheimer lymphocytes from control ones. Brain Res. Bull. 2002; 58: 203-205.
Impact factor: 2.283

Palotás A, Kálmán J, Laskay G, Juhász A, Janka Z, Penke B. Comparative studies on $[Ca^{2+}]_i$-level of fibroblasts from Alzheimer patients and control individuals. Neurochem. Res. 2001; 26: 817-820.
Impact factor: 1.638

4. **List of articles directly not connected to this work**

Palotás A, Puskás LG, Kitajka K, Palotás M, Molnár J, Pákáski M, Janka Z, Penke B, Kálmán J. Altered response to mirtazapine on gene expression profile of lymphocytes from Alzheimer's patients. Eur. J. Pharmacol. 2004; 497: 247-254.
Impact factor (2003): 2.352

Palotás M, **Palotás A**, Puskás LG, Kitajka K, Pákáski M, Janka Z, Molnár J, Penke B, Kálmán J. Gene expression profile analysis of the rat cortex following treatment with imipramine and citalopram. Int. J. Neuropsychopharmacol. 2004; 7: 1-13.
Impact factor (2003): 4.000

Palotás A, Puskás LG, Kitajka K, Palotás M, Molnár J, Pákáski M, Janka Z, Penke B, Kálmán J. The effect of citalopram on gene expression profile of Alzheimer lymphocytes. Neurochem. Res. 2004; 29: 1563-1570.
Impact factor (2003): 1.511

Palotás A, Lázár Gy, Paszt A, Szentpáli K. Alkali ingestion predisposes to developing giant mid-esophageal pulsion diverticulum – a report of a medical rarity. Med. Hypotheses 2004; 62: 931-934.
Impact factor (2003): 0.684

Palotás A, Penke B, Kemény L, Janka Z, Kálmán J. A chapter in the unity of variety – calcium is the sole author? Brain Res. 2004; 1000: 57-59.
Impact factor (2003): 2.474

Szentpáli K, **Palotás A**, Wolfárd A, Tiszlavicz L, Balogh Á. A gastrointestinal stromal tumor presenting in a perforated Meckel's diverticulum. Can. J. Surg. 2004; 47: 70.
Impact factor (2003): 0.627

Szentpáli K, **Palotás A**, Lázár Gy, Paszt A, Balogh Á. Endoscopic intubation with conventional plastic stents – a safe and cost-effective palliation for inoperable esophageal cancer. Dysphagia 2004; 19: 22-27.
Impact factor (2003): 1.091

Kálmán J, Juhász A, Rimanóczy Á, **Palotás A**, Palotás M, Boda K, Márki-Zay J, Csibri É, Janka Z. The nitric oxide synthase-3 codon 298 polymorphism is not associated with late-onset sporadic Alzheimer's dementia and Lewy body disease in a sample from Hungary. Psychiat. Genet. 2003; 13: 201-204.
Impact factor: 2.414

Palotás A, Szentpáli K, Paszt A, Balogh Á, Lázár Gy. Palliation of inoperable esophageal tumor with endoscopic intubation. Magy. Onkol. 2003; 47: 385-389.
Impact factor: 0

Palotás M, **Palotás A**, Pákáski M, Hugyecz M, Janka Z, Penke B, Kálmán J. Effect of antidepressants on the metabolism of amyloid precursor protein in rat brain. Neuropsychopharm. Hung. 2003; V/3: 133-137.
Impact factor: 0

Palotás A, Paszt A, Szentpáli K, Lázár Gy. Esophageal cancer complicated with azygos continuation of the inferior vena cava. Int. Cardiovasc. Thorac. Surg. 2003; 2: 361-363.
Impact factor: 0

Kálmán J, Juhász A, Rimanóczy Á, **Palotás A**, Palotás M, Szabó Z, Boda K, Márki-Zay J, Janka Z. Lack of influence of the apolipoprotein E genotype on the outcome of selegiline treatment in Alzheimer's disease. Dement. Geriatr. Cogn. Disord. 2003; 16: 31-34.
Impact factor: 2.445

Szentpáli K, **Palotás A**, Balogh Á, Lázár Gy. Medical and surgical evaluation of Barrett's esophagus and Barrett's cancer. Chir. Gastroenterol. 2003; 19: 176-180.
Impact factor: 0.157

Palotás A, Kálmán J, Palotás M, Matin K, Szentpáli K, Paszt A, Janka Z, Penke B. Whole blood samples from Alzheimer patients and control donors demonstrate fluorimetric differences. Neurochem. Res. 2002; 27: 1581-1583.
Impact factor: 1.672

Palotás A, Kálmán J, Palotás M, Juhász A, Janka Z, Penke B. Fibroblasts and lymphocytes from Alzheimer patients are resistant to β-amyloid-induced increase in the intracellular calcium concentration. Prog. Neuro-Psychopharmacol. Biol. Psychiatry. 2002; 26: 971-974.
Impact factor: 1.433

Palotás A, Kálmán J, Laskay G, Juhász A, Janka Z, Penke B. β-amyloid peptide-induced intracellular calcium level changes in Alzheimer fibroblasts. Clin. Neurosci./Ideggy. Szle. 2002; 55: 164-167.
Impact factor: 0

5. List of abstracts presented at scientific meetings

Palotás A, Penke B, Kemény L, Janka Z, Kálmán J. Calcium-approach to neurodegeneration. FENS Abstr. 2004; 2: 159.20.
Impact factor: 0

Palotás A, Penke B, Kemény L, Janka Z, Kálmán J. Neurodegenerative disorders: a single disease? Eur. Psychiatry 2004; 19/Suppl.1: 152.
Impact factor (2003): 1.329

Palotás A, Penke B, Kemény L, Janka Z, Kálmán J. New chapter in skin biopsy: diagnostic tool for neurodegenerative disorders. 1st International Meeting on Neurobiology of the Skin. 2004. Münster, Germany.
Impact factor: 0

Palotás A, Penke B, Kemény L, Janka Z, Kálmán J. Calcium in neurodegenerative disorders – a holistic approach. J. Neurochem. 2004; 88/Suppl.1: 53
Impact factor (2003): 4.825

Palotás A. Effect of antipsychotics on β-amyloid-induced calcium-imbalance on fibroblasts. Clin. Neurosci./Ideggy. Szle. 2003; 56: 342
Impact factor: 0

Hugyecz M, Pákáski M, Bjelik A, **Palotás A**, Palotás M, Molnár J, Janka Z, Kálmán J. *In vivo* and *in vitro* effects of hydroxizine on the metabolism of amyloid precursor protein. Clin. Neurosci./Ideggy. Szle. 2003; 56: 334
Impact factor: 0

Bjelik A, Pákáski M, Hugyecz M, **Palotás A**, Palotás M, Molnár J, Janka Z, Kálmán J. *In vivo* treatment with the antidepressant imipramine and the amyloid precursor protein metabolism. Clin. Neurosci./Ideggy. Szle. 2003; 56: 331
Impact factor: 0

Palotás A, Janka Z, Penke B, Pákáski M, Hugyecz M, Palotás M, Kálmán J. Effect of antipsychotics on amyloid-precursor protein level. First International Conference of the National Neuroscience Society of Romania. 2003. Bucharest, Romania.
Impact factor: 0

Palotás A, Janka Z, Penke B, Palotás M, Kálmán J. Antipsychotics in the treatment of Alzheimer's disease. Acta Neurobiol. Experiment. 2003; 63 Suppl: 36
Impact factor: 0.694

Palotás A, Kálmán J, Palotás M, Janka Z, Penke B. Beneficial effect of haloperidol in Alzheimer's disease. Eur. J. Neurology 2003; 10/Suppl.1: 226
Impact factor: 2,000

Palotás A, Palotás M, Janka Z, Penke B, Kálmán J. Alzheimer-specific biochemical alterations in the periphery. 6th AD/PD Abstr. 2003; 1: 48
Impact factor: 0

Palotás A, Palotás M, Janka Z, Penke B, Kálmán J. Haloperidol stabilizes calcium-imbalance in Alzheimer's disease. J. Neurochem. 2003; 87/Suppl.1: 92
Impact factor: 4.825

Palotás A, Palotás M, Janka Z, Penke B, Kálmán J. Haloperidol attenuates β-amyloid-induced calcium-imbalance. IBRO Abstr. 2003; 1: 100
Impact factor: 0

Palotás A, Paszt A. Surgical management of esophageal cancer complicated with azygos continuation utilizing neoadjuvant chemo-radiation. ESS Abstr. 2002; 1: 53
Impact factor: 0

Palotás A, Palotás M, Pákáski M, Hugyecz M, Kása P, Janka Z, Kálmán J. Effects of antipsychotic treatment on the amyloid-precursor-protein metabolism *in vivo*. Clin. Neurosci./Ideggy. Szle. 2002; 55/Suppl.1: 11
Impact factor: 0

Palotás M, **Palotás A**, Pákáski M, Hugyecz M, Kása P, Janka Z, Kálmán J. *In vivo* effect of antidepressants on amyloid precursor protein metabolism. Clin. Neurosci./Ideggy. Szle. 2002; 55/Suppl.1: 11-12
Impact factor: 0

Palotás A, Palotás M, Pákáski M, Hugyecz M, Kása P, Janka Z, Kálmán J. Typical and atypical antipsychotic drugs in Alzheimer's disease. Neuropsychopharm. Hung. 2002; IV/Suppl.1: 25
Impact factor: 0

Palotás M, **Palotás A**, Pákáski M, Hugyecz M, Kása P, Janka Z, Kálmán J. Antidepressant treatment in Alzheimer's disease. Neuropsychopharm. Hung. 2002; IV/Suppl.1: 25-26
Impact factor: 0

Palotás A, Kálmán J, Palotás M, Juhász A, Janka Z, Penke B. Biphasic effect of β-amyloid peptide. Int. J. Psychophysiol. 2002; 25: 143
Impact factor: 2.055

Palotás A, Kálmán J, Palotás M, Juhász A, Janka Z, Penke B. β-amyloid peptide: a calcium antagonist? Neurobiol. Aging 2002; 23/Suppl.1: 390-391
Impact factor: 6.155

Pákáski M, Kálmán J, Palotás M, **Palotás A**, Juhász A, Molnár J, Hugyecz M, Janka Z. Imipramine and citalopram modify the amyloid precursor protein metabolism. Neurobiol. Aging 2002; 23/Suppl.1: 392
Impact factor: 6.155

Palotás A, Kálmán J, Palotás M, Juhász A, Janka Z, Penke B. β-amyloid-induced decrease in the intracellular calcium level. Can. J. Neurol. Sci. 2002; 29/Suppl.1: 17
Impact factor: 1.014

Palotás A, Kálmán J, Palotás M, Juhász A, Janka Z, Penke B. β-amyloid peptide decreases the calcium concentration of cells on the long-run. FENS Abstr. 2002; 1: 222.14
Impact factor: 0

Kálmán J, Pákáski M, Palotás M, **Palotás A**, Juhász A, Molnár J, Hugyecz M, Janka Z. Imipramine and citalopram modify the amyloid precursor protein metabolism. Int. J. Neuropsychopharmacol. 2002; 3/Suppl.1: 14
Impact factor: 3.341

Palotás A. Fibroblast and Alzheimer's disease. Conference for Young Scientists of the Albert Szent-Györgyi Medical University. 1999. Szeged, Hungary.
Impact factor: 0

Palotás A. Role of amyloid peptides in the pathogenesis of Alzheimer's disease. Conference for Young Scientists of the Albert Szent-Györgyi Medical University. 1998. Szeged, Hungary.
Impact factor: 0

Palotás A, Huszka Cs. Effect of β-amyloid peptides on primary rat astroglia cultures. Conference for Young Scientists of the Albert Szent-Györgyi Medical University. 1997. Szeged, Hungary.
Impact factor: 0

REFERENCES

1 Alzheimer A. Über eine eigenartige Erkrankung der Hirnrinde. Allgemeine Zeitschrift für Psychiatrie und Psychisch-gerichtliche Medizin 1907; 64: 146-148.

2 Brookmeyer R, Gray S, Kawas C. Projections of Alzheimer's disease in the United States and the public health impact of delaying disease onset. Am. J. Public Health 1998; 88: 1337-1342.

3 American Psychiatric Association, Diagnostic and Statistical Manual of Mental Disorders. 4th Ed. Washington, D.C., 1994.

4 Tariska P. A gerontopszichiátriai beteg komplex klinikai vizsgálata. In: Simkó A (Ed) A gerontopszichiátria aktuális kérdései. Print-X, Budapest, 1994.

5 Tariska P. Alzheimer-kór: okok, tünetek, diagnózis, differenciáldiagnózis, terápiás lehetőségek. Golden Book, Budapest, 2000.

6 Tariska I. Az öregedő agy. In: Tariska I (Ed) Öregkori ideg- és elmegyógyászati kórképek. Medicina, Budapest, 1967.

7 Tariska P. A demencia mai szemlélete. Animula, Budapest, 1988.

8 Small GW, Rabins PV, Barry PP, Buckholtz NS, DeKosky ST, Ferris SH, Finkel SI, Gwyther LP, Khachaturian ZS, Lebowitz BD, McRae TD, Morris JC, Oakley F, Schneider LS, Streim JE, Sunderland T, Teri LA, Tune LE. Diagnosis and treatment of Alzheimer's disease and related disorders. Consensus statement of the American Association for Geriatric Psychiatry, the Alzheimer's Association, and the American Geriatrics Society. JAMA 1997; 278: 1363-1371.

9 Rabins PV, Lyketsos CG, Steele CD. Practical Dementia Care. New York: Oxford University Press.

10 Tariska P. Gyakorlati útmutató az emlékezészavarok általános orvosi megközelítéséhez. Pharma Press, Budapest, 1995.

11 Selkoe DJ, Abraham CR, Podlisny MB, Duffy LK. Isolation of low-molecular-weight proteins from amyloid plaque fibers in Alzheimer's disease. J. Neurochem. 1986; 46: 1820-1834.

12 Masters CL, Simms G, Weinman NA, Multhaup G, McDonald BL, Beyreuther K. Amyloid plaque core protein in Alzheimer disease and Down syndrome. Proc. Natl. Acad. Sci. USA 1985; 82: 4245-4249.

13 Glenner GG, Wong CW. Alzheimer's disease: initial report of the purification and characterization of a novel cerebrovascular amyloid protein. Biochem. Biophys. Res. Commun. 1984; 120: 885-890.

14 Cummings JL, Vinters HV, Cole GM, Khachaturian ZS. Alzheimer's disease: etiologies, pathophysiology, cognitive reserve, and treatment opportunities. Neurology 1998; 51: S2-S17.

15 Whitehouse PJ, Price DL, Struble RG, Clark AW, Coyle JT. Alzheimer's disease and senile dementia: loss of neurons in the basal forebrain. Science 1982; 215: 1237-1239.

16 Kidd M. Paired helical filaments in electron microscopy of Alzheimer's disease. Nature 1963; 197: 192-193.

17 Terry RD. The fine structure of neurofibrillary tangles in Alzheimer's disease. J. Neuropathol. Exp. Neurol. 1963; 22: 629-642.

18 Trojanowski JQ, Lee VM. Paired helical filament tau in Alzheimer's disease. The kinase connection. Am. J. Pathol. 1994; 144: 449-453.

19 Estus S, Golde TE, Kunishita T, Blades D, Lowery D, Eisen M, Usiak M, Qu XM, Tabira T, Greenberg BD. Potentially amyloidogenic, carboxyl-terminal derivatives of the amyloid protein precursor. Science 1992; 255: 726-728.

20 Golde TE, Estus S, Younkin LH, Selkoe DJ, and Younkin SG. Processing of the amyloid protein precursor to potentially amyloidogenic derivatives. Science 1992; 255: 728-730.

21 Seubert P, Vigo-Pelfrey C, Esch F, Lee M, Dovey H, Davis D, Sinha S, Schlossmacher M, Whaley J, Swindlehurst C, McCormack R, Wolfert R, Selkoe D, Lieberberg I, Schenk D. Isolation and quantification of soluble Alzheimer's β-peptide from biological fluids. Nature 1992; 359: 325-327.

22 Schulz PE. Beta-peptides enhance the magnitude and probability of long-term potentiation. Soc. Neurosci. Abstr. 1996; 22: 2111.

23 Wu J, Anwyl R, Rowan MJ. β-amyloid selectively augments NMDA receptor-mediated synaptic transmission in rat hippocampus. NeuroReport 1995; 6: 2409-2413.

24 Huber G, Bailly Y, Martin JR, Mariani J, Brugg B. Synaptic β-amyloid precursor proteins increase with learning capacity in rats. Neuroscience 1997; 80: 313-320.

25 Kamenetz FR, Tomita T, Borchelt DR, Sisodia SS, Iwatsubo T, Malinow R. Activity dependent secretion of β-amyloid: roles of β-amyloid in synaptic transmission. Soc. Neurosci. Abstr. 2000; 26: 491.

26 Heese K, Nagai Y, Sawada T. Identification of a new synaptic vesicle protein 2B mRNA transcript which is up-regulated in neurons by amyloid-β peptide fragment (1-42). Biochem Biophys. Res. Commun. 2001; 289: 924-928.

27 Pike CJ, Burdick D, Walencewicz AJ, Glabe CG, Cotman CW. Neurodegeneration induced by β-amyloid peptides *in vitro*: The role of peptide assembly state. J. Neurosci. 1993; 13: 1676-1687.

[28] Dumery L, Bourdel F, Soussan Y, Fialkowsky A, Viale S, Nicolas P, Reboud-Ravaux M. β-Amyloid protein aggregation: its implication in the physiopathology of Alzheimer's disease. Pathol. Biol. (Paris) 2001; 49: 72-85.
[29] Mehta PD, Pirttila T, Patrick BA, Barshatzky M, Mehta SP. Amyloid-β protein 1-40 and 1-42 levels in matched cerebrospinal fluid and plasma from patients with Alzheimer disease. Neurosci. Lett. 2001; 304: 102-106.
[30] Younkin SG. Evidence that Aβ42 is the real culprit in Alzheimer's disease. Ann. Neurol. 1995; 37: 287-288.
[31] Joachim CL, Mori H, Selkoe DJ. Amyloid β-protein deposition in tissues other than brain in Alzheimer's disease. Nature (Lond) 1989; 341: 226-230.
[32] Gearing M, Wilson RW, Unger ER, Shelton ER, Chan HW, Masters CL, Beyreuther K, Mirra SS. Amyloid precursor protein (APP) in the striatum in Alzheimer's disease: an immunohistochemical study. J Neuropathol. Exp. Neurol. 1993; 52: 22-30.
[33] Einstein G, Buranosky R, Crain BJ. Dendritic pathology of granule cells in Alzheimer's disease is unrelated to neuritic plaques. J. Neurosci. 1994; 14: 5077-5088.
[34] Cochran E, Bacci B, Chen Y, Patton A, Gambetti P, Autilio-Gambetti L. Amyloid precursor protein and ubiquitin immunoreactivity in dystrophic axons is not unique to Alzheimer's disease. Am. J. Pathol. 1991; 139: 485-489.
[35] Wilson CA, Doms RW, Lee VM. Intracellular APP processing and Aβ production in Alzheimer disease. J. Neuropathol. Exp. Neurol. 1999; 58: 787-794.
[36] Klein WL, Krafft GA, Finch CE. Targeting small Aβ oligomers: the solution to an Alzheimer's disease conundrum? Trends. Neurosci. 2001; 24: 219-224.
[37] Wilson D, Doms R, Lee V. Intracellular APP processing and Aβ production in Alzheimer's disease. J. Neuropathol. Exp. Neurol. 1999; 58: 787-794.
[38] Emre M, Geula C, Ransil BJ, Mesulam MM. The acute neurotoxicity and effects upon cholinergic axons of intracerebrally injected β amyloid in the rat brain. Neurobiol. Aging 1992; 13: 553-560.
[39] Kowall NW, McKee AC, Yankner BA, Beal MF. *In vivo* neurotoxicity of β-amyloid [β(1-40)] and the [β(25-35)] fragment. Neurobiol. Aging 1992; 13: 537-542.
[40] Pike CJ, Burdick D, Walencewicz AJ, Glabe CG, Cotman CW. Neurodegeneration induced by β-amyloid peptides *in vitro*: the role of peptide assembly state. J. Neurosci. 1993; 13: 1676-1687.
[41] Glenner GG, Wong CW. Alzheimer's disease and Down's syndrome: sharing of a unique cerebrovascular amyloid fibril protein. Biochem. Biophys. Res. Commun. 1984; 122: 1131-1135.
[42] Hardy JA, Higgins GA. Alzheimer's disease: the amyloid cascade hypothesis. Science 1992; 256: 184-185.
[43] Mattson MP, Cheng D, Davis D, Bryant K, Lieberburg I, Rydel RE. β-amyloid peptides destabilize calcium homeostasis and render human cortical neurons vulnerable to excitotoxicity. J. Neurosci. 1992; 12: 376-389.
[44] Mattson MP, Barger SW, Cheng B, Lieberburg I, Smith-Swintosky VL, Rydel RE. β-Amyloid precursor protein metabolites and loss of neuronal Ca^{2+} homeostasis in Alzheimer's disease. Trends Neurosci. 1993; 16: 409-414.
[45] Ueda K, Shinohara S, Yagami T, Asakura K, Kawasaki K. Amyloid β protein potentiates Ca^{2+} influx through L-type voltage-sensitive Ca^{2+} channels: a possible involvement of free radicals. J. Neurochem. 1997; 68: 265-271.
[46] Mark RJ, Hensley K, Butterfield DA, Mattson MP. Amyloid β-peptide impairs ion-motive ATPase activities: evidence for a role in loss of neuronal Ca^{2+} homeostasis and cell death. J. Neurosci. 1995; 15: 6239-6249.
[47] Wu A, Derrico CA, Hatem L, Colvin RA. Alzheimer's amyloid-β peptide inhibits sodium/calcium exchange measured in rat and human brain plasma membrane vesicles. Neuroscience 1997; 80: 675-684.
[48] Good TA, Smith DO, Murphy RM. β-amyloid peptide blocks the fast-inactivating K^+ current in rat hippocampal neurons. Biophys. J. 1996; 70: 296-304.
[49] Arispe N, Pollard HB, Rojas E. β-Amyloid Ca^{2+}-channel hypothesis for neuronal death in Alzheimer disease. Mol. Cell Biochem. 1994; 140: 119-125.
[50] Harkány T, Ábrahám I, Timmerman W, Laskay G, Tóth B, Sasvári M, Kónya C, Sebens JB, Korf J, Nyakas C, Zarándi M, Soós K, Penke B, Luiten PG. β-Amyloid neurotoxicity is mediated by a glutamate-triggered excitotoxic cascade in rat nucleus basalis. Eur. J. Neurosci. 2000; 12: 2735-2745.
[51] Hensley K, Carney JM, Mattson MP, Aksenova M, Harris M, Wu JF, Floyd RA, Butterfield DA. A model for β-amyloid aggregation and neurotoxicity based on free radical generation by the peptide: relevance to Alzheimer's disease. Proc. Natl. Acad. Sci. USA 1994; 91: 3270-3274.
[52] Butterfield DA, Hensley K, Harris M, Mattson MP, Carney J. β-amyloid peptide free radical fragments initiate synaptosomal lipoperoxidation in a sequence-specific fashion: implications to Alzheimer's disease. Biochem. Biophys. Res. Commun. 1994; 200: 710-715.
[53] Lynch T, Cherny RA, Bush AI. Oxidative processes in Alzheimer's disease: the role of Aβ-metal interactions. Exp. Gerontol. 2000; 35: 445-451.
[54] Zou H, Henzel WJ, Liu X, Lutschg A, Wang X. Apaf-1, a human protein homologous to *C. elegans* CED-4, participates in cytochrome c-dependent activation of caspase-3. Cell 1997; 90: 405-413.
[55] Martinou JC, Desagher S, Antonsson B. Cytochrome c release from mitochondria: all or nothing. Nat. Cell. Biol. 2000; 2: 41-43.
[56] Green DR, Reed JC. Mitochondria and apoptosis. Science 1998; 281: 1309-1312.
[57] Dumery L, Bourdel F, Soussan Y, Fialkowsky A, Viale S, Nicolas P, Reboud-Ravaux M. β-Amyloid protein aggregation: its implication in the physiopathology of Alzheimer's disease. Pathol. Biol. (Paris) 2001; 49: 72-85.

[58] Selkoe DJ. Alzheimer's disease: genes, proteins and therapy. Physiol. Rev. 2001; 81: 741-766.
[59] Chen S, Frederickson RC, Brunden KR. Neuroglial-mediated immunoinflammatory responses in Alzheimer's disease: complement activation and therapeutic approaches. Neurobiol. Aging 1996; 17: 781-787.
[60] Patrick GN, Zukerberg L, Nikolic M, de la Monte S, Dikkes P, Tsai LH. Conversion of p35 to p25 deregulates Cdk5 activity and promotes neurodegeneration. Nature (Lond) 1999; 402: 615-622.
[61] Williamson R, Scales T, Clark BR, Gibb G, Reynolds CH, Kellie S, Bird IN, Varndell IM, Sheppard PW, Everall I, Anderton BH. Rapid tyrosine phosphorylation of neuronal proteins including tau and focal adhesion kinase in response to amyloid-β peptide exposure: involvement of Src family protein kinases. J. Neurosci. 2002; 22: 10-20.
[62] Rapoport M, Ferreira A. PD98059 prevents neurite degeneration induced by fibrillar β-amyloid in mature hippocampal neurons. J. Neurochem. 2000; 74: 125-133.
[63] Mattson MP. Calcium as sculptor and destroyer of neural circuitry. Exp. Gerontol. 1992; 27: 29-49.
[64] Bootman MD, Collins TJ, Peppiatt CM, Prothero LS, MacKenzie L, De Smet P, Travers M, Tovey SC, Seo JT, Berridge MJ, Ciccolini F, Lipp P. Calcium signalling: an overview. Semin. Cell Dev. Biol. 2001; 12: 3-10.
[65] Watt F. Nuclear microscope analysis in Alzheimer's and Parkinson's disease: a review. Cell. Mol. Biol. 1996; 42: 17-26.
[66] Nixon RA, Saito KI, Grynspan F, Griffin WR, Katayama S, Honda T, Mohan PS, Shea TB, Beermann M. Calcium-activated neutral proteinase (calpain) system in aging and Alzheimer's disease. Ann. NY Acad. Sci. 1994; 747: 77-91.
[67] Selkoe DJ. Cell biology of the amyloid β-protein precursor and the mechanism of Alzheimer's disease. Annu. Rev. Cell Biol. 1994; 10: 373-403.
[68] Kang J, Lemaire HG, Unterbeck A, Salbaum JM, Masters CL, Grzeschik KH, Multhaup G, Beyreuther K, Muller-Hill B. The precursor of Alzheimer's disease amyloid A4 protein resembles a cell-surface receptor. Nature (Lond) 1987; 325: 733-736.
[69] Selkoe DJ, Podlisny MB, Joachim CL, Vickers EA, Lee G, Fritz LC, Oltersdorf T. β-amyloid precursor protein of Alzheimer disease occurs as 110- to 135-kilodalton membrane-associated proteins in neural and nonneural tissues. Proc. Natl. Acad. Sci. USA 1988; 85: 7341-7345.
[70] Manning RW, Reid CM, Lampe RA, Davis LG. Identification in rodents and other species of an mRNA homologous to the human β-amyloid precursor. Brain Res. 1988; 427: 293-297.
[71] Querfurth HW, Wijsman EM, St. George-Hyslop PH, Selkoe DJ. βAPP mRNA transcription is increased in cultured fibroblats from the familial Alzheimer's disease-1 family. Mol. Brain Res. 1995; 28: 319-337.
[72] Tanzi RE, McClatchey AI, Lamperti ED, Villakomaroff L, Gusella JF. Protease inhibitor domain encoded by an amyloid protein-precursor messenger-RNA associated with Alzheimer's-disease. Nature 1988; 331: 528-530.
[73] Ho L, Fukuchi K, Younkin SG. The alternatively spliced Kunitz protease inhibitor domain alters amyloid β-protein precursor processing and amyloid β-protein production in cultured cells. J. Biol. Chem. 1996; 271: 30929-30934.
[74] Goedert M. Neuronal localization of amyloid β-protein precursor mRNA in normal human brain and in Alzheimer's disease. EMBO J. 1987; 6: 3627-3632.
[75] Sandbrink R, Masters CL, Beyreuther K. βA4-amyloid protein precursor mRNA isoforms without exon 15 are ubiquitously expressed in rat tissues including brain, but not in neurons. J. Biol. Chem. 1994; 269: 1510-1517.
[76] Tanzi RE, Wenniger JJ, Hyman BT. Cellular specificity and regional distribution of amyloid-β protein precursor alternative transcripts are unaltered in Alzheimer's hippocampal formation. Mol. Brain Res. 1993; 18: 246-252.
[77] Esch FS, Keim PS, Beattle EC, Blacher RW, Culwell AR, Oltersdorf T, McClure D, Ward PJ. Cleavage of amyloid-β peptide during constitutive processing of its precursor. Science 1990; 248: 1122-1124.
[78] Bowes MP, Masliah E, Otero DA, Zivin JA, Saitoh T. Reduction of neurological damage by a peptide segment of the amyloid β/A4 protein precursor in a rabbit spinal cord ischemia model. Exp. Neurol. 1994; 129: 112-119.
[79] Smith-Swintosky VL, Pettigrew LC, Craddock SD, Culwell AR, Rydel RE, Mattson MP. Secreted forms of β-amyloid precursor protein protect against ischemic brain injury. J. Neurochem. 1994; 63: 781-784.
[80] Fraser SP, Suh Y, Djamgoz MBA. Ionic effects of the Alzheimer's disease β-amyloid precursor protein and its metabolic fragments. Trends Neurosci. 1997; 20: 67-72.
[81] Milward EA, Papadopoulos R, Fuller SJ, Moir RD, Small D, Beyreuther K, Masters CL. The amyloid protein precursor of Alzheimer's disease is a mediator of the effects of nerve growth factor on neurite outgrowth. Neuron 1992; 9: 129-137.
[82] Saitoh T, Sundsmo M, Roch JM, Kimura N, Cole G, Schubert D, Oltersdorf T, Schenk DB. Secreted form of amyloid-β protein precursor is involved in the growth regulation of fibroblasts. Cell 1989; 58: 615-622.
[83] Araki W, Kitaguchi N, Tokushima Y, Ishii K, Aratake H, Shimohama S, Nakamura S, Kimura J. Trophic effect of β-amyloid precursor protein on cerebral cortical neurons in culture. Biochem. Biophys. Res. Commun. 1991; 181: 265-271.
[84] Mattson MP, Cheng B, Culwell AR, Esch FS, Lieberburg I, Rydel RE. Evidence for excitoprotective and intraneuronal calcium-regulating roles for secreted forms of the β-amyloid precursor protein. Neuron 1993; 10: 243-254.

[85] Kihara T, Shimohama S, Sawada H, Kimura J, Kume T, Kochiyama H, Maeda T, Akaike A. Nicotinic receptor stimulation protects neurons against β-amyloid toxicity. Ann. Neurol. 1997; 42: 159-163.
[86] Barger SW, Mattson MP. Induction of neuroprotective κB-dependent transcription by secreted forms of the Alzheimer's β-amyloid precursor. Mol. Brain Res. 1996; 40: 116-126.
[87] Ishiguro M, Ohsawa I, Takamura C, Morimoto T, Kohsaka S. Secreted from of β-amyloid precursor protein activates protein kinase C and phospholipase C-α1 in cultured embryonic rat neocortical cells. Mol. Brain Res. 1998; 53: 24-32.
[88] Golde TE, Estus S, Younkin LH, Selkoe DJ, Younkin SG. Processing of the amyloid protein precursor to potentially amyloidogenic derivatives. Science 1992; 255: 728-730.
[89] Jarrett JT, Berger EP, Lansbury PT Jr. The carboxy terminus of the β-amyloid protein is critical for the seeding of amyloid formation: implications for the pathogenesis of Alzheimer's disease. Biochemistry 1993; 32: 4693-4697.
[90] Iwatsubo T, Odaka A, Suzuki N, Mizusawa H, Nukina N, Ihara Y. Visualization of Aβ42(43) and Aβ40 in senile plaques with end-specific Aβ monoclonals: evidence that an initially deposited species is Aβ 42(43). Neuron 1994; 13: 45-53.
[91] Wolfe MS, Xia W, Ostaszewski BL, Diehl TS, Kimberly WT, Selkoe DJ. Two transmembrane aspartates in presenilin-1 required for presenilin endoproteolysis and γ-secretase activity. Nature 1999; 398: 513-517.
[92] Ancolio K, Dumanchin C, Barelli H, Warter JM, Brice A, Campion D, Frebourg T, Checler F. Unusual phenotypic alteration of β-amyloid precursor protein (βAPP) maturation by a new Val-715 → Met βAPP-770 mutation responsible for probable early-onset Alzheimer's disease. Proc. Natl. Acad. Sci. USA 1999; 96: 4119-4124.
[93] Finkel SI. The signs of the behavioural and psychological symptoms of dementia. Clinician 1998; 16: 33-42.
[94] Frisoni GB, Rozzini L, Gozzetti A, Binetti G, Zanetti O, Bianchetti A, Trabucchi M, Cummings JL. Behavioral syndromes in Alzheimer's disease: description and correlates. Dement. Geriatr. Cogn. Disord. 1999; 10: 130-138.
[95] Arnold SE, Franz BR, Trojanowski JQ. Elderly patients with schizophrenia exhibit infrequent neurodegenerative lesions. Neurobiol. Aging 1994; 15: 299-303.
[96] Casanova MF, Carosella NW, Gold JM, Kleinman JE, Weinberger DR, Powers RE. A topographical study of senile plaques and neurofibrillary tangles in the hippocampi of patients with Alzheimer's disease and congnitively impaired patients with schizophrenia. Psychiatry Res. 1993; 49: 41-62.
[97] Sisodia SS. Evidence that β-amyloid protein in Alzheimer's disease is not derived by normal processing. Science 1990; 248: 492-495.
[98] Soininen H, Syrjanen S, Heinonen O, Neittaanmaki H, Miettinen R, Paljarvi L, Syrjanen K, Beyreuther K, Riekkinen P. Amyloid-β protein deposition in skin of patients with dementia. Lancet 1992; 339: 245.
[99] Etcheberrigaray R, Bhagavan S. Ionic and signal transduction alterations in Alzheimer's disease: relevance of studies on peripheral cells. Mol. Neurobiol. 1999; 20: 93-109.
[100] Bergman M, Salman H, Beloosesky Y, Djaldetti M, Bessler H. Are peripheral blood cells from patients with Alzheimer's disease more sensitive to apoptotic stimuli? Alzheimer Dis. Assoc. Dis. 2002; 16: 156-160.
[101] Eckert A, Cotman CW, Zerfass R, Hennerici M, Muller WE. Lymphocytes as cell model to study apoptosis in Alzheimer's disease: vulnerability to programmed cell death appears to be altered. J. Neural. Transm. Suppl. 1998; 54: 259-67.
[102] Mórocz M, Kálmán J, Juhász A, Sinkó I, McGlynn AP, Downes CS, Janka Z, Raskó I. Elevated levels of oxidative DNA damage in lymphocytes from patients with Alzheimer's disease. Neurobiol. Aging 2002; 23: 47-53.
[103] Zubenko GS, Cohen BM, Growdon J, Corkin S. Cell membrane abnormality in Alzheimer's disease. Lancet 1984; 2: 235.
[104] Kálmán J, Dey I, Ilona SV, Matkovics B, Brown D, Janka Z, Farkas T, Joó F. Platelet membrane fluidity and plasma malondialdehyde levels in Alzheimer's demented patients with and without family history of dementia. Biol. Psychiat. 1994; 35: 190-194.
[105] Zubenko GS. Endoplasmic reticulum abnormality in Alzheimer's disease: selective alteration in platelet NADH-cytochrome C reductase activity. J. Geriatr. Psychiat. Neurol. 1989; 2: 3-10.
[106] Sevush S, Jy W, Horstman LL, Mao WW, Kolodny L, Ahn YS. Platelet activation in Alzheimer disease. Arch. Neurol. 1998; 55: 530-536.
[107] Perry RH, Wilson ID, Bober MJ, Atack J, Blessed G, Tomlinson BE, Perry EK. Plasma and erythrocyte acetylcholinesterase in senile dementia of Alzheimer type. Lancet 1982; 1: 174-175.
[108] Peterson C, Gibson GE, Blass JP. Altered calcium uptake in cultured skin fibroblasts from patients with Alzheimer's disease. N. Engl. J. Med. 1985; 312: 1063-1065.
[109] Peterson C, Goldman JE. Alterations in calcium content and biochemical processes in cultured skin fibroblasts from aged and Alzheimer donors. Proc. Natl. Acad. Sci. USA 1986; 83: 2758-2762.
[110] Sims NR, Finegan JM, Blass JP. Altered glucose metabolism in fibroblasts from patients with Alzheimer's disease. N. Engl. J. Med. 1985; 313: 683-684.
[111] Paoletti F, Tombaccini D. Proteolytic imbalance in Alzheimer fibroblasts as potential pathological trait of disease. FASEB J. 1998; 12: 925-927.

[112] Gibson G, Martins R, Blass J, Gandy S. Altered oxidation and signal transduction systems in fibroblasts from Alzheimer patients. In: Mailer D, Gispen W (Eds.) The current status of the calcium hypothesis of brain aging and Alzheimer's disease. Life Science 1996; 59: 477-490.

[113] Li JC, Kaminskas E. Deficient repair of DNA lesions in Alzheimer's disease fibroblasts. Biochem. Biophys. Res. Commun. 1985; 129: 733-738.

[114] Connolly GP. Fibroblast models of neurological disorders: fluorescence measurement studies. Trends Pharmacol. Sci. 1998; 19: 171-177.

[115] Dolman CL. Diagnosis of neurometabolic disorders by examination of skin biopsies and lymphocytes. Semin. Diagn. Pathol. 1984; 1: 82-97.

[116] Idoate-Gastearena MA, Vega-Vazquez F. Diagnosis of neurometabolic and neurodegenerative diseases by cutaneous biopsy. Rev. Neurol. 1997; 25: S269-S280.

[117] Huang HM, Martins R, Gandy S, Etcheberrigaray R, Ito E, Alkon DL, Blass JP, Gibson GE. The use of cultured fibroblasts in elucidating the pathophysiology and diagnosis of Alzheimer's disease. In: Disterhoft JF, Gispen WH, Traber J Khachaturian ZS (Eds.) Calcium Hypothesis of Aging and Dementia. New York Academy of Science, New York, 1994; 225-244.

[118] Giambalvo CT. Protein kinase C and dopamine release – II: Effect of dopamine acting drugs *in vivo*. Biochem. Pharmacol. 1988; 37: 4009-4017.

[119] Walker JM, Bowen WD, Walker FO, Matsumoto RR, De Costa B, Rice KC. Sigma receptors: biology and function. Pharmacol. Rev. 1990; 42: 355-401.

[120] Behl C, Lezoualc'h F, Widmann M, Rupprecht R, Holsboer F. Oxidative stress-resistant cells are protected against haloperidol toxicity. Brain Res. 1996; 717: 193-195.

[121] Avent KM, Usuki E, Eyles DW, Keeve R, van der Schyf CJ, Castagnoli N, Pond SM. Haloperidol and its tetrahydropyridine derivative (HPTP) are metabolized to potentially neurotoxic pyridium species in the baboon. Life Sci. 1996; 59: 1473-1482.

[122] Prokopenko RA, Mogilevich SE, Luik AI, Naydyenova IY, Batrak GN, Hawryluk BR, Degtiar VY. Effects of haloperidol and chlorpromazine on smooth muscle contractility, platelet aggregation and neuronal calcium current. Gen. Physiol. Biophys. 1995; 14: 349-357.

[123] Higaki J, Murphy GM Jr, Cordell B. Inhibition of β-amyloid formation by haloperidol: a possible mechanism for reduced frequency of Alzheimer's disease pathology in schizophrenia. J. Neurochem. 1997; 68: 333-336.

[124] Lane HY, Chang YC, Su MH, Chiu CC, Huang MC, Chang WH. Shifting from haloperidol to risperidone for behavioral disturbances in dementia: safety, response predictors, and mood effects. J. Clin. Psychopharmacol. 2002; 22: 4-10.

[125] Chan WC, Lam LC, Choy CN, Leung VP, Li SW, Chiu HF. A double-blind randomised comparison of risperidone and haloperidol in the treatment of behavioural and psychological symptoms in Chinese dementia patients. Int. J. Geriatr. Psychiatry 2001; 16: 1156-1162.

[126] Borc JJ, Larson DB, Lyons JS, Beardsley RS. Expenditures for psychotropic medications in the United States. Am. J. Psychiatry 1991; 148: 644-647.

[127] Volavka J, Cooper TB. Review of haloperidol blood level and clinical response: looking through the window. J. Clin. Psychopharmacol. 1987; 7: 25-30.

[128] vanPutten T, Marder SR, Mintz J, Poland RE. Haloperidol plasma levels and clinical response: a therapeutic window relationship. Psyhcopharmacol. Bull. 1988; 24: 172-175.

[129] Aravagiri M, Marder SR, Wirshing D, Wirshing WC. Plasma concentrations of risperidone and its 9-hydroxy metabolite and their relationship to dose in schizophrenic patients: simultaneous determination by a high performance liquid chromatography with electrochemical detection. Pharmacopsychiatry 1998; 31: 102-109.

[130] Ereshefsky L, Lacombe S. Pharmacological profile of risperidone. Can. J. Psychiatry 1993; 38: S80-S88.

[131] Laskay G, Zarándi M, Varga J, Jost K, Fónagy A, Torday Cs, Latzkovits L, Penke B. A putative tetrapeptide antagonist prevents β-amyloid-induced long-term elevation of $[Ca^{2+}]_i$ in rat astrocytes. Biochem. Biophys. Res. Commun. 1997; 235:479-481.

[132] Lowry OH, Rosenbrough NJ, Farr AL, Randall RJ. Protein measurement with the Folin-phenol reagents. J. Biol. Chem. 1951; 193: 265-275.

[133] Stewart J M, Young JD. Solid Phase Peptide Synthesis. 2nd Ed. Pierce, Rockford, IL. 1984.

[134] Kaiser E. Color test for detection of free terminal amino groups in the solid-phase synthesis of peptides. Anal. Biochem. 1970; 34: 595-598.

[135] Campbell A, Baldessarini RJ. Effects of maturation and aging on behavioral responses to haloperidol in the rat. Psychopharmacology (Berl) 1981; 73: 219-222.

[136] Dunn LA, Atwater GE, Kilts CD. Effects of antipsychotic drugs on latent inhibition: sensitivity and specificity of an animal behavioral model of clinical drug action. Psychopharmacology (Berl) 1993; 112: 315-323.

[137] Di Matteo V, Cacchio M, Di Giulio C, Di Giovanni G, Esposito E. Biochemical evidence that the atypical antipsychotic drugs clozapine and risperidone block $5\text{-}HT_{2C}$ receptors *in vivo*. Pharmacol. Biochem. Behav. 2002; 71: 607-613.

[138] Broerse A, Timmerman W, Westerink BH, Den BJ. Antipsychotics and single-cell activity in the rat superior colliculus. Prog. Neuropsychopharmacol. Biol. Psychiatry 2002; 26: 327-33.
[139] Hess HH, Lees MB, Derr JE. A linear Lowry-Folin assay for both water-soluble and sodium dodecyl sulfate-solubilized proteins. Ann. Biochem. 1978; 85: 295-300.
[140] Puskás LG, Zvara Á, Hackler L Jr, Micsik T, van Hummelen P. Production of bulk amounts of universal RNA for DNA microarrays. Biotechniques 2002; 33: 898-904.
[141] Puskás LG, Hackler L Jr, Kovács G, Kupihár Z, Zvara Á, Micsik T, van Hummelen P. Recovery of cyanine-dye nucleotide triphosphates. Anal. Biochem. 2002; 305, 279-281.
[142] Onody A, Zvara Á, Hackler L Jr, Vígh L, Ferdinándy P, Puskás LG. Effect of classic preconditioning on the gene expression pattern of rat hearts: a DNA microarray study. FEBS Lett. 2003; 536: 35-40.
[143] Kitajka K, Puskás LG, Zvara Á, Hackler L Jr, Barcelo-Coblijn G, Yeo YK, Farkas T. The role of n-3 polyunsaturated fatty acids in brain: modulation of rat brain gene expression by dietary n-3 fatty acids. Proc. Natl. Acad. Sci. USA 2002; 99: 2619-2624.
[144] Cleveland WS. Robust locally weighted regression and smoothing scatterplots. J. Am. Statist. Assoc. 1974; 74: 829-836.
[145] Yang YH, Dudoit S, Luu P, Lin DM, Peng V, Ngai J, Speed TP. Normalization for cDNA microarray data: a robust composite method addressing single and multiple slide systematic variation. Nucleic Acids Res. 2002; 30: 15.
[146] Pfaffl MW. A new mathematical model for relative quantification in real-time RT-PCR. Nucleic Acids Res. 2001; 29: 45.
[147] Hickey WF, Hsu BL, Kimura H. T-lymphocyte entry into the central nervous system. J. Neurosci. Res. 1991; 28: 254-260.
[148] Fabry Z, Raine CS, Hart MN. Nervous tissue as an immune compartment: the dialect of the immune response in the CNS. Immunol. Today 1994; 15: 218-224.
[149] Nicoll JAR, Wilkinson D, Holmes C, Steart P, Markham H, Weller R. Neuropathology of human Alzheimer disease after immunization with amyloid-β peptide: a case report. Nat. Med. 2003; 9: 448-452.
[150] Etienne-Manneville S, Adamson P, Manneville JB, Wilbourn B, Greenwood J, Couraud PO. ICAM-1 coupled cytoskeletal rearrangements and lymphocyte migration across brain endothelium involves intracellular calcium signalling. J. Immunol. 2000; 165: 3375-3383.
[151] Schwarz MJ, Chiang S, Müller N, Ackenheil M. T-helper-1 and T-helper-2 responses in psychiatric disorders. Brain Behav. Immun. 2001; 15: 340-370.
[152] Meda L, Cassatella MA, Szendrei GI, Ötvös L Jr, Baron P, Villalba M, Ferrari D, Rossi F. Activation of microglial cells by β-amyloid protein and interferon-γ. Nature 1995; 374: 647-650.
[153] Brod SA. Unregulated inflammation shortens human functional longevity. Inflamm. Res. 2000; 49: 561-570.
[154] Clayton A, Evans RA, Pettit E, Hallett M, Williams JD, Steadman R. Cellular activation through the ligation of intercellular adhesion molecule-1. J. Cell. Sci. 1998; 111: 443-453.
[155] Baldwin AS Jr. The NF-κB and IκB proteins: new discoveries and insights. Annu. Rev. Immunol. 1996; 14: 649-683.
[156] Bondy B, Hofmann M, Muller-Spahn F, Witzko M, Hock C. Reduced β-amyloid response in lymphocytes of patients with Alzheimer's disease. Pharmacopsychiatry 1995; 28: 143-146.
[157] Eckert A, Forstl H, Hartmann H, Muller WE. Decreased β-amyloid sensitivity in Alzheimer's disease. Lancet 1993; 342: 805-806.
[158] Samelson LE. Signal transduction mediated by the T cell antigen receptor: the role of adapter proteins. Annu. Rev. Immunol. 2002; 20: 371-394.
[159] Müller KM, Bickel M, Wiesmann UN, Spörri B. Natural killer cells activate human dermal fibroblasts. Cytokine 2000; 12: 1755-1762.
[160] Chirathaworn C, Kohlmeier JE, Tibbetts SA, Rumsey LM, Chan MA, Benedict SH. Stimulation through intercellular adhesion molecule-1 provides a second signal for T cell activation. J. Immunol. 2002; 168: 5530-5537.
[161] Greenwood J, Calder VL. Lymphocyte migration through cultured endothelial cell monolayers derived from the blood-retinal barrier. Immunology 1993; 80: 401-406.
[162] Pryce G, Male D, Campbell I, Greenwood J. Factors controlling T-cell migration across rat cerebral endothelium *in vitro*. J. Neuroimmunol. 1997; 75: 84-94.
[163] Muller WE, Koch S, Eckert A, Hartmann H, Scheuer K. β-Amyloid peptide decreases membrane fluidity. Brain Res. 1995; 674: 133-136.
[164] Mattson MP. Cellular actions of β-amyloid precursor protein and its soluble and fibrillogenic derivatives. Physiol. Rev. 1997; 77: 1081-1132.
[165] Mogensen HS, Beatty DM, Morris SJ, Jorgensen OS. Amyloid β-peptide (25-35) changes [Ca^{2+}] in hippocampal neurons. NeuroReport 1998; 9: 1553-1558.
[166] Stix B, Reiser B. β-Amyloid peptide 25-35 regulates basal and hormone-stimulated Ca-levels in cultured rat astrocytes. Neurosci. Lett. 1998; 243: 121-124.

[167] Cowburn RF, Wiehager B, Sundstrom E. β-Amyloid peptides enhance binding of the calcium mobilising second messengers, inositol-(1,4,5)trisphosphate and inositol (1,3,4,5)tetrakis-phosphate to their receptor sites in rat cortical membranes. Neurosci. Lett. 1995; 191: 31-34.

[168] Pascale A, Etcheberrygaray R. Calcium alterations in Alzheimer's disease: pathophysiology, models and therapeutic opportunities. Pharmacol. Res. 1999; 39: 81-88.

[169] Ishikawa H, Ozawa H, Saito T, Takahata N, Takemura H. Calcium mobilization evoked by amyloid-β protein involves inositol 1,4,5-triphosphate production in human platelets. Life Sci. 1998; 62: 705-713.

[170] Crawford KW, Bowen WD. Sigma-2 receptor agonists activate a novel apoptotic pathway and potentiate antineoplastic drugs in breast tumor cell lines. Cancer Res. 2002; 62: 313-322.

[171] Mitchell IJ, Cooper AC, Griffiths MR, Cooper AJ. Acute administration of haloperidol induces apoptosis of neurones in the striatum and substantia nigra in the rat. Neuroscience 2002; 109: 89-99.

[172] Santi CM, Cayabyab FS, Sutton KG, McRory JE, Mezeyova J, Hamming KS, Parker D, Stea A, Snutch TP. Differential inhibition of T-type calcium channels by neuroleptics. J. Neurosci. 2002; 22: 396-403.

[173] Kontkanen O, Toronen P, Lakso M, Wong G, Castren E. Antipsychotic drug treatment induces differential gene expression in the rat cortex. J. Neurochem. 2002; 83: 1043-1053.

[174] Fletcher EJ, Church J, MacDonald JF. Haloperidol blocks voltage-activated Ca^{2+} channels in hippocampal neurones. Eur. J. Pharmacol. 1994; 267: 249-252.

[175] Kagan BL, Hirakura Y, Azimov R, Azimova R, Lin MC. The channel hypothesis of Alzheimer's disease: current status. Peptides 2002; 23: 1311-1315.

[176] Edell WS, Tunis SL. Antipsychotic treatment of behavioral and psychological symptoms of dementia in geropsychiatric inpatients. Am. J. Geriatr. Psychiatry 2001; 9: 289-297.

[177] Hermann N, Black SE. Behavioral disturbances in dementia: will the real treatment please stand up? Neurology 2000; 55: 1247-1248.

[178] Reuss B, Unsicker K. Atypical neuroleptic drugs downregulate dopamine sensitivity in rat cortical and striatal astrocytes. Neurosci. 2001; 18: 197-209.

[179] Fu W, Luo H, Parthasarathy S, Mattson MP. Catecholamines potentiate amyloid β-peptide neurotoxicity: involvement of oxidative stress, mitochondrial dysfunction, and perturbed calcium homeostasis. Neurobiol. Dis. 1998; 5: 229-243.

[180] DesJarlais RL, Scibel GL, Kuntz ID, Furth PS, Alvarez JC, Ortiz de Montellano PR, DeCamp DL, Babe LM, Craik CS. Structure-based design of nonpeptide inhibitors specific for the human immunodeficiency virus 1 protease. Proc. Natl. Acad. Sci. USA 1990; 87: 6644-6648.

[181] Paul SM, Purdy RH. Neuroactive steroids. FASEB J. 1992; 6: 2311-2322.

[182] French-Mullen JM, Spence KT. Neurosteroids block Ca^{2+} channel current in freshly isolated hippocampal CA_1 neurons. Eur. J. Pharmacol. 1995; 202: 269-273.

[183] Vilner BJ, Bowen WD. Dual modulation of cellular calcium by sigma receptor ligands: release from intracellular stores and blockade of voltage-dependent influx. Soc. Neurosci. Abstr. 1995; 21: 1608.

[184] Chen M. Alzheimer's α-secretase may be a calcium-dependent protease. FEBS Lett. 1997; 417: 163-167.

[185] Matsuno K, Matsunaga K, Senda T, Mita S. Increase in extracellular acetylcholine level by sigma ligands in rat frontal cortex. J. Pharmac. Exp. Ther. 1993; 265: 851-859.

[186] Maurice T, Su TP, Privat A. Sigma-1 (σ_1) receptor agonists and neurosteroids attenuate $\beta_{25\text{-}35}$-amyloid peptide-induced amnesia in mice through a common mechanism. Neuroscience 1997; 83: 413-428.

[187] Cardounel A, Regelson W, Kalimi M. Dehydroepiandrosterone protects hippocampal neurons against neurotoxin-induced cell death: mechanism of action. Proc. Soc. Exp. Biol. Med. 1999; 222: 145-149.

[188] Dwivedi Y, Pandey GN. Effects of treatment with haloperidol, chlorpromazine, and clozapine on protein kinase C (PKC) and phosphoinositide-specific phospholipase C (PI-PLC) activity and on mRNA and protein expression of PKC and PLC isozymes in rat brain. J. Pharm. Exp. Ther. 1999; 291: 688-704.

[189] Buxbaum JD, Gandy SE, Cicchetti P. Processing of Alzheimer β/A4 amyloid precursor protein: modulation by agents that regulate protein phosphorylation. Proc. Natl. Acad. Sci. USA 1990; 87: 6003-6006.

[190] Cedazo-Minguez A, Wiehager B, Winblad B, Huttinger M, Cowburn RF. Effects of apolipoprotein E (apoE) isoforms, β-amyloid (Aβ) and apoE/Aβ complexes on protein kinase C-α (PKC-α) translocation and amyloid precursor protein (APP) processing in human SH-SY5Y neuroblastoma cells and fibroblasts. Neurochem. Int. 2001; 38: 615-625.

[191] Pákáski M, Baláspiri L, Checler F, Kása P. Human amyloid-β causes changes in the levels of endothelial protein kinase C and its α-isoform *in vitro*. Neurochem. Int. 2002; 41: 409.

[192] Stea A, Soong TW, Snutch TP. Determinants of PKC-dependent modulation of a family of neuronal calcium channels. Neuron 1995; 15: 929-940.

[193] Westmark CJ, Malter JS. Extracellular-regulated kinase controls β-amyloid precursor protein mRNA decay. Mol. Brain Res. 2001; 90: 193-201.

[194] Masliah E, Westland CE, Rockenstein EM, Abraham CR, Mallory M, Veinberg I, Sheldon E, Mucke L. Amyloid precursor proteins protect neurons of transgenic mice against acute and chronic excitotoxic injuries *in vivo*. Neuroscience 1997; 78: 135-146.

[195] Papp H, Pákáski M, Kása P. Presenilin-1 and the amyloid precursor protein are transported bidirectionally in the sciatic nerve of adult rat. Neurochem. Int. 2002; 41: 429-435.
[196] Stephenson DT, Rash K, Clemens JA. Amyloid precursor protein accumulates in regions of neurodegeneration following focal cerebral ischemia in the rat. Brain Res. 1992; 593: 128-135.
[197] Kalaria RN, Bhatti SU, Palatinsky EA, Pennington DH, Shelton ER, Chan HW, Perry G, Lust WD. Accumulation of the β-amyloid precursor protein at sites of ischemic injury in rat brain. NeuroReport 1993; 4: 211-214.
[198] Post A, Rücker M, Ohl F, Uhr M, Holsboer F, Almeida OFX, Michaelidis TM. Mechanisms underlying the protective potential of α-tocopherol (vitamin E) against haloperidol-associated neurotoxicity. Neuropsychopharmacology 2002; 26: 397-407.
[199] Barger SW, Mattson MP. Induction of neuroprotective κB-dependent transcription by secreted forms of Alzheimer's β-amyloid precursor. Mol. Brain Res. 1996; 40: 116-126.
[200] Mattson MP, Camandola S. NF-κB in neuronal plasticity and neurodegenerative disorders. J. Clin. Invest. 2001; 107: 247-254.
[201] Nishimoto I, Okamoto T, Matsuura Y. Alzheimer amyloid protein precursor complexes with brain GTP-binding protein G_o. Nature 1993; 362: 75-79.
[202] Nitsch RM, Deng A, Growdon JH, Wurtman RJ. Serotonin 5-HT_{2A} and 5-HT_{2C} receptors stimulate amyloid precursor protein ectodomain secretion. J. Biol. Chem. 1996; 271: 4188-4194.
[203] Wallace W, Haroutunian V. Using the subcortically lesioned rat cortex to understand the physiological role of amyloid precursor protein. Behav. Brain Res. 1993; 57: 199-206.
[204] Buxbaum JD, Ruefli AA, Parker CA, Cypess AM, Greengard P. Calcium regulates processing of the Alzheimer amyloid protein precursor in a protein kinase C-independent manner. Proc. Natl. Acad. Sci. USA 1994; 91: 4489-4493.
[205] Checler F. Processing of the β-amyloid precursor protein and its regulation in Alzheimer's disease. J. Neurochem. 1995; 65: 1431-1444.
[206] Querfurth HW, Selkoe DJ. Calcium ionophore increases amyloid-β peptide production by cultured cells. Biochemistry 1994; 33: 4550-4561.
[207] Sennvik K, Benedikz E, Fastbom J, Sundstrom E, Winblad B, Ankarcrona M. Calcium ionophore A23187 specificially decreases the secretion of β-secretase cleaved amyloid precursor protein during apoptosis in primary rat cortical cultures. J. Neurosci. Res. 2001; 63: 429-437.
[208] Walter J, Fluhrer R, Hartung B, Willem M, Kaether C, Capell A, Lammich S, Multhaup G, Haass C. Phosphorylation regulates intracellular trafficking of β-secretase. J. Biol. Chem. 2001; 276: 14634-14641.
[209] Lockhart DJ, Winzeler EA. Genomics, gene expression and DNA arrays. Nature 2000; 405: 827-836.
[210] McCullumsmith RE, Stincic TL, Agrawal SM, Meador-Woodruff JH. Differential effects of antipsychotics on haloperidol-induced vacuous chewing movements and subcortical gene expression in the rat. Eur. J. Pharmacol. 2003; 477: 101-112.
[211] Schmitt A, Zink M, Petroianu G, May B, Braus DF, Henn FA. Decreased gene expression of glial and neuronal glutamate transporters after chronic antipsychotic treatment in rat brain. Neurosci. Lett. 2003; 347: 81-84.
[212] Coderre TJ, Katz J, Vaccarino AL, Melzack R. Contribution of central neuroplasticity to pathological pain: review of clinical and experimental evidence. Pain 1993; 52: 259-285.
[213] Moore KA, Baba H, Woolf CJ. Synaptic transmission and plasticity in the superficial dorsal horn. Prog. Brain Res. 2000; 129: 63-80.
[214] Guo Q, Robinson N, Mattson MP. Secreted β-amyloid precursor protein counteracts the proapoptotic action of mutant presenilin-1 by activation of NF-κB and stabilization of calcium homeostasis. J. Biol. Chem. 1998; 273: 12341-12351.
[215] Jimerson DC, Post RM, Carman JS, van Kammen JS, Wood JH, Goodwin FK, Bunney WE. CSF calcium: clinical correlates in affective illness and schizophrenia. Biol. Psychiatry 1979; 14: 37-51.
[216] Riley DM, Watt DC. Hypercalcemia in the etiology of puerperal psychosis. Biol. Psychiatry 1985; 20: 479-488.
[217] Yarlagadda A. Role of calcium regulation in pathophysiology model of schizophrenia and possible interventions. Med. Hypotheses 2002; 58: 182-186.
[218] Xing G, Chavko M, Zhang LX, Yang S, Post RM. Decreased calcium-dependent constitutive nitric oxide synthase (cNOS) activity in prefrontal cortex in schizophrenia and depression. Schizophr. Res. 2002; 58: 21-30.
[219] Suzuki K, Kusumi I, Sasaki Y, Koyama T. Serotonin-induced platelet intracellular calcium mobilization in various psychiatric disorders: is it specific to bipolar disorder? J. Affect. Disord. 2001; 64: 291-296.
[220] Koller CW. Neuroprotective Therapy for Parkinson's Disease. Exp. Neurol. 1997; 144: 24-28.
[221] Panov AV, Burke JR, Strittmatter WJ, Greenamyre JT. *In vitro* effects of polyglutamine tracts on Ca^{2+}-dependent depolarization of rat and human mitochondria: relevance to Huntington's disease. Arch. Biochem. Biophys. 2003; 410: 1-6.
[222] Yan HD, Lim W, Lee KW, Kim J. Sera from amyotrophic lateral sclerosis patients reduce high-voltage activated Ca^{2+} currents in mice dorsal root ganglion neurons. Neurosci. Lett. 1997; 235: 69-72.
[223] Gailly P. New aspects of calcium signaling in skeletal muscle cells: implications in Duchenne muscular dystrophy. Biochim. Biophys. Acta 2002; 1600: 38-44.

[224] Frasson M, Sahel JA, Fabre M, Simonutti M, Dreyfus H, Picaud S. Retinitis pigmentosa: rod photoreceptor rescue by a calcium-channel blocker in the rd mouse. Nat. Med. 1999; 5: 1183-1187.
[225] Desikan R, Mackerness SAH, Hancock JT, Neill SJ. Regulation of the Arabidopsis transcriptome by oxidative stress. Plant Physiol. 2001; 127: 159-172.
[226] Wagner U, Edwards R, Dixon DP, Mauch F. Probing the diversity of the Arabidopsis glutathione S-transferase gene family. Plant Mol. Biol. 2002; 49: 515-532.
[227] Karoum F, Karson CN, Bigelow LB, Lawson WB, Wyatt RJ. Preliminary evidence of reduced combined output of dopamine and its metabolites in chronic schizophrenia. Arch. Gen. Psychiat. 1987; 44: 604-607.
[228] van den Buuse M, Webber KM. Endothelin and dopamine release. Prog. Neurobiol. 2000; 60: 385-405.
[229] Reiser G, Donié F. Endothelin induces a rise of inositol 1,4,5-triphosphate, inositol 1,3,4,5-tetrakisphosphate levels and of cytosolic Ca^{2+} activity in neural cell lines. Eur. J. Neurosci. 1990; 2: 769-775.
[230] Choi DW. Calcium-mediated neurotoxicity: relationship to specific channel types and role in ischemic damage. Trends Neurosci. 1988; 11: 465-469.
[231] Kataoka Y, Koizumi S, Kohzuma M, Shibaguchi H, Shigematsu K, Niwa M, Taniyama K. NMDA receptor involvement in endothelin neurotoxicity in rat striatal slices. Eur. J. Pharmacol. 1995; 273: 285-289.